

THE RECOMBINATION OF ATOMIC OXYGEN
IN THE PRESENCE OF INERT GASES

and

A STUDY OF VIBRATIONALLY EXCITED NITROGEN
PRODUCED BY A MICROWAVE DISCHARGE AND
BY CHEMICAL REACTION

by

J. E. MORGAN

A thesis submitted to the Faculty of
Graduate Studies and Research in partial
fulfilment of the requirements for the
degree of Doctor of Philosophy

Department of Chemistry,
McGill University,
Montreal.

December 1962

TABLE OF CONTENTS

| <u>PART I</u> | | <u>Page</u> |
|--|---------|-------------|
| I. <u>INTRODUCTION</u> | | 1 |
| II. <u>PRODUCTION OF OXYGEN ATOMS</u> | | 3 |
| (i) Photolytic dissociation | | 3 |
| (ii) Thermal dissociation | | 5 |
| (iii) Electrical dissociation | | 7 |
| III. <u>MEASUREMENT OF OXYGEN ATOM CONCENTRATION</u> | | 11 |
| (i) Catalytic probe | | 11 |
| (ii) Wrede-Harteck gauges | | 13 |
| (iii) Nitrogen dioxide titration | | 14 |
| (iv) Electron spin resonance | | 17 |
| (v) Mass spectrometric methods | | 17 |
| IV. <u>KINETICS OF OXYGEN-ATOM RECOMBINATION</u> | | 19 |
| Reaction mechanism | | 19 |
| Thermal Decomposition of Ozone | | 21 |
| Direct Measurement of Oxygen-Atom Recombination | | 27 |
| Heterogeneous Recombination of Oxygen Atoms | | 28 |
| Homogeneous Recombination of Oxygen Atoms | | 30 |
| Shock Tube Measurements of the Second Order Recombination | | 33 |
| Measurement of the Second Order Recombination at Room Temperature | | 39 |

| | <u>Page</u> |
|--|-------------|
| V. <u>THE PRESENT PROBLEM</u> | 41 |
| Production of an O ₂ Free System .. | 41 |
| The Reaction between N and NO | 41 |
| VI. <u>EXPERIMENTAL</u> | 46 |
| Materials | 46 |
| Apparatus | 47 |
| Calibration of flowmeters F ₁ and F ₃ .. | 54 |
| Nitric oxide flowmeter F ₂ | 56 |
| Limitations of fast-flow systems .. | 58 |
| Production and measurement of oxygen atoms | 61 |
| Verification of the stoichiometry of the N - NO reaction | 65 |
| Alternative method for determining the oxygen-atom concentration | 68 |
| Integrated rate expressions for oxygen-atom recombination in the absence of O ₂ .. | 71 |
| VII. <u>RESULTS</u> | 74 |
| (i) Using ostensibly 'bone' dry nitrogen without further water vapour removal | 74 |
| (ii) Effect of water vapour on the homogeneous recombination rate | 83 |
| (iii) Efficiencies of various third bodies in the homogeneous recombination reaction | 83 |
| VIII. <u>DISCUSSION</u> | 89 |
| Heterogeneous recombination | 89 |
| Homogeneous recombination | 90 |
| Efficiencies of third bodies | 92 |
| Conclusions | 94 |
| <u>BIBLIOGRAPHY</u> | 97 |

| <u>PART II</u> | | <u>Page</u> |
|---|---------|-------------|
| I. <u>INTRODUCTION</u> | | 103 |
| Vibrational excitation of diatomic molecules | | 103 |
| Vibrational excitation produced by chemical reaction | | 106 |
| Vibrational excitation produced by electrical discharge | | 111 |
| The present problem | | 112 |
| II. <u>EXPERIMENTAL</u> | | 114 |
| Apparatus | | 114 |
| Operation of detector | | 114 |
| Preparation of the catalytic surface | | 119 |
| III. <u>RESULTS</u> | | 122 |
| Relaxation rate of N_2^* | | 130 |
| Magnitude of the energy of N_2^* | | 136 |
| Efficiency of molecules in deactivating N_2^* | | 138 |
| Examination of vibrationally excited N_2 produced by reaction of N and NO | | 149 |
| IV. <u>DISCUSSION</u> | | 157 |
| Vibrational relaxation times | | 158 |
| Temperature dependence of relaxation times | | 161 |
| Vibrational relaxation of nitrogen | | 161 |
| Effect of impurity on relaxation rate | | 162 |
| Energy distribution between the vibrational levels of nitrogen | | 166 |
| Excitation produced by the N/NO reaction | | 167 |
| <u>BIBLIOGRAPHY</u> | | 169 |

| | <u>Page</u> |
|--|-------------|
| <u>APPENDIX A</u> | 172 |
| <u>APPENDIX B</u> | 173 |
| <u>SUMMARY AND CONTRIBUTIONS TO KNOWLEDGE</u> .. | 180 |

PART I

THE RECOMBINATION OF ATOMIC OXYGEN
IN THE PRESENCE OF INERT GASES

I. INTRODUCTION

It is a rather sobering thought that advances in an increasing number of fields should depend for their stimulus on political and military need rather than purely academic interest.

While this is by no means generally true, the connection in certain cases, particularly the physical sciences, is very apparent.

Consider, for example, the reactions involving nitrogen and oxygen atoms. Research in this field dates back at least fifty years to Lord Rayleigh's studies of discharged nitrogen and also to the considerable amount of qualitative data obtained two or three decades ago by workers such as Harteck and Kopsch, Geib, Rodebush, etc.

Interest in this field was revived about 1950 and the increasingly rapid progress to the present day parallels, and can in part be traced to, the advent and development of the science of rocketry with its attendant concern with conditions in the upper atmosphere.

It is in an attempt to analyse the reactions and processes responsible for various radiative emissions from the upper atmosphere that has led to the laboratory study of the kinetics of dissociated and ionized atmospheric gases.

Since the major constituents of the atmosphere are nitrogen and oxygen, it might be assumed that such a system would be relatively uncomplicated. In fact the reverse is

true when cognizance is taken of the possible reactions of atoms, ions, and excited molecules not only with themselves but with species such as ozone and the oxides of nitrogen which are readily formed in primary reactions. (See for example 'The Threshold of Space' by M. Zelikoff, Pergamon Press, 1957.) This thesis then will be devoted to a very small section of this field, the apparently simple problem of the kinetics of oxygen atom recombination.

The first consideration in such an investigation is the choice of a suitable source of atom production.

II. PRODUCTION OF OXYGEN ATOMS

In its simplest terms, the production of gaseous atoms reduces to the problem of supplying energy in sufficiently large quantities to an undissociated gas.

In practice, the methods available can be divided into three main groups:

- (i) Photolytic dissociation
- (ii) Thermal dissociation
- (iii) Electrical dissociation.

(i) Photolytic dissociation

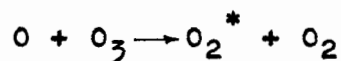
The following processes can all be realized by the action of solar radiation in the upper atmosphere⁽¹⁾:

| <u>Process</u> | <u>Spectral Region</u> |
|--|---|
| (a) $O_2 + h\nu \rightarrow O(^3P) + O(^1D)$ | Schumann-Runge continuum $\leq 1760 \text{ \AA}$ |
| (b) $O_2 + h\nu \rightarrow 2 O(^3P)$ | Herzberg continuum $\leq 2420 \text{ \AA}$ |
| (c) $O_3 + h\nu \rightarrow O_2 + O(^1D)$ | Hartley continuum $\leq 2550 \text{ \AA}$ |
| (d) $O_3 + h\nu \rightarrow O_2 + O(^3P)$ | Chappius continuum 6100 \AA |
| (e) $NO + h\nu \rightarrow N + O$ | 1900 \AA |
| (f) $NO + h\nu \rightarrow NO^+ + e; e + NO^+ \rightarrow N + O$ | Lyman α |
| (g) $NO_2 + h\nu \rightarrow NO + O$ | $\leq 3700 \text{ \AA}$ |
| (h) $N_2O + h\nu \rightarrow N_2 + O$ | $\leq 2000 \text{ \AA}$ |

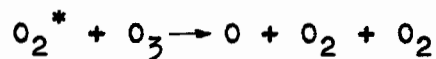
Of these processes (e), (f) and (g) can be eliminated as practical laboratory sources of oxygen atoms because of the concomitant production of other reactive species⁽²⁾.

The direct photo-dissociation of oxygen is difficult to achieve in practice since the regions of continuous absorption lie in the short ultra-violet where experimental difficulties abound. Kistiakowsky⁽³⁾, however, has been able to obtain about 1% dissociation of O₂ using 1860 Å and 1720 Å radiation.

The photolysis of ozone has been investigated by McGrath and Norrish^(4,4a). The energetic state of the oxygen atoms so produced, however, will depend on the spectral distribution of the illumination used to effect the dissociation. As a laboratory source of oxygen atoms, the system is further complicated by the production of substantial amounts of vibrationally excited O₂ in the secondary reaction



This vibrationally excited O₂ may effect further decomposition of the ozone by an energy chain mechanism



The direct photolysis of nitrous oxide has been examined by several workers^(5,6,7), but the production of quite large amounts of nitric oxide render the process unsuitable for kinetic studies. However, the mercury-sensitized photolysis of N₂O studied by Cvetanovic⁽⁸⁾ appears

to be considerably cleaner and has been successfully used by this author to examine the reactions of hydrocarbons with atomic oxygen. Unfortunately, for kinetic studies, the presence of variable amounts of mercuric oxides make the system somewhat unattractive.

(ii) Thermal dissociation

The objections raised against most of the photolytic dissociations are equally valid for thermal decompositions. That is, an oxygen atom source is required which is uncontaminated with other reactive molecular fragments.

In practice this reduces the field to the dissociation of ozone and oxygen.

(a) Thermal decomposition of ozone:

This process does not appear to have been utilized to any great extent as a source of oxygen atoms per se. However, the data obtained from studies of this system have been both extensive and very important in understanding the kinetics of oxygen atom recombination^(9,10,11,12). These results will be discussed subsequently.

(b) Thermal dissociation of oxygen:

In general, quite high temperatures are necessary to obtain appreciable dissociation of a gas into its constituent atoms depending, of course, to a large extent on the magnitude of the dissociation energy. This method is eminently satisfactory for the

dissociation of say sodium or chlorine but much less so for oxygen and nitrogen. In particular, thermal dissociation of oxygen, using a heated tungsten filament, is impossible because of the extremely rapid oxidation of the filament at the temperatures involved. The use of Nernst type 'glo bars' has been attempted to overcome this difficulty, but no significant dissociation was observed⁽¹³⁾.

However, the high temperatures necessary for dissociation of oxygen have been successfully obtained by the use of shock waves. In this method a shock wave is produced by the sudden rupture of a diaphragm separating a high pressure 'driver' gas from the low pressure gas which is to be dissociated. The resulting shock wave propagates through the low pressure gas with molecular velocity and results in a shock front across which temperature pressure and density change discontinuously. In this way temperatures of the order of 5000°K may be readily produced. This method is generally employed to determine the kinetics of the dissociation process by following the approach to equilibrium of the shocked gas. The method can therefore hardly be described as a source of atoms but, since the dissociation rate can be related to the recombination rate through the equilibrium

constant, it is capable of providing valuable kinetic data. A considerable amount of data in the dissociation of oxygen has been obtained in this way^(14,15,16,17,18,19,20).

(iii) Electrical dissociation

Electrical discharges are probably the most useful sources of atomic species.

The generally accepted mechanism of electrical dissociation⁽²¹⁾ involves as a primary step the production of electrons by ionizing collisions in the discharge. Dissociation may then follow by direct electron impact or by indirect processes. For example, a metastable particle may be formed in the initial electron-molecule encounter which dissociates on a secondary encounter with a neutral molecule. Alternatively, dissociation may result by initial ion formation followed by dissociative recombination of the positive ion with an electron.

The possibility that the dissociated gas may contain energetic species other than atoms can therefore not be ignored.

Types of discharge

(a) Low frequency discharges:

This type of discharge is exemplified by the Woods tube⁽²²⁾. In essence it is simply a U-shaped tube approximately one metre in length containing two cylindrical electrodes between which a low frequency (60 c.p.s.) high voltage (2 Kv) discharge

may be produced. The gas to be dissociated is led into the tube in the neighbourhood of the electrodes and withdrawn near the base of the U. For production of atomic oxygen, it can be operated on D.C. or low frequency A.C.⁽²³⁾. It is of interest to note that, for the production of atomic nitrogen, it has been found necessary to use an intermittent discharge in which strong electrical fields exist^(24,25). Although these low frequency discharges produce a high degree of dissociation, they suffer from the disadvantages inherent with an internal electrode system. The main disadvantage is that oxidation and sputtering of the electrodes can add unknown amounts of impurities such that kinetic studies may be almost completely vitiated.

(b) Radio frequency discharges:

As the name implies, these discharges operate at much higher frequencies (≈ 30 Mc) than the conventional A.C. discharges. This radio frequency energy can be fed into the gas by means of an external electrode system. The elimination of internal electrodes represents the most important single advantage of the system.

In practice the radio frequency energy is fed into the gas by either capacitative or inductive coupling. For efficient transfer of energy to the gas, it is necessary to reduce dielectric losses in

the discharge tube walls. Such losses not only represent wasted power but, in some cases (e.g. Pyrex), the dielectric heating may even melt the discharge tube which necessitates the use of air blast cooling. Alternatively, quartz discharge tubes may be used. Well-designed radio frequency discharges have been described in the literature^(26,27).

(c) Microwave discharges:

The present widespread use of microwave discharges resulted from the development during World War II of a powerful source of microwave energy - the magnetron.

Commercial magnetron oscillators are now available which can produce continuous wave energy in the thousands of megacycles range with output energies of up to 1000 watts. Initially the microwave generator was used to dissociate hydrogen^(28,29). Subsequently, Broida et al.⁽³⁰⁾ utilized the microwave discharge for dissociating nitrogen and oxygen. In addition to the advantages of the radio frequency discharge, the much shorter wavelength of the microwave radiation results in a more sharply-defined discharge region. Furthermore, the ease of coupling is such that a satisfactory discharge can be obtained by using a commercial diathermy unit with its director contiguous to a discharge

tube, although higher efficiency may be obtained by the use of correctly designed wave guides⁽³¹⁾. The energy fed into the discharge can be controlled in the commercial units by variation of the output power. Alternatively, a water attenuator may be lowered into the resonance cavity of the wave guide⁽³²⁾.

III. MEASUREMENT OF OXYGEN ATOM CONCENTRATION

There are numerous ways of determining oxygen atom concentrations depending upon the type of system employed. Methods of limited utility, as exemplified by indirect density measurements behind shock fronts^(15,18), will not be presently discussed. However, there are five more widely applicable methods for determining oxygen atom concentrations which are particularly suited for use in fast flow systems.

(1) Catalytic probes

The mode of action of all such probes is basically similar. A catalytic surface, capable of recombining all or part of the atoms, is introduced into the dissociated gas stream. The rate of liberation of heat to the probe is then a function of the atomic flow rate.

Harteck and Kopsch⁽³³⁾ described such a probe as long ago as 1931. They used a fine coil of platinum wire which was heated to incandescence by atom recombination. The temperature of the probe (determined by an optical pyrometer) was then taken as a measure of the atom concentration.

This method of temperature rise, due to atom recombination, has also been utilized by Linnett and Marsden⁽³⁴⁾ and by Greaves and Linnett⁽³⁵⁾. These workers used copper-constantan thermocouple probes whose junctions were coated with silver peroxide⁽³⁶⁾. The resulting E.M.F. was taken as a measure of the oxygen atom concentration.

This E.M.F. was later shown by Greaves and Linnett⁽³⁷⁾ to be proportional to the atom concentration as determined by a Wrede-Harteck gauge^(38,39).

It will be appreciated that such probes are capable of yielding relative measurements only, since the temperature rise is a function of

- (a) the efficiency of the probe for recombination,
- (b) the thermal capacity of the probe and gas stream,
- (c) the radiative efficiency of the probe.

Instead of measuring the temperature rise of such a probe, Tollefson and Le Roy⁽⁴⁰⁾ eliminated factors (b) and (c) by using a filament through which a current was passed. In the presence of the atomic species (in their case hydrogen atoms) this current was reduced sufficiently to retain the filament at its original temperature. When operated in this isothermal mode, the heat liberated by atom recombination can be directly equated to the reduction of electrical power supplied to the filament.

This technique has been modified and improved by Schiff and co-workers⁽⁴¹⁾ for absolute oxygen atom concentration measurements by ensuring that all the atoms are recombined rather than an unknown fraction.

The most important fault to be found in these probes lies in their lack of specificity. It is obvious that any excited species capable of deactivation on the probe surface will lead to a spuriously high atom concentration. For example, it has been shown that a microwave discharge in

oxygen produces, in addition to ground state atoms, a significant amount (10 - 20%) of electronically excited ($^1\Delta_g$) oxygen molecules^(42,43a). Furthermore, the presence of vibrationally excited molecules cannot be excluded. This lack of specificity has been noted by Elias, Ogryzlo and Schiff⁽⁴¹⁾ who found oxygen atom concentrations determined by such a probe to be 10% greater than indicated by a Wrede-Harteck gauge and 25% greater than indicated by the NO₂ titration⁽³²⁾.

It is therefore evident that these probes must be used with caution unless it is known unequivocally that only a single energetic species is present in the gas stream.

(11) Wrede-Harteck gauges

These gauges, developed by Wrede⁽³⁹⁾ and Harteck⁽³⁸⁾ in 1928, utilize the difference in effusion rates of atoms and their parent molecules through an aperture whose dimensions are small compared with the mean free paths of the particles. They are capable of absolute atom concentration measurements and, more important, are sensitive only to atomic species.

A small chamber is put in contact with the dissociated gas by means of a small aperture. Inside this chamber is placed a piece of catalytic material capable of recombining the atoms so that atoms and molecules diffuse into the chamber but only molecules diffuse out. The condition of no net mass transfer across the orifice thus leads to a pressure differential, ΔP , which for diatomic molecules can easily be shown to be related to α , the

fractional concentration of atoms in the gas stream, by

$$\alpha = \frac{2}{2 - \sqrt{2}} \left(\frac{\Delta P}{P} \frac{T(C)}{T(G)} + 1 - \frac{T(C)}{T(G)} \right)$$

where $T(C)$ = temperature of gas inside the chamber.

$T(G)$ = temperature of the main gas stream.

P = pressure of the main gas stream.

Provided there is no temperature gradient across the orifice, this reduces to

$$\alpha = \frac{\Delta P}{P} \frac{2}{2 - \sqrt{2}}$$

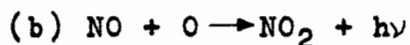
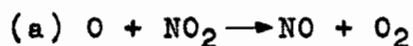
The disadvantages associated with this gauge are mainly operational. Perhaps the most exacting condition to be met is the reduction of temperature gradients produced by recombination inside the chamber.

The original design has been modified by several workers in efforts to reduce the long equilibration times involved^(44,45,37). A recent publication by Sharpless, Young and Clark⁽⁴⁶⁾ illustrates very well the complexity and precision required in these gauges if accurate determinations are required.

(iii) Nitrogen dioxide titration

Spealman and Rodebush⁽⁴⁷⁾ investigated the reaction between oxygen atoms and nitrogen dioxide in 1935.

The mechanism is now fairly well established as



This reaction sequence has been used by Kaufman⁽³²⁾ as a titration technique to determine oxygen-atom concentrations in fast flow system.

Provided reaction (a) is much faster than either (b) or (c), it can be seen that addition of NO_2 to an oxygen-atom stream will result in the rapid consumption of an equivalent amount of oxygen atoms and the concomitant production of an equal amount of nitric oxide. This nitric oxide then reacts comparatively slowly via reactions (b) and (c) to emit radiation. The intensity of this radiation has been shown to be proportional to both the oxygen atom concentration and the nitric oxide concentration⁽³²⁾. Thus addition of nitrogen dioxide to an oxygen-atom stream will result in a light intensity immediately below the mixing point given by

$$I = C(\text{NO})(\text{O})$$

where for convenience (NO) and (O) represent flow rates rather than concentrations.

$$\begin{aligned} \text{However } (\text{NO}) &= \text{molar flow rate of } \text{NO}_2 \text{ consumed} \\ &= (\text{NO}_2)_o \end{aligned}$$

$$\begin{aligned} (\text{O}) &= \text{residual oxygen-atom flow after} \\ &\quad \text{partial consumption by } \text{NO}_2 \\ &= (\text{O})_o - (\text{NO}_2)_o \end{aligned}$$

$$\text{Therefore } I = C(\text{NO}_2)_o \left((\text{O})_o - (\text{NO}_2)_o \right)$$

The emitted light intensity, I , will therefore be zero when $(\text{NO}_2)_o = 0$ (trivial case) or when $(\text{NO}_2)_o = (\text{O})_o$.

Differentiation of the last equation with respect to $(\text{NO}_2)_0$ further shows that I will be a maximum when

$$(\text{NO}_2)_0 = \frac{1}{2}(\text{O})_0$$

Either of these two conditions can be, and have been, used to determine oxygen-atom flow rates, and hence concentrations, in dissociated oxygen flow streams. Kaufman favours the former, using the condition $I = 0$ as the end-point for the titration.

A modification of the method, using the latter condition, has been employed by Reeves, Manella and Harteck⁽⁴⁸⁾.

These workers add sufficient NO_2 to achieve the condition of maximum light intensity, i.e. $(\text{NO}_2)_0 = \frac{1}{2}(\text{O})_0$. The nitrogen dioxide was then shut off and replaced by nitric oxide until the same intensity was obtained. It is easily seen from $I = C(\text{NO}_2)_0 \left((\text{O})_0 - (\text{NO}_2)_0 \right)$ that

$$I_{\max}(\text{NO}_2) = C \frac{1}{4}(\text{O})_0^2$$

and that

$$I(\text{NO}) = C(\text{NO})_0(\text{O})_0$$

Equating these expressions gives

$$(\text{NO})_0 = \frac{1}{4}(\text{O})_0$$

The advantage claimed by these workers lies in the elimination of the need for determining the NO_2 flow. Since NO_2 is less easily monitored than NO because of its corrosive nature and partial dimerization to N_2O_4 , this is certainly advantageous but it must also be weighed against the disadvantage of determining a much smaller flow rate. For very low atom flow rates this disadvantage can become very important. This

technique is also much more time-consuming than the direct titration.

An alternative method successfully employed by Elias⁽¹³⁾ involves adding an excess of NO_2 such that the oxygen atoms are quantitatively converted to NO . The nitric oxide thus formed is then trapped out downstream during a known time interval and subsequently determined by oxidation to NO_2 . Although this method is time consuming, it does eliminate the difficulty of accurately determining flow rates of nitrogen dioxide.

(iv) Electron spin resonance

This comparatively new technique for determining oxygen-atom concentrations⁽⁴⁹⁾ has the advantage that it is highly specific and furthermore can distinguish between different electronic states of the atom. However, for kinetic measurements, it has several disadvantages:

(i) High cost and complexity.

(ii) It measures a space average concentration over the length of the flow tube within the resonance cavity and thus the spatial resolution is poor.

(iii) Calculations of absolute concentrations are difficult since the signal is a function of a large number of system and instrumental parameters. In practice the instrument has to be calibrated independently.

(v) Mass spectrometric methods

While the mass spectrometer is capable of yielding

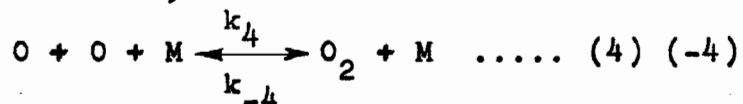
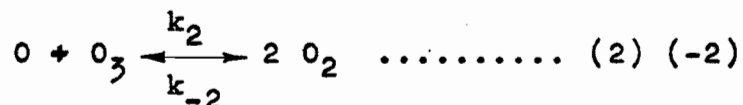
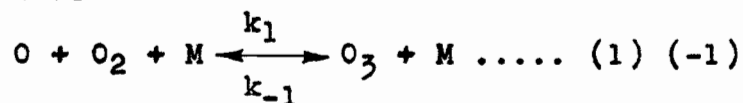
unequivocal evidence for the presence of atomic species, its use in kinetic studies has several limitations.

- (i) High cost and complexity.
- (ii) Although it can sample from a well-defined position in the flow stream, i.e. good spatial resolution, this sampling point is fixed and it can be difficult to vary the reaction time.
- (iii) The sometimes large and variable amount of recombination taking place within the ion source renders imperative an independent calibration. Nevertheless the instrument has been used with some success in determining both atomic nitrogen and atomic oxygen concentrations in partially dissociated gas streams^(43,43a).

IV KINETICS OF OXYGEN-ATOM RECOMBINATION

Reaction Mechanism

In any system containing both oxygen atoms and oxygen molecules, cognizance must be taken of at least the following reactions:



where M represents any molecule in the gas, i.e. O₂, O₃ or O.

Under certain conditions there is also the possibility of heterogeneous recombination which can be represented by



This is the simplest possible set of reactions capable of describing the mechanism of oxygen-atom recombination. Furthermore, because of the reversibility of reactions (1), (2) and (3), it should also be adequate to describe the mechanism of the thermal decomposition of ozone.

Before any evidence for these reactions is introduced, consider first the thermodynamic features of this system.

From the heats of reaction of the steps outlined above in conjunction with a knowledge of the heat capacities

and free energies of the various components, it is possible to calculate the equilibrium constants involved in the above mechanism.

Campbell and Nudelman⁽⁵⁰⁾ have derived an expression for the equilibrium constant as a function of temperature for the i^{th} reaction in the form

$$K_i(T) = d_i T^{e_i} \exp\left(-\frac{\theta_i}{T} + \sum_{l>1} b_{il} T^l\right)$$

and have computed the values of d_i , e_i , b_{il} and θ_i for the reactions (1) through (4) (see Appendix A).

Evaluations of these equilibrium constants at $T = 300^\circ\text{K}$ yield

$$K_1 = 2.30 \times 10^{16} \text{ cm}^3 \text{ mole}^{-1}$$

$$K_2 = 4.96 \times 10^{68}$$

$$K_3 = 2.55 \times 10^{52}$$

$$K_4 = 1.10 \times 10^{85} \text{ cm}^3 \text{ mole}^{-1}$$

Consider a system of equimolar concentrations of ozone and oxygen with a total pressure of 4 cm Hg at 300°K . The concentration of ozone and oxygen is thus approximately 10^{-6} moles cm^{-3} . The relative rates of (3) and (-3) are therefore

$$\frac{\text{Rate of (3)}}{\text{Rate of (-3)}} = \frac{k_3 [O_3]^2}{k_{-3} [O_2]^3} = \frac{2.55 \times 10^{52} \times 10^{-12}}{10^{-18}} = 2.55 \times 10^{58}$$

The final equilibrium concentration of ozone is approximately 10^{-71} mole cm^{-3} .

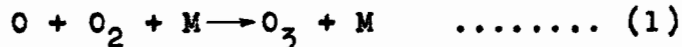
Since ozone can be stored indefinitely at these

temperatures provided no oxygen atoms are present, it is apparent that reaction (3) must be extremely slow. Therefore both (3) and (-3) can be set equal to zero without undue error.

Similar considerations show that reaction (1) is approximately 10^{10} times faster than (-1) for equimolar concentrations of oxygen atoms and ozone at 4 cm Hg pressure.

Reactions (-2) and (-4) are also vanishingly small compared with their respective forward reactions under these conditions.

Thus the kinetics of oxygen-atom recombination at moderate temperatures and pressures can be simplified to the following reactions:



Thermal Decomposition of Ozone

A considerable amount of information concerning the above reactions has been obtained by studying the kinetics of ozone decomposition at somewhat elevated temperatures.

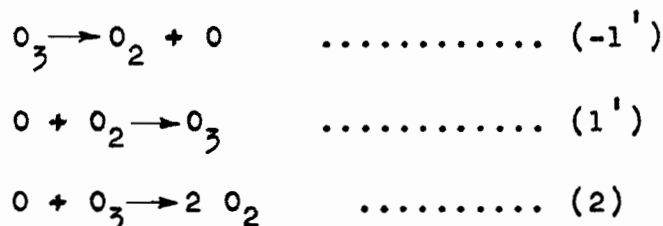
The many early investigations of the thermal decomposition of ozone conflicted drastically concerning the relative importance of homogeneous and heterogeneous

decomposition and also upon the relative significance of various homogeneous reactions⁽⁵¹⁻⁵⁷⁾. Prior to the work of Schumacher et al.^(58,58a), these erratic results were probably due to heterogeneous catalysis by stopcock grease⁽⁵⁹⁾ and other impurities. Benson and Axworthy⁽¹⁰⁾ have shown that the decomposition is extremely sensitive to homogeneous and heterogeneous catalysis by a wide variety of substances.

The most commonly accepted mechanism for ozone decomposition is the modification of the Jahn mechanism⁽⁵⁵⁾ due to Benson and Axworthy⁽¹⁰⁾. Jahn found that the rate of disappearance of ozone in dilute O₃/O₂ mixtures could be represented by

$$-\frac{d[O_3]}{dt} = k_{obs} \frac{[O_3]^2}{[O_2]}$$

and he proposed the following mechanism



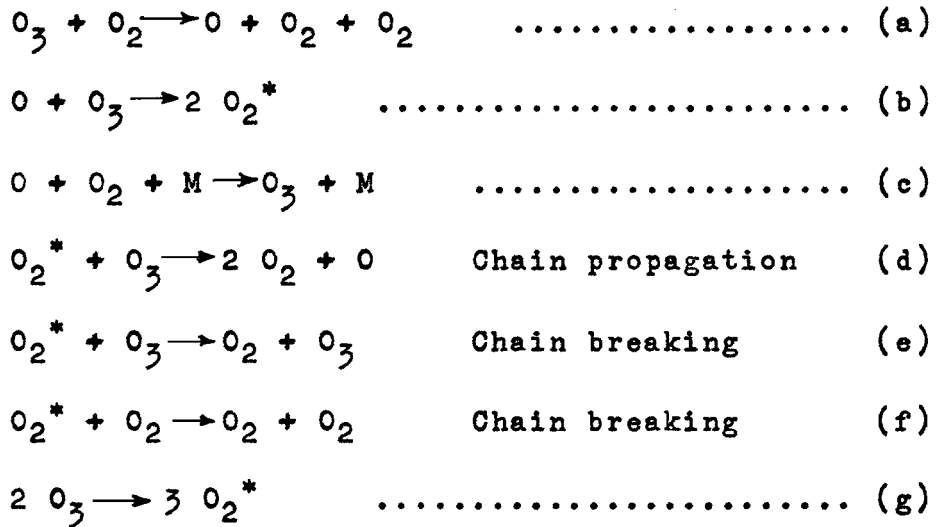
Assumption of a steady-state concentration for oxygen atoms leads to the following expression

$$-\frac{d[O_3]}{dt} = \frac{2k_2 k_{-1}' [O_3]^2}{k_1' [O_2] + k_2 [O_3]}$$

To fit the experimental rate law requires the ozone to be sufficiently dilute such that $k_2 [O_3] \ll k_1' [O_2]$.

Such a mechanism will always predict a decrease in rate on addition of oxygen. However, Glissman and

Schumacher⁽⁵⁸⁾ found that the rate was increased by adding oxygen, provided the ozone concentration was sufficiently high. This led them to propose the following energy chain mechanism:



In the above mechanism, the asterisk represents an energetically excited species. This mechanism leads to the following rate expression based upon steady-state concentrations for both O_2^* and O .⁽⁵⁰⁾

$$- \frac{d[\text{O}_3]}{dt} = k_g [\text{O}_3]^2 + \frac{2k_b [\text{O}_2] [\text{O}] \left(1 + \frac{k_c}{k_d} + \frac{k_f}{k_d} \frac{[\text{O}_2]}{[\text{O}_3]} \right) + 3k_g [\text{O}_3]^2}{\frac{k_c}{k_d} \frac{[\text{O}_2] [\text{M}]}{[\text{O}_3]} \left(1 + \frac{k_c}{k_d} + \frac{k_f}{k_d} \frac{[\text{O}_2]}{[\text{O}_3]} \right) - 1 + \frac{k_c}{k_d} + \frac{k_f}{k_d} \frac{[\text{O}_2]}{[\text{O}_3]}}$$

This rather cumbersome expression is obviously difficult to test experimentally. It should be noted, however, that for concentrated ozone, i.e. $[\text{O}_2] = 0$, it successfully predicts the observed second order decay of ozone

$$- \frac{d[\text{O}_3]}{dt} = k_g [\text{O}_3]^2 \left(1 - \frac{3k_d}{k_d - k_c} \right) \quad [\text{O}_2] = 0$$

The importance of energy chains has been challenged by Benson and Axworthy⁽¹⁰⁾ who have been able to correlate both their own data and those of Glissman and Schumacher, using the following simple mechanism:



A steady-state assumption for $[O]$ then yields

$$-\frac{d[O_3]}{dt} = \frac{2k_2 k_{-1} [O_3]^2 \sum a_m [M]}{k_2 [O_3] + k_1 [O_2] \sum a_m [M]}$$

where $[M]$ is the concentration of any particular third body (O_2 , O_3 or O) and a_m its efficiency relative to O_3 .

As $[O_2]$ tends to zero, this expression also yields a second decay for ozone

$$-\frac{d[O_3]}{dt} = 2k_{-1} [O_3]^2 \quad [O_2] = 0$$

but the observed second order rate constant is attributed to a different reaction than that of Glissman and Schumacher.

The various rate constants and efficiencies obtained by Benson and Axworthy from their own data and that of Glissman and Schumacher are as follows:

$$k_{-1}(M = O_3) = (4.61 \pm 0.25) \times 10^{15} \exp(-24,000/RT) \text{ cm}^3 \text{ mole}^{-1} \text{ sec}^{-1}$$

$$k_1(M = O_3) = 6.00 \times 10^{13} \exp(600/RT) \text{ cm}^6 \text{ mole}^{-2} \text{ sec}^{-1}$$

$$k_2 = 2.96 \times 10^{13} \exp(-6,000/RT) \text{ cm}^3 \text{ mole}^{-1} \text{ sec}^{-1}$$

with efficiencies of various third bodies of

$$a_{O_3} = 1 \quad a_{O_2} = 0.44 \quad a_{N_2} = 0.41 \quad a_{CO_2} = 1.06 \quad a_{He} = 0.34$$

More recent data have also been interpreted on the basis of the Benson and Axworthy mechanism.

Zaslowsky et al. (11,11a,11b) working with concentrated ozone have reported the following values:

$$k_{-1} = 8 \times 10^{15} \exp(-24,300/RT) \text{ cm}^3 \text{ mole}^{-1} \text{ sec}^{-1}$$

$$k_1(M = O_3) = 2.57 \times 10^{14} \exp(-300/RT) \text{ cm}^6 \text{ mole}^{-2} \text{ sec}^{-1}$$

$$k_1(M = O_2) = 1.44 \times 10^{14} \exp(-300/RT) \text{ cm}^6 \text{ mole}^{-2} \text{ sec}^{-1}$$

$$k_2 = 426 \times 10^{12} \exp(-3,200/RT) \text{ cm}^3 \text{ mole}^{-1} \text{ sec}^{-1}$$

Jones and Davidson⁽¹²⁾ have studied the decomposition of ozone in shock pyrolyzed ozone-nitrogen and ozone-argon mixtures. They also used the Benson and Axworthy mechanism with the simplifying assumption that reaction (1) is negligible in comparison with (-1) at the shock temperature (700 - 900°K).

They report the following values:

$$k_{-1} = (5.0 \pm 0.5) \times 10^{14} \exp(-23,000/RT) \text{ cm}^3 \text{ mole}^{-1} \text{ sec}^{-1}$$

$$k_1 = (8.9 \pm 0.9) \times 10^{12} \exp(-11,800 \pm 400)/RT \text{ cm}^6 \text{ mole}^{-2} \text{ sec}^{-1}$$

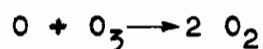
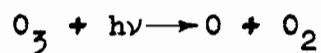
$$k_2 = (3.0 \pm 0.3) \times 10^{13} \exp(-6,000 \pm 700)/RT \text{ cm}^3 \text{ mole}^{-2} \text{ sec}^{-1}$$

The possibility of the participation of energy chains in the thermal decomposition of ozone has been the subject of some controversy. For example, it is of interest to note that Benson and Axworthy's mechanism shows signs of breaking down at high decomposition rates ($> 10^{-9}$ moles $\text{cm}^{-3} \text{ sec}^{-1}$). These authors have considered the possibility of

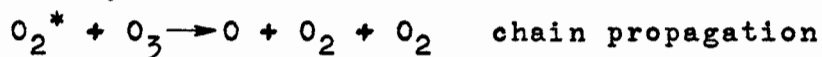
this being due to the participation of an energy chain but have rejected this explanation in favour of temperature gradients set up by the high decomposition rate.

Evidence in favour of energy chains has been put forward by Schumacher et al. (60,61) from studies of the photolytic decomposition of ozone.

If the photolytic mechanism was simply



one would not expect a quantum yield greater than two. However, experiments with both red⁽⁶⁰⁾ and ultra-violet light⁽⁶¹⁾ indicate quantum yields greater than two. This can only be explained by an energy chain mechanism of the type



where O_2^* has sufficient energy to participate in the chain propagation step.

Evidence supporting this mechanism has been obtained by McGrath and Norrish⁽⁴⁾ who found that photolysis of ozone with short wavelength radiation produced substantial quantities of vibrationally excited O_2 with an energy spectrum peaked at the thirteenth level. On purely energetic grounds, this energy chain could be initiated by either $O(^3P)$ or $O(^1D)$. However, these authors showed subsequently^(4a) that, while $O(^1D)$ atoms did indeed initiate

an energy chain, the ground state $O(^3P)$ did not.

This finding of course casts doubt on the results of photolysis with red light obtained by Schumacher, since at these wavelengths the primary photolytic step produces only $O(^3P)$.

Other workers^(12,61a,61b) have subsequently confirmed the non-existence of energy chains in the thermal decomposition of ozone. In spite of these data, Schumacher has remained unconvinced and has engaged in a lengthy controversy with Benson on this point^(62,63).

Very recently, however, Schumacher^(62a) has reinvestigated the photolytic decomposition of ozone at long wavelengths and now finds no evidence for a quantum yield greater than two, and has expressed his agreement with Benson on the non-existence of energy chains in the thermal decomposition of ozone.

Direct Measurement of Oxygen-Atom Recombination

In general, oxygen atom recombination has been studied in fast flow systems at quite low pressures (< 5 mm Hg). In such systems the ozone concentration is very low (vide infra) and hence reaction (4) could be expected to become competitive with (1) and (2) in the removal of oxygen atoms. Furthermore, since flow systems employ relatively narrow flow tubes, the surface to volume ratio of the reaction tube may become large enough to render important the effects of heterogeneous recombination.

Heterogeneous Recombination of Oxygen Atoms

Linnett and Marsden⁽³⁴⁾ and Greaves and Linnett^(35,37,64,65) have measured the rate of heterogeneous recombination for a wide variety of materials. They have found in general that the process is first order in oxygen atoms and can be represented by



The first order rate constant so obtained will be a function both of the efficiency of the walls for recombination and the geometry of the reaction vessel. A more meaningful number is the recombination coefficient defined as the fraction of the collisions which lead to recombination.

Kinetic theory shows that the number of collisions per unit area of a surface per second is given by

$$\text{No. of collisions} = [N] \frac{\bar{c}}{4} \text{ cm}^{-2} \text{ sec}^{-1}$$

where $[N]$ = concentration in particles cm^{-3}

\bar{c} = average velocity of particles.

Therefore the total number of collisions per second = $[N] \frac{\bar{c}}{4} A$

where A = surface area of vessel.

Therefore the number of particles disappearing per second =

$$\gamma [N] \frac{\bar{c}}{4} A.$$

Experimentally $-\frac{d[N]}{dt} = k_5 [N]$

Therefore the number of particles disappearing per second =

$$- V \frac{d[N]}{dt} = k_5 [N] V$$

where V = volume of reaction vessel.

$$\text{Thus } \gamma = \frac{4k_5}{\bar{c}} \cdot \frac{V}{A}$$

For a cylindrical vessel of radius r , $V/A = r/2$

$$\text{Therefore } \gamma = \frac{2k_5 r}{\bar{c}}$$

The above workers determined γ by measuring the concentration gradient produced by diffusive flow down a closed side-arm under pressure conditions low enough that homogeneous decay by reactions (1), (2) and (4) could be neglected in comparison with heterogeneous decay by reaction (5). This method is essentially that due to Smith⁽⁶⁶⁾.

Other investigators^(67,68) using different techniques have also obtained values of γ for some of the materials investigated by Linnett et al.

In general, the lack of agreement is quite pronounced both in absolute magnitudes and in the temperature dependence⁽⁶⁸⁾. This lack of agreement is demonstrated in the following table which lists published values of γ for Pyrex glass.

Table I

| Worker | γ | Ref. |
|--------------------------------|-----------------------|------|
| Kaufman | 2×10^{-5} | (32) |
| Herron and Schiff | 1.1×10^{-4} | (43) |
| Elias, Ogryzlo and Schiff | 7.7×10^{-5} | (41) |
| Harteck, Reeves and Manella | $10^{-6} - 10^{-7}$ * | (69) |
| Kretschmer | 5×10^{-6} * | (70) |
| Hacker, Marshall and Steinberg | 4.0×10^{-5} | (71) |

*Pyrex coated with phosphoric acid.

It is thus apparent that heterogeneous recombination is very dependent on the history of the surface.

Homogeneous Recombination of Oxygen Atoms

It has been found experimentally by a number of workers (72,41,32,71) that the recombination of oxygen atoms in the presence of a relatively large excess of O₂ (80 - 90%) is first order in oxygen atoms. This has led to the following assumptions.

(a) The reaction $O + O + M \rightarrow O_2 + M$ is negligible compared with recombination via reactions (1), (2) and (5).

(b) Reaction (2) is sufficiently fast compared with (1) that the ozone obeys the steady state condition

$$-\frac{d[O_3]}{dt} = 0.$$

These assumptions lead immediately to the following differential rate expression

$$-\frac{d[O]}{dt} = 2k_1 [O] [O_2] [M] + k_5 [O]$$

Provided $[O] \ll [O_2]$ the concentration of O₂ will remain essentially constant and the first order kinetics follow immediately

$$-\frac{d[O]}{dt} = k_{obs} [O]$$

$$\text{where } k_{obs} = 2k_1 [O_2] [M] + k_5$$

A number of techniques have been employed to follow the oxygen-atom concentration in these experiments. Table II on P. 31 lists the values obtained for k₁ interpreted on the basis of the above mechanism with M = O₂.

Table II

| Worker | Method | $k_1 \times 10^{-14}$ $\text{cm}^6 \text{mole}^{-2}$ sec^{-1} at 300°K |
|---|----------------------------------|---|
| Kaufman ⁽³²⁾ | Air afterglow | 2.0 |
| Elias, Ogryzlo & Schiff ⁽⁴¹⁾ | Catalytic probe | 1.0 |
| Harteck and Reeves ⁽⁷³⁾ | Air afterglow | 2.2 |
| Hacker, Marshall and Steinberg ⁽⁷¹⁾ | E.P.R. and Catalytic probe | 2.5 |
| Kretschmer and Petersen ⁽⁷⁴⁾ | Air afterglow (Static system) | 1.1 ($T \approx 350^\circ\text{K}$) |

For comparison, the thermal decomposition of ozone (vide supra) yields the following values of k_1 evaluated at 300°K .

| <u>Worker</u> | <u>$k_1 \times 10^{-14} \text{ cm}^6 \text{ mole}^{-2} \text{ sec}^{-1}$</u> |
|-------------------------------------|---|
| Benson and Axworthy ⁽¹⁰⁾ | 0.73 |
| Jones and Davidson ⁽¹²⁾ | 1.9 |
| Zaslowsky et al. ⁽¹¹⁾ | 0.86 |

Kaufman⁽⁶⁸⁾ has since expressed the opinion that k_1 must be less than $2.0 \times 10^{14} \text{ cm}^6 \text{ mole}^{-2} \text{ sec}^{-1}$ and has presented data which favour a value of $0.7 \times 10^{14} \text{ cm}^6 \text{ mole}^{-2} \text{ sec}^{-1}$.

The temperature dependence of k_1 appears to be quite small. Benson and Axworthy report a negative Arrhenius activation energy of 600 cal; Jones and Davidson

a negative energy of 1800 ± 400 , and Zaslowsky et al. a positive activation energy of 300 cal.

The simplifying assumptions invoked in the interpretation of oxygen-atom recombination deserve a closer scrutiny.

Assumption (b) above requires that the steady state concentration of ozone be

$$[\text{O}_3]_{\text{s.s.}} = \frac{k_1}{k_2} [\text{O}_2] [\text{M}] \approx \frac{k_1}{k_2} [\text{O}_2]^2$$

Using $k_1 = 1 \times 10^{14} \text{ cm}^6 \text{ mole}^{-2} \text{ sec}^{-1}$ and $k_2 = 1.3 \times 10^9 \text{ cm}^3 \text{ mole}^{-1} \text{ sec}^{-1}$ (10) implies that

$$[\text{O}_3]_{\text{s.s.}} = 7.7 \times 10^4 [\text{O}_2]^2$$

Thus for an O_2 concentration of $1 \times 10^{-7} \text{ mole cm}^{-3}$ at 300°K ($\approx 1.9 \text{ mm Hg}$) the steady state ozone concentration should be 0.77% of the O_2 concentration.

However, Schiff and Herron⁽⁴³⁾ were unable to detect ozone mass spectrometrically in the concentrations required by the above expression. This implies that either k_1 must be considerably smaller than $1 \times 10^{14} \text{ cm}^6 \text{ mole}^{-2} \text{ sec}^{-1}$ or conversely that k_2 must be considerably larger than $1.3 \times 10^9 \text{ cm}^3 \text{ mole}^{-1} \text{ sec}^{-1}$. This latter alternative is borne out by the value of $2 \times 10^{10} \text{ cm}^3 \text{ mole}^{-1} \text{ sec}^{-1}$ obtained for k_2 by Zaslowsky et al.^(11a,11b) and the value of $1.5 \times 10^{10} \text{ cm}^3 \text{ mole}^{-1} \text{ sec}^{-1}$ reported for k_2 by Schiff and Phillips⁽⁷⁵⁾.

Assumption (a), however, cannot be so readily justified. The criterion of linear logarithmic plots of

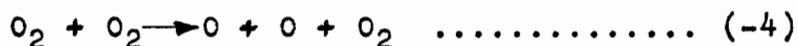
oxygen-atom concentration as a function of time has been invoked by Kretschmer and Petersen⁽⁷⁴⁾ and by Elias, Ogryzlo and Schiff⁽⁴¹⁾ to put upper limits on k_4 of $2 \times 10^{14} \text{ cm}^6 \text{ mole}^{-2} \text{ sec}^{-1}$ and $4 \times 10^{14} \text{ cm}^6 \text{ mole}^{-2} \text{ sec}^{-1}$ respectively. The insensitivity of logarithmic plots is such that k_4 could be much larger than these estimates without introducing noticeable curvature into the first order plot.

It is therefore imperative that k_4 be determined independently, not only for its own sake but because it could lead to a re-evaluation of k_1 .

Shock Tube Measurements of the Second Order Recombination

To date most of the information regarding the direct second order recombination of oxygen atoms has been obtained from shock tube data.

Matthews⁽¹⁷⁾ and Byron⁽¹⁸⁾ have both examined the rate of dissociation of O_2 by shock wave heating of oxygen and oxygen/argon mixtures in which they measured the rate of attainment of the equilibrium density behind the shock front. From these data it is possible to calculate the rate constant for the process



The rate constant, k_{-4} , can then be related to k_4 via the equilibrium constant.

For this method to yield meaningful values of k_4 at temperatures outside the experimental range (3000-5000°K) requires a very accurate determination of the temperature

dependence of k_{-4} .

Fowler and Guggenheim⁽⁷⁶⁾ have derived the following expression for a bimolecular rate constant

$$k = 2\rho\sigma_{1,2}^2 \left(\frac{2\pi RT}{M}\right)^{\frac{1}{2}} e^{-E^*/RT} \sum_{y=0}^{\frac{1}{2}t+1} \frac{1}{\Gamma(y+1)} \left(\frac{E^*}{RT}\right)^y$$

where E^* = minimum energy required for reaction,

ρ = probability of collision between molecules with energy E^* will lead to reaction,

M = reduced mass of collision pair,

$\sigma_{1,2}$ = collision diameter.

This expression assumes that the energy in t square terms (rotational and vibrational) plus three translational square terms can all contribute to the reaction. If the energy in s vibrational and r rotational nodes can contribute, then $t = 2s + r$, since each vibration contributes two square terms.

If the energy $E^* \gg \frac{1}{2}tRT$, the summation in the above expression may be replaced by the last term. In addition, if $\frac{1}{2}t$ is integral, the expression becomes

$$k = 2\rho\sigma_{1,2}^2 \left(\frac{2\pi RT}{M}\right)^{\frac{1}{2}} \frac{1}{(\frac{1}{2}t+1)!} \left(\frac{E^*}{RT}\right)^{\frac{1}{2}t+1} \exp\left(-\frac{E^*}{RT}\right)$$

Alternatively, if one assumes that only one translational square term (along the line of centres) can contribute to E^* , then t must be replaced by $t - 2$. The expression then becomes

$$k = 2\rho\sigma_{1,2}^2 \left(\frac{2\pi RT}{M}\right)^{\frac{1}{2}} \frac{1}{(\frac{1}{2}t)!} \left(\frac{E^*}{RT}\right)^{\frac{1}{2}t} \exp\left(-\frac{E^*}{RT}\right)$$

Either of these two expressions can be used to express k_{-4} in the form

$$k_{-4} = p_0 T^{\frac{1}{2}} \left(\frac{D}{RT} \right)^n \exp(-D/RT)$$

where D = dissociation energy of O_2 .

Matthews⁽¹⁷⁾ favours $n = \frac{1}{2}t + 1$ (three translational degrees of freedom) with $t = 4$ (one vibration and two rotations) i.e. $n = 3$.

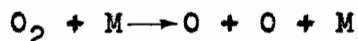
His experimental data between 3000 - 5000°K can then be fitted by

$$k_{-4} = p 7.43 \times 10^{11} T^{\frac{1}{2}} \left(\frac{59380}{T} \right)^3 \exp(-59380/T)$$

with $p = 0.073$.

However, he also mentions that the data are consistent with $n = 2$ and $p = 0.35$.

Byron⁽¹⁸⁾ used a similar expression for k_{-4} except that he considered the possibility of reactions such as



where $M = O, O_2$ and Ar .

His overall rate constant $k_{-4}(\text{obs})$ therefore has the form

$$k_{-4}(\text{obs}) = C' T^{\frac{1}{2}} \left(\frac{\sum p_M}{(n_M)} \left(\frac{D}{RT} \right)^{n_M} \right) \exp \left(- \frac{D}{RT} \right)$$

In addition, he favours the contribution of only one translational square term. The numerical values obtained by Byron for p_M and n_M are:

| M | $\frac{n_M(-\frac{1}{2}t)}{M}$ | P_M |
|----------------|--------------------------------|-------|
| O ₂ | 2.00 | 0.24 |
| A | 1.00 | 0.10 |
| O | 1.00 | 1.7 |

The P_M 's of course give the relative efficiencies of the various collision partners in reaction (-4).

It is apparent from the magnitude of the activation energy of reaction (-4) that the pre-exponential temperature dependence of k_{-4} is completely overshadowed by the exponential temperature dependence, and n can be varied within wide limits and still be capable of interpreting the experimental data.

Since the equilibrium constant for reaction (-4) has the same exponential temperature dependence as k_{-4} (reaction (4) has little or no activation energy) the temperature dependence of k_4 derived from k_{-4} and the equilibrium constant will simply be that due to the combined pre-exponential terms.

The resulting uncertainty in the temperature dependence of k_4 is well illustrated by attempting to extrapolate the data of Matthews and Byron to 300°K.

| | $k_4 \text{ cm}^6 \text{ mole}^{-2} \text{ sec}^{-1}$ | | |
|----------|---|----------------------|----------------------|
| | <u>300</u> | <u>1400</u> | <u>3500</u> |
| Matthews | 150×10^{15} | 5×10^{15} | 0.8×10^{15} |
| Byron | 6×10^{15} | 1.3×10^{15} | 0.5×10^{15} |

While the results are in good agreement at the experimental

temperature (3500°K) they differ by a factor of 25 at 300°K.

It has become apparent that k_4 at 300°K cannot be much larger than $1 \times 10^{15} \text{ cm}^6 \text{ mole}^{-2} \text{ sec}^{-1}$ which implies that the temperature dependence chosen by Matthews, and to a lesser extent that of Byron, must be incorrect.

Matthews has computed an upper limit for k_4 from the theoretical treatment of Wigner⁽⁷⁷⁾ and has obtained

$$k = 18.5 \times T^{-\frac{1}{2}} \times 10^{16} \text{ cm}^6 \text{ mole}^{-2} \text{ sec}^{-1}$$

Thus $k_4 \leq 10.7 \times 10^{15} \text{ cm}^6 \text{ mole}^{-2} \text{ sec}^{-1}$ at 300°K.

If the Wigner temperature dependence is applied to Matthews' and Byron's data, the following values are obtained:

$$k_4 (300^\circ\text{K}) \text{ Matthews} = 2.74 \times 10^{15} \text{ cm}^6 \text{ mole}^{-2} \text{ sec}^{-1}$$

$$k_4 (300^\circ\text{K}) \text{ Byron} = 1.71 \times 10^{15} \text{ cm}^6 \text{ mole}^{-2} \text{ sec}^{-1}$$

both of which are not unreasonable.

More recently Rink, Knight and Duff⁽²⁰⁾ have performed shock tube experiments on mixtures of O_2/Xe at temperatures from 3000 - 6000°K.

These authors state that the temperature dependence of k_4 cannot be assigned an accuracy greater than $T^{-\frac{1}{2}}$ to T^{-2} . They arbitrarily choose T^{-1} and report the following values for k_4 :

| M | $k_4 \text{ cm}^6 \text{ mole}^{-2} \text{ sec}^{-1}$ | |
|--------------|---|-----------------------|
| | <u>3500°K</u> | <u>300°K</u> |
| O_2 | 4.57×10^{14} | 5.33×10^{15} |
| O | 13.7×10^{14} | 16.0×10^{15} |
| Xe | 13.4×10^{14} | 15.7×10^{15} |

A choice of $T^{-\frac{1}{2}}$ would yield a value for k_4 at 300°K ($M = \text{O}_2$) of 1.56×10^{15} .

Of all the shock tube data, only those of Camac and Vaughan⁽¹⁹⁾ have an accuracy sufficient to predict values of k_4 outside the experimental temperature range. These workers derive an expression for k_{-4} of the form

$$k_{-4} (M = \text{Ar}) = 6 \times 10^{13} \left(\frac{D}{RT}\right)^{1.0 \pm 0.2} \exp(-D/RT)$$

where $D = 5.116 \text{ e.v.} = 117,934 \text{ cal mole}^{-1}$.

Using a simplified expression for the equilibrium constant of⁽⁵⁰⁾

$$K_4 = 3.907 \times 10^{-2} \exp\left(\frac{59704}{T}\right)$$

leads to an expression for k_4 of

$$k_4 (M = \text{Ar}) = \frac{1.39 \times 10^{17}}{T} \exp\left(\frac{331}{T}\right)$$

Thus $k_4 (M = \text{Ar}) T = 3500^\circ\text{K} = 0.436 \times 10^{14} \text{ cm}^6 \text{ mole}^{-2} \text{ sec}^{-1}$

$k_4 (M = \text{Ar}) T = 300^\circ\text{K} = 1.4 \times 10^{15} \text{ cm}^6 \text{ mole}^{-2} \text{ sec}^{-1}$

It should be noted that the value of D used by Camac and Vaughan is lower than the present accepted value of $119,120$ ⁽⁷⁸⁾ and is also different from the value used in the expression for K_4 . Complete cancellation of the exponential term yields

$$k_4 (M = \text{Ar}) = \frac{1.39 \times 10^{17}}{T}$$

which at 300°K evaluates as $0.46 \times 10^{15} \text{ cm}^6 \text{ mole}^{-2} \text{ sec}^{-1}$.

Thus, even now, it would appear that k_4 cannot be

predicted to better than a factor of three by extrapolation of the high temperature results.

Measurement of the Second Order Recombination
at Room Temperature

Attempts at measuring the rate of reaction (4) at room temperature have been rather sparse.

Reeves, Manella and Harteck⁽⁴⁸⁾ have studied this reaction by dissociating dilute O₂/Ar mixtures (5 - 20% O₂) in a flow system and following the decay by a modified NO₂ titration (see P.14). With such a system it is possible to attain a high degree of dissociation of the oxygen with a consequent diminution of the indirect recombination via ozone formation. These authors showed that even under the most adverse conditions the ozone mechanism could only account for approximately 20% of the observed recombination rate. After correcting for this contribution, they obtained a value for k₄ (M = Ar) of 0.97 x 10¹⁵ cm⁶ mole⁻² sec⁻¹. This result will be discussed subsequently.

Golden and Myerson⁽⁷⁹⁾ have also estimated k₄ by dissociating O₂/Ar mixtures in a static system and following the rate of repopulation of the ground state O₂ by absorption spectroscopy. They report a value for k₄ of 1 x 10¹⁵ cm⁶ mole⁻² sec⁻¹. This result is uncorrected for wall decay and also for processes such as O₂(¹Δ_g) → ground state.⁽⁶⁸⁾

Finally, Krongelb and Strandberg⁽⁴⁹⁾ using a paramagnetic resonance spectrometer in conjunction with a discharged oxygen flow system report k₄ (M = O₂) = 5 x 10¹⁵

$\text{cm}^6 \text{ mole}^{-2} \text{ sec}^{-1}$. Their data, however, were taken under conditions where the ozone mechanism is likely to be more important. Kaufman⁽⁶⁸⁾ has reinterpreted these data to yield a value for k_1 of $1 - 2 \times 10^{14} \text{ cm}^6 \text{ mole}^{-2} \text{ sec}^{-1}$.

V. THE PRESENT PROBLEM

Production of an O₂ Free System

It is apparent from the foregoing that the high temperature shock tube studies cannot predict with any accuracy the rate constant for the second order recombination of oxygen atoms at room temperature.

Of the low temperature studies designed to estimate this rate constant that of Krongelb and Strandberg⁽⁴⁹⁾ must be viewed with suspicion. The only other reported values are those of Harteck, Reeves and Manella⁽⁴⁸⁾ and Golden and Myerson⁽⁷⁹⁾. This latter result also appears to be the subject of some criticism⁽⁶⁸⁾.

In view of the difficulty in separating the direct second order mechanism from the first order ozone mechanism, it would appear that complete elimination of the ozone mechanism would be more likely to lead to a successful evaluation of k_4 . Such a system was partially realized by Harteck et al. (above) by dissociation of small amounts of oxygen in the presence of large amounts of inert gas.

The present investigation, initiated before the publication of Harteck et al., has the same aim but a different approach.

The Reaction between N and NO

It has been known for some time⁽⁸⁰⁾ that addition of nitric oxide to discharged ('active') nitrogen causes the normal yellow Lewis-Rayleigh afterglow to undergo colour

changes ranging from orange through pink to blue as the amount of added nitric oxide is increased. Spectral studies of this afterglow have shown strong emission of the β and γ bands of excited nitric oxide^(81,82,83,84). The mechanism responsible for this emission could be either excitation of the nitric oxide by the active nitrogen or it could arise from recombination processes. To clarify this point, Kaufman and Kelso⁽⁸⁵⁾ added $N^{15}O$ to discharged nitrogen. In every case the resulting β and γ emission arose from $N^{14}O$, demonstrating unequivocally that the emission could not be due to excitation of the added nitric oxide.

It was also noted that addition of excess nitric oxide resulted in the appearance of the greenish-yellow air afterglow which, as has been noted previously, conclusively demonstrates the presence of atomic oxygen. These observations are consistent with the following simple mechanism



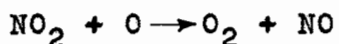
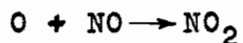
followed by



In a later publication⁽⁸⁶⁾ these workers repeated these results and, in addition, estimated the rate constant for the primary step as being greater than $10^{11} - 10^{12} \text{ cm}^3 \text{ mole}^{-1} \text{ sec}^{-1}$.

Kistiakowsky and Volpi⁽⁸⁷⁾ in 1957 also examined this reaction mass spectrometrically. They used a flow system with quite long residence times (c. 0.35 secs) and

found no nitric oxide in the effluent gas until a critical flow rate of nitric oxide into the reaction vessel was reached. Above this value the effluent nitric oxide increased linearly with the influx nitric oxide flow rate. The only other product found in the effluent gas was oxygen. Significantly the oxygen flow rate was one-half the critical flow rate of nitric oxide. This behaviour is completely explicable on the basis of the above mechanism with the oxygen atoms produced in reaction (6) having recombined before reaching the sampling leak into the mass spectrometer. This recombination, of course, was accelerated by the excess nitric oxide



It is significant that when only a slight excess of nitric oxide was present the O_2 flow rate was found to be less than indicated by the stoichiometry of (6). However, under these conditions, a contribution to the ion current at mass 16 was noticed. Unfortunately the instrument was not calibrated for atomic oxygen, so that a quantitative mass balance of O and O_2 could not be made.

These authors were able to put a lower limit on the rate constant for reaction (6) of $4 \times 10^{11} \text{ cm}^3 \text{ mole}^{-1} \text{ sec}^{-1}$. Subsequently they have raised this lower limit to $5 \times 10^{13} \text{ cm}^3 \text{ mole}^{-1} \text{ sec}^{-1}$ (88).

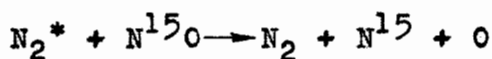
Other workers have since studied this reaction with a continuing refinement of the value for the rate

constant.

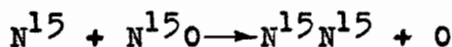
Clyne and Thrush⁽⁸⁹⁾ find $k_6 = 2.5 \pm .5 \times 10^{13} \text{ cm}^3 \text{ mole}^{-1} \text{ sec}^{-1}$ in the temperature range 476 - 755°K.

Phillips and Schiff⁽⁹⁰⁾, using a mass spectrometer in conjunction with a fast flow system, report a value of $1.3 \pm .3 \times 10^{13} \text{ cm}^3 \text{ mole}^{-1} \text{ sec}^{-1}$ at 300°K.

Herron⁽⁹¹⁾ has also made a mass spectrometric study using N^{15}O and reports the presence of $\text{N}^{14}\text{N}^{15}$ in the effluent gas. The absence of $\text{N}^{15}\text{N}^{15}$ would appear to rule out the participation of reactions such as



invoked by Winkler et al.⁽⁹²⁾ since this would necessarily lead to $\text{N}^{15}\text{N}^{15}$ by the reaction



Herron reports a value for k_6 of $1.0 \pm 0.5 \times 10^{13} \text{ cm}^3 \text{ mole}^{-1} \text{ sec}^{-1}$.

The mechanism therefore seems to be fairly well established as



followed by



The rapidity of (6) compared with (7), (8) and (9), coupled with the radiative emissions associated with (7) and (8), should therefore allow this reaction to be conducted as

a gas phase titration with a visual end point.

With a flow rate of nitric oxide less than that of the nitrogen atoms, all the nitric oxide will be immediately consumed by reaction (6) to form oxygen atoms. These oxygen atoms can then react with the residual nitrogen atoms to emit the blue β and γ emission of nitric oxide by reaction (7). (This will be superimposed upon the yellow Lewis-Rayleigh afterglow resulting from the residual nitrogen atoms to yield a purplish emission.) With excess nitric oxide, all of the nitrogen atoms will be immediately consumed with a concomitant production of an equivalent flow of oxygen atoms. These oxygen atoms can now react with the excess nitric oxide by reactions (8) and (9) accompanied by the characteristic greenish-yellow air afterglow.

The equivalence or end point will therefore be defined by the absence of either of these afterglows, and the system will consist of oxygen atoms and nitrogen molecules only.

Subsequent to the initiation of this work, Barth et al. (93) have demonstrated this behaviour quite convincingly.

Such a system is therefore admirably suited to the study of oxygen atom recombination, since it effectively eliminates the participation of the ozone mechanism by eliminating molecular oxygen.

VI. EXPERIMENTAL

Materials

Nitrogen:

Of the many different grades of nitrogen available, two seemed to be significantly superior. These were Matheson 'Prepurified' and Dinsmore 'Premium' grade. Primarily, because of availability, the Dinsmore product was used throughout this investigation. No further purification other than water vapour removal was attempted.

Nitric oxide:

Cylinder nitric oxide of better than 98% purity (Matheson) was further purified by passage through a column of 8 - 20 mesh 'caroxite' (Fisher Scientific Co.) to remove most of the nitrogen dioxide. This was followed by trap to trap distillation through the 'caroxite' column. On the final distillation, the trap was warmed to -80°C by immersion in a dry-ice-acetone bath and the residue, consisting largely of water vapour, was discarded.

The nitric oxide thus purified condensed at liquid air temperature initially to a greyish-blue liquid and finally to a blueish-white solid.

The colour of the condensed material affords a sensitive criterion of purity, since very small amounts of nitrogen dioxide impart a dirty green colour to the solid.

Furthermore, if the nitric oxide is evaporated slowly (M.P. -163.6°C , B.P. -151.8°C), any NO_2 present will remain as N_2O_3 , a bright blue solid (M.P. -102°C , B.P. 3.5°C).

It is possible in this way to detect milligram quantities of NO_2 in the presence of several grams of nitric oxide and affords a very sensitive criterion of purity.

The purified nitric oxide was stored in a twelve litre bulb at about 60 - 70 cms Hg pressure.

Nitrogen dioxide:

Purified nitric oxide was converted to nitrogen dioxide by addition of good quality tank oxygen (Imperial Oxygen Co.). After allowing sufficient time for complete mixing, the nitrogen dioxide was condensed in a dry-ice-acetone trap and the excess oxygen pumped off. As before, the absence of any blue N_2O_3 in the condensed NO_2 (white) was taken as a criterion of purity. To prevent partial decomposition, the nitrogen dioxide was stored in a twelve litre bulb with the addition of a small excess of oxygen. The presence of this oxygen did not affect the subsequent use of the nitrogen dioxide.

Inert gases:

Argon (Canadian Liquid Carbonic), helium (Air Reduction Canada), carbon-dioxide (Matheson Coleman grade), and sulphur hexafluoride (Matheson) were used directly from cylinders as required.

Apparatus

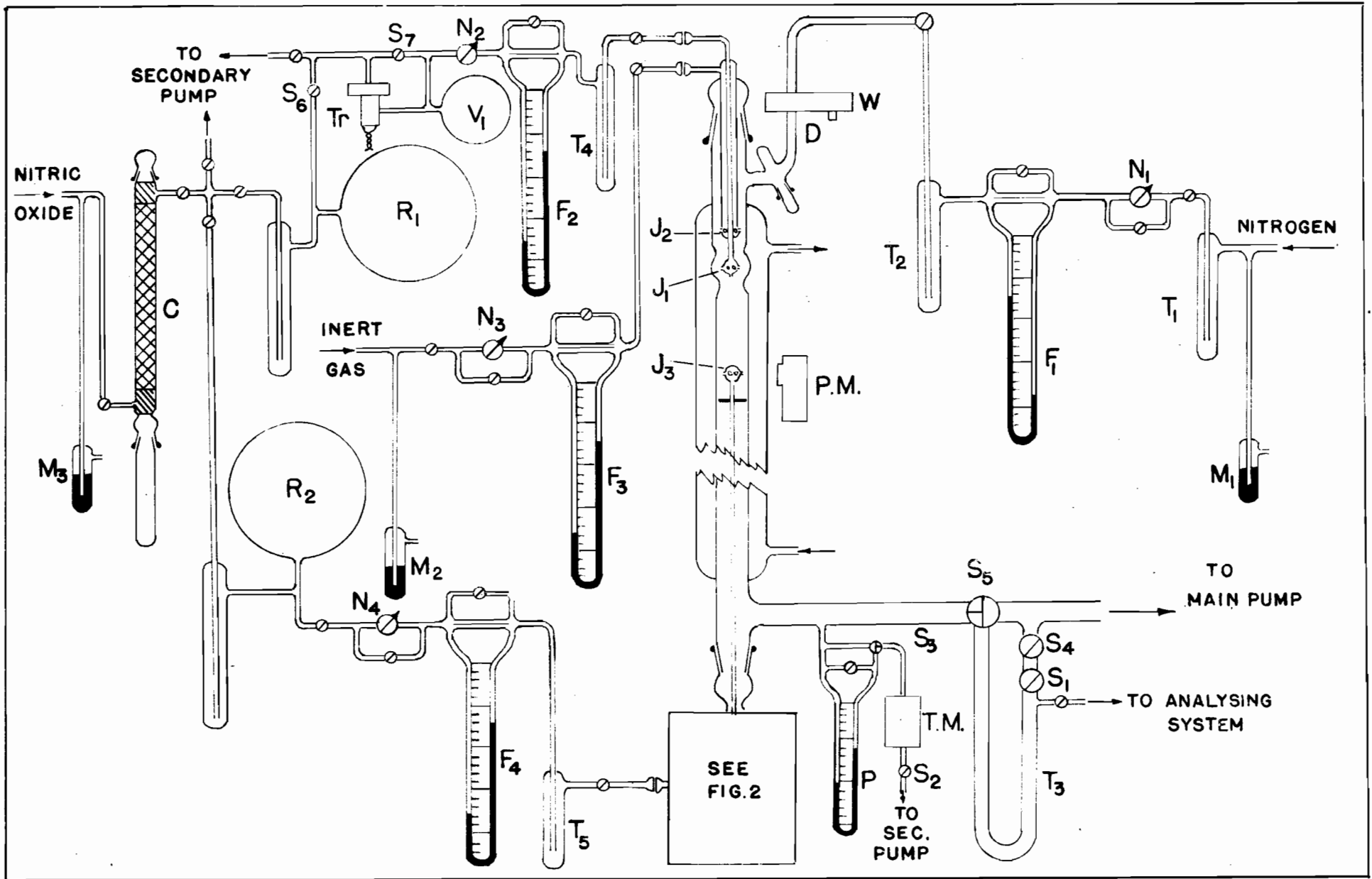
The apparatus used is shown schematically in Fig. 1.

Nitrogen, maintained at atmospheric pressure by the manostat M_1 , was dried by passage through the liquid air trap T_1 and its flow rate controlled and monitored by the

Figure 1

DIAGRAM OF APPARATUS

- M - Manostat
- T - Trap
- N - Needle valve
- F - Capillary flowmeter
- R - Gas reservoir
- S - Stopcock
- D - Quartz discharge tube
- W - Waveguide
- Tr - Pressure transducer
- J - Reactant inlet
- P.M. - Photomultiplier tube
- P - Oil manometer
- T.M. - Tilting McLeod gauge
- C - Caroxite column



needle valve N_1 and associated capillary flowmeter F_1 . Before entering the discharge tube, the nitrogen was passed through a second liquid air trap T_2 to remove any water vapour which might have escaped T_1 . In addition, this trap served to eliminate possible contamination by mercury vapour from the flowmeter. Elimination of mercury vapour was also aided by covering the exposed mercury surfaces with a small amount of 'octoil'.

The discharge tube D consisted of a length of 13 mm I.D. vycor tubing which was coated externally with 'aquadag' to reduce the intense light emitted from the discharge.

Atomic nitrogen was produced by a microwave discharge from a Raytheon diathermy unit capable of providing up to 125 watts of 2450 Mc/sec C.W. radiation. The microwave generator was coupled to the system by means of the wave guide W. It is necessary, of course, to ensure that the graphite coating on the discharge tube does not extend right through the discharge region, since it provides a very effective shield and the discharge will not operate. The whole wave-guide assembly was then enclosed by an asbestos paper box to reduce stray light still further.

The pressure prevailing in the reaction tube could be measured either with the tilting McLeod gauge, T.M., or by the octoil manometer, P, by suitable manipulation of the stopcocks S_2 and S_3 .

The two-way stopcock, S_3 , enabled the closed limb

of the manometer to be continually evacuated by the secondary pump. In this position the McLeod gauge provided a check on the pressure in the closed limb.

Variations in pressure in the reaction tube were produced by the throttling stopcock, S_1 , while stopcocks, S_4 and S_5 , allowed the main gas stream to be bypassed to allow removal of the products retained in the U-tube trap T_3 .

Nitric oxide from the reservoir, R_1 , was controlled by the needle valve, N_2 , and the octoil flowmeter, F_2 , after which it was passed through a dry-ice-acetone trap T_4 . The dry nitric oxide then entered the atomic nitrogen stream through the jet J_1 .

To obtain rapid mixing, it was found necessary to use a jet with six peripheral holes of $0.2 \pm .01$ mm diameter and a seventh axial hole of 0.1 mm diameter. Uniformity of these holes was found to be essential if good mixing was to be achieved.

Introduction of the various inert gases was effected by a flow-line similar to the nitrogen line, consisting of the manostat M_2 , needle valve N_3 and flowmeter F_3 . The gas in question entered the flow stream through the jet, J_2 , which was co-axial to J_1 and had six peripheral holes of 0.2 ± 0.01 mm diameter.

Since it was necessary to add other gases downstream from J_1 (nitric oxide and nitrogen dioxide) a fourth flow-line was included as shown. This line was similar to the nitric oxide flow-line feeding J_1 and consisted of the reservoir R_2 ,

needle valve, N_4 , and flowmeter, F_4 , and dry-ice trap, T_5 . This line was terminated by a movable jet assembly J_3 which enabled the reactant in question to be introduced into the flow stream at any desired point downstream from J_1 .

This movable jet assembly is shown in more detail in Fig. 2, from which the mode of operation is apparent.

The reaction tube was made of 26 mm I.D. pyrex tubing fitted with a cooling water jacket. The 'zero point' of the reaction tube is defined by the position of admixture of the nitric oxide, i.e. at J_1 . The length of the tube over which measurements could be made was 33 cms.

A 1P21 (RCA) photomultiplier tube (P.M.) was mounted in a light-proof enclosure that could be moved parallel to the reaction tube on a set of rails. This enclosure was fitted with a set of collimating slits such that a length of the reaction tube of 1 mm could be viewed. The output of the phototube was fed to an amplifier, and relative light intensities were read off on a meter (Eldorado Electronics).

N_2O_3 analysis system:

The nitric oxide formed by the reaction of oxygen atoms with nitrogen dioxide (vide infra) was analysed in the apparatus shown in Fig. 3. It consisted essentially of two interconnected calibrated volumes, V_A and V_B , and an oxygen reservoir, R_3 . The method of analysis will be described in the next section.

Figure 2

MOVABLE JET ASSEMBLY

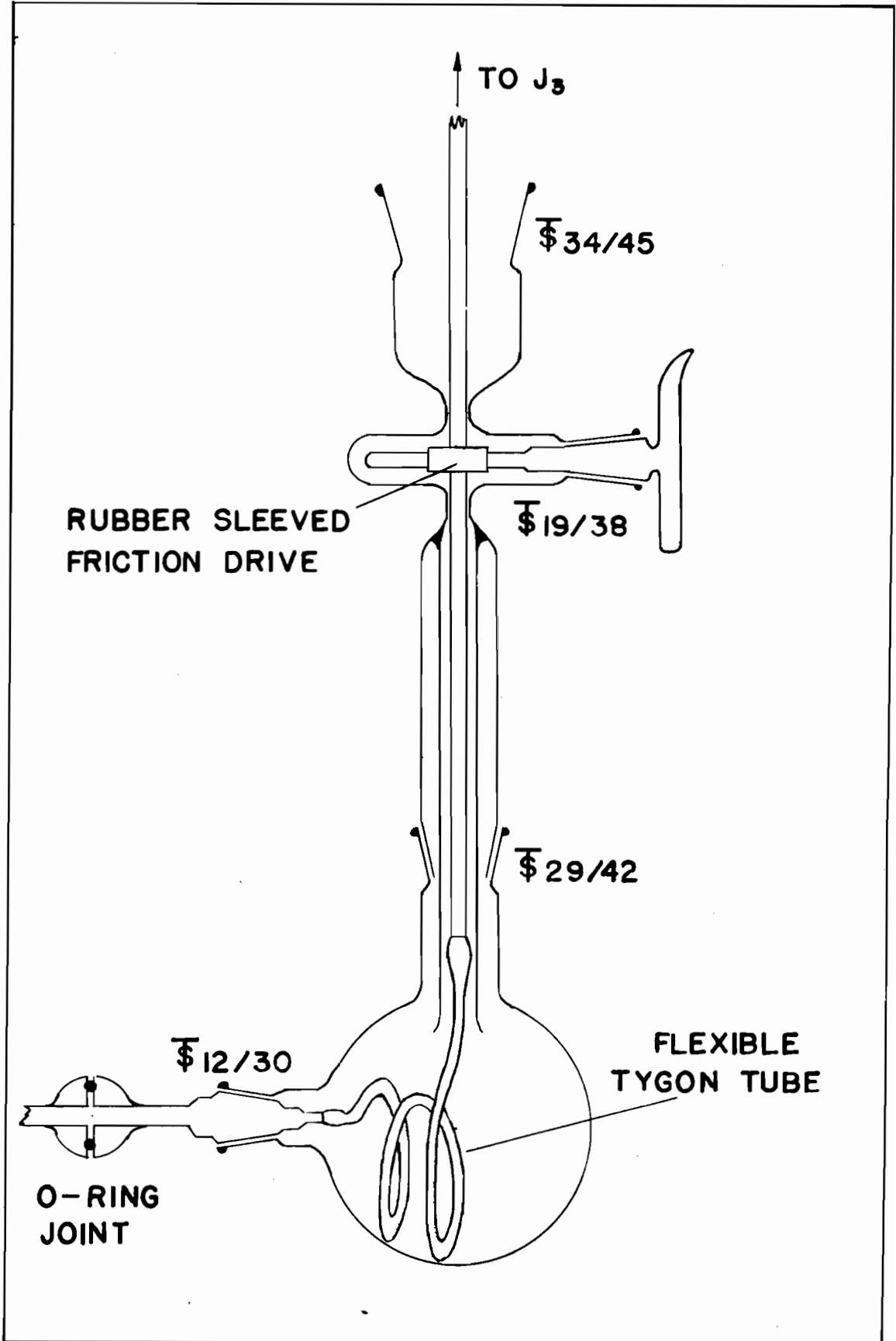
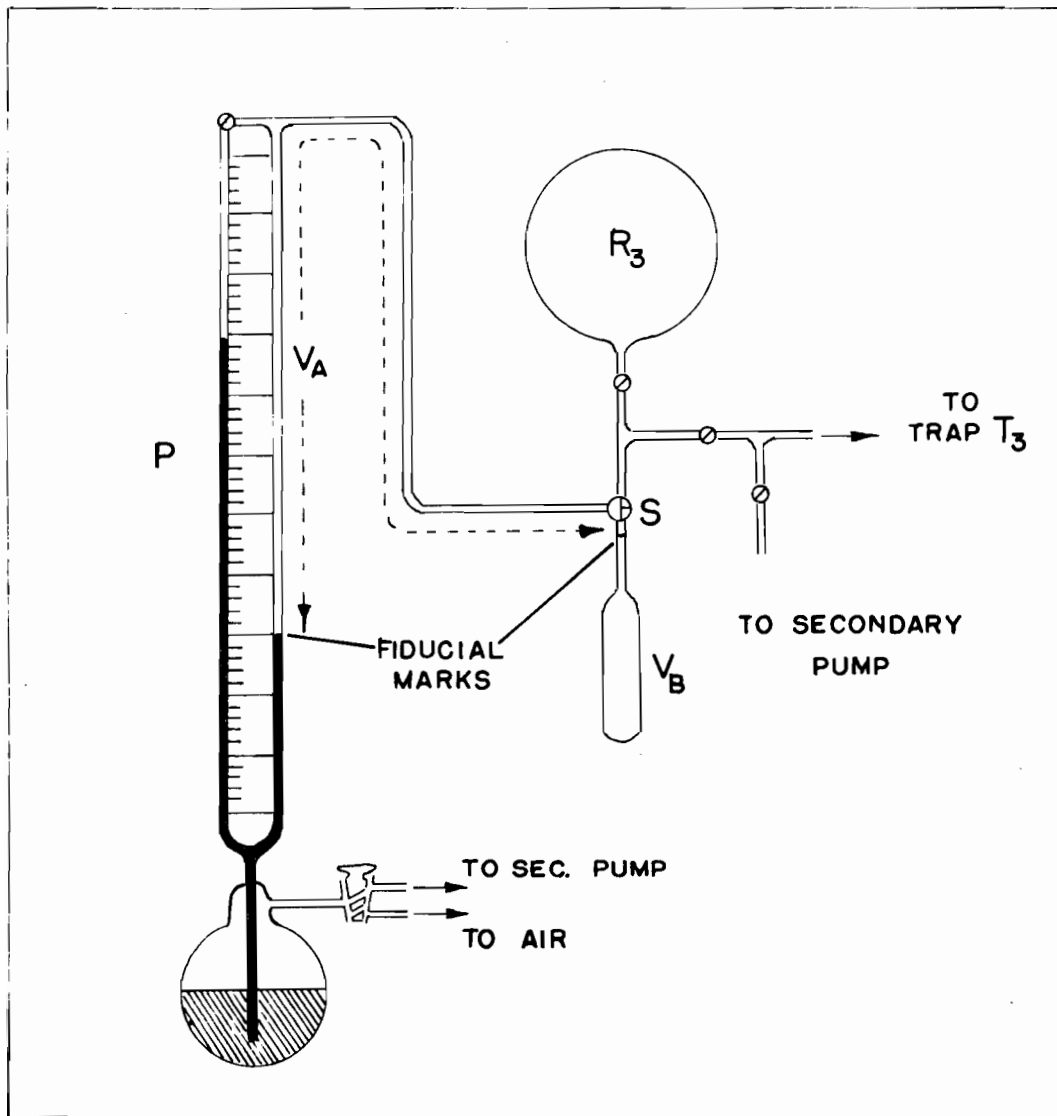


Figure 3

ANALYSING SYSTEM

- S - Stopcock
- R₃ - Oxygen reservoir
- P - Mercury levelling manometer
- V_A, V_B - Calibrated volumes



Calibration of flowmeters F_1 and F_3

These two flowmeters, which were designed to pass quite high flow rates (c. 100 μ moles/sec), were calibrated in the following manner.

The apparatus shown in Fig. 4 was connected to the inlet of the flow-line, and the rate of gas flow at atmospheric pressure determined by introducing a soap film into the burette tube by means of the rubber bulb. The time taken for the soap film to sweep out a known volume was then determined by a stopwatch. Since it is necessary to have a slight excess of gas issuing from the jet, J, the pressure in the apparatus will be in excess of atmospheric by the amount, ΔP , indicated by the octoil manometer, P. Of course, this pressure must not be large enough to cause gas to issue from the manostat, M_1 , in Fig. 1.

The molar flow rate was then calculated from the expression

$$F = \frac{V}{t} \frac{(P + \Delta P)}{RT}$$

where V = volume swept out in time, t .

$(P + \Delta P)$ = pressure in apparatus.

T = ambient temperature.

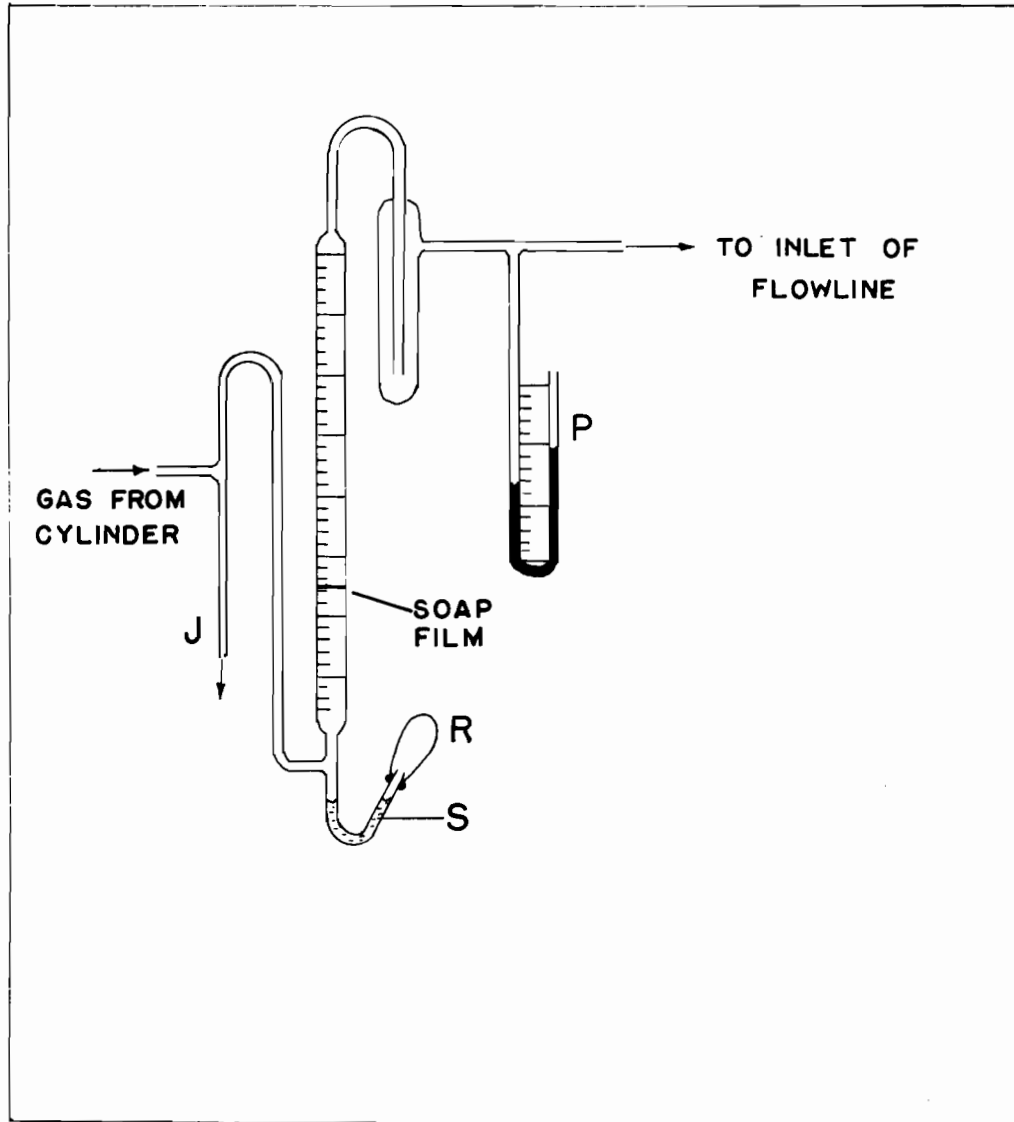
The pressure difference developed across the capillary flowmeter is related to the molar flow rate by the Poiseuille equation

$$F = \frac{(P_1^2 - P_2^2) \pi r^4}{16L \eta RT}$$

Figure 4

APPARATUS FOR CALIBRATING FLOWMETERS

- J - Outlet for excess gas
- S - Soap solution
- R - Rubber bulb
- P - Octoil manometer



where r = radius of capillary.

L = length of capillary.

P_1 = pressure on high side of capillary.

P_2 = pressure on low side of capillary.

η = coefficient of viscosity of the gas.

This equation can be written as

$$F = C(P_1 - P_2)(P_1 + P_2) = C(\Delta P^2 + 2P_2 \Delta P)$$

where $\Delta P = P_1 - P_2$.

For the high flow-rate meters, F_1 and F_3 , the capillary dimensions ($r = 2 \times 10^{-2}$ cms, $L = 5 - 10$ cms) were such that ΔP was of the order of 20 cms Hg. Since P_2 , which is approximately equal to the pressure in the reaction tube, was of the order of a 2 - 3 mm Hg, the second term in the above expression amounts to about 2% of ΔP^2 .

Thus the flow rate will be approximately proportional to ΔP^2 and the calibration relatively unaffected by changes in the pressure in the reaction tube. Nevertheless the calibration was performed at the two extreme conditions of P_2 likely to be encountered (1 mm and 7 mm Hg) and, when necessary, a linear interpolation made to determine the flow rate at intermediate pressures.

Nitric oxide flowmeter F_2

Since the flow rate measured by this flowmeter was of the order of 1 micromole sec^{-1} , the pressure drop across a capillary of 0.2 mm radius was insufficiently large to

satisfy the requirement that the calibration be independent of the pressure in the reaction tube. Reduction of the capillary diameter to satisfy this criterion would result in inconveniently long response times. For this line therefore, a capillary essentially the same as those described above was employed and the much smaller pressure drop measured by an octoil rather than a mercury manometer.

Furthermore, the presence of the jet, J_1 , resulted in a further pressure drop and thus P_2 was not known. The simplest solution to this was to determine the nitric oxide flow independently at the completion of every experiment. This was readily accomplished in the following manner.

During the experiment stopcocks, S_6 and S_7 , were normally open. To determine the flow rate, stopcock S_7 was closed and the rate of differential pressure drop between the reservoir, R_1 , and the calibrated volume, V_1 , was measured as a function of time by the pressure transducer, T_r (Statham Instruments). This transducer was sufficiently sensitive that a pressure drop of less than 1 mm Hg could be determined with better than 1% accuracy. This small pressure drop ($< 0.2\%$) ensured that the determination did not perturb the flow rate. The molar flow rate could then be easily calculated from

$$F = \frac{\Delta P}{t} \frac{V_1}{RT}$$

where $\Delta P/t$ = rate of differential pressure drop.

V_1 = volume of calibrated bulb.

T = ambient temperature.

This procedure was found to be very rapid and accurate for determining flow rates of 1μ mole/sec or less.

Flowmeter, F_4 , was not calibrated since it was not necessary to know the flow rate of the reactant added through this line (vide infra).

Limitations of fast-flow systems

The use of flow systems has been very valuable in the study of the kinetics of fast reactions. In general, the premixed reactants are allowed to flow through a reaction vessel of known volume. From a knowledge of the volume flow rate at the existing pressure, the residence time within the reaction vessel can be easily calculated.

There are two extreme cases which are amenable to simple mathematical analysis in the study of reaction kinetics:

- (a) Complete longitudinal mixing (stirred flow reactor).
- (b) No longitudinal mixing.

Detailed analyses of these two cases have been published (94,95,96).

The second case is the one of interest in the present work. It is evident that for a tubular reaction vessel of constant cross-section, provided the volume flow rate of the gas does not alter, the reaction time will be directly proportional to distance measured in the flow direction. In fact, provided that the above criteria are satisfied, the concentration at any point, l , in the flow system is equal to the concentration in an equivalent closed

system which has reacted for a time $t = \frac{lA}{u}$
where A = cross-sectional area of flow tube, and
 u = volume flow rate.

Obviously $\frac{u}{A}$ is simply the linear velocity of the gas through the reaction vessel.

However, a number of precautions must be taken to ensure the fulfilment of the above criteria.

(1) If the reaction is accompanied by a change in the number of molecules, then obviously the volume flow rate will not be constant and the simple rate expression of the constant volume case will no longer be valid.

The integrated rate expressions for a number of such cases have been derived by Hougen and Watson⁽⁹⁷⁾. In the present work, although the recombination reaction is accompanied by a change in the number of molecules, the concentration of the reacting species ($\approx 1\%$) is sufficiently low that even complete recombination will produce a negligible change in the total volume flow rate.

(2) For high linear velocities an appreciable viscous pressure drop may be produced along the length of the reaction tube. As pointed out by Kaufman⁽⁹⁸⁾, this pressure change might inadvertently be ascribed to a change in concentration due to reaction. This error, of course, would be additional to that arising from the variation in linear flow rate due to the pressure variation. The magnitude of the pressure drop along the tube can be calculated from the Poiseuille equation.

$$(P_1^2 - P_2^2) = \frac{16 \eta l R T f}{\pi r^4}$$

where r = radius of tube

l = length of tube

f = molar flow rate

η = coefficient of viscosity.

For small pressure gradients, this can be rearranged to give

$$\frac{\Delta P}{P} = \frac{8 \eta l R T f}{P^2 \pi r^4}$$

For the following typical operating conditions

$$P = 3 \text{ mm Hg} \quad T = 300^\circ\text{K} \quad f = 10^{-4} \text{ moles sec}^{-1}$$

$$r = 1.3 \text{ cms} \quad \eta (N_2) = 1.8 \times 10^{-4} \text{ poises} \quad l = 30 \text{ cms}$$

it is easily shown that the pressure drop is approximately 0.075%. Even at lower pressures, e.g. 1 mm Hg, it still amounts to only 0.68%. This source of error therefore is not important under the present operating conditions.

(3) The essential criterion of no longitudinal mixing can only be satisfied if diffusion is slow compared with the linear velocity. The concentration gradient set up in the flow tube will obviously lead to a diffusive flow tending to remove the gradient. This effect is reduced by working with high linear velocities and, since the diffusion coefficient is inversely proportional to pressure, high pressures. This first condition, however, is limited by the viscous pressure drop noted above. The error arising from axial diffusion is dependent upon the first derivative of the concentration gradient and will therefore be a function both of the linear

velocity and the recombination rate. As shown in Appendix B, a necessary condition for diffusion effects to be negligible is that

$$1 \gg \frac{nDkc^{n-1}}{V^2}$$

where V = linear velocity of the gas stream.

D = diffusion coefficient of the reactive species.

k = rate constant of the removal reaction.

n = order of the removal reaction.

At 3 mm Hg in the present system

$$c \approx 1.6 \times 10^{-9} \text{ mole cm}^{-3}$$

$$k \approx 10^{15} \times 1.6 \times 10^{-7} \text{ cm}^3 \text{ mole}^{-2} \text{ sec}^{-1}$$

$$D < 150 \text{ cm}^2 \text{ sec}^{-1}$$

$$V \approx 120 \text{ cm sec}^{-1}$$

$$n = 2$$

$$\begin{aligned} \text{Therefore } \frac{nDkc^{n-1}}{V^2} &\sim \frac{2 \times 150 \times 1.6 \times 10^8 \times 1.6 \times 10^{-9}}{1.2^2 \times 10^4} \\ &= 5.4 \times 10^{-3} \end{aligned}$$

The required inequality is therefore adequately satisfied.

Production and measurement of oxygen atoms

Production of atomic oxygen:

The proposed method of atomic oxygen production has already been described.

An O_2 free oxygen atom system was produced by the titration of nitrogen atoms with nitric oxide. This was achieved by adding nitric oxide through the jet, J_1 , into a

discharged nitrogen stream with the end-point of the titration being defined by the absence of the afterglow associated with reaction (7) or (8).

In practice this end-point was impossible to achieve accurately by simple adjustment of the nitric oxide flow rate, mainly because of the lack of sensitivity of the needle valve at these very low flow rates. However, an approximate end-point could be attained in this way and final adjustment made by altering the nitrogen flow rate and the power supplied to the discharge.

This system is obviously rather unstable since there is only a single operating point. Any perturbation capable of changing the atom or nitric oxide flow rates at the titration jet will therefore cause the system to move off the end-point. Such factors include pressure fluctuations caused by introduction of even small amounts of reactants downstream, introduction of liquid air traps, etc.

In practice, it was found necessary to allow the system to stabilize for about thirty minutes before any measurements were made.

Measurement of oxygen-atom concentration:

Various methods for determining oxygen-atom concentrations have been discussed previously.

For simplicity and specificity, it was decided to use the nitrogen dioxide reaction. To recapitulate, this method takes advantage of the following mechanism:



As noted previously, the primary reaction is much faster than the two subsequent reactions. Because of the light-emitting step, this mechanism can be used as a gas phase titration, the extinction of the afterglow due to (8) marking the end-point.

However, despite claims to the contrary, it was found that this end-point was insufficiently sharp to determine the atom concentration with sufficient accuracy.

It was decided therefore to utilize the alternative method of adding an excess of nitrogen dioxide and determining the amount of nitric oxide produced. Provided this excess is sufficiently large, the flow rate of nitric oxide should be exactly equal to the original oxygen-atom flow rate. However, nitric oxide cannot be trapped quantitatively at liquid air temperatures. There are two alternatives available to overcome this limitation.

(a) The use of pumped down liquid nitrogen as the refrigerant.

(b) Addition of sufficient nitrogen dioxide to form N_2O_3 . This compound (M.P. -102°C) can be trapped quantitatively at liquid air temperatures.

It was found in practice that a flow rate of nitrogen dioxide approximately equal to three times the

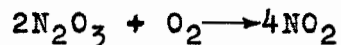
oxygen-atom flow rate was sufficient to ensure quantitative formation and trapping of the nitric oxide.

Analysis of N_2O_3 :

The above method for determining oxygen-atom flow rates involves the trapping of the N_2O_3 during a measured time interval. This N_2O_3 must then be assayed quantitatively. The procedure was as follows.

The residual non-condensable gas (nitrogen) in the trap, T_3 , was first pumped off by means of the secondary pump. The N_2O_3 was then distilled into the evacuated bulb, V_B (Fig. 3), which was immersed in liquid air to a fiducial mark just below the stopcock, S. Oxygen was then added from the reservoir, R_3 , and its pressure, P_1 , measured on the levelling manometer, P_2 . Stopcock, S, was then closed and the bulb, V_B , allowed to warm to room temperature. (Care must be exercised to ensure that the amount of condensed material initially present in V_B is small enough that the resulting pressure on evaporation is not greatly in excess of atmospheric.)

In the gaseous state, the N_2O_3 is rapidly oxidized to nitrogen dioxide.



Complete oxidation can be checked by the colour of the solid material present after recondensation by liquid air. It was found experimentally that less than 1% of N_2O_3 could be detected by its blue coloration. The NO_2 was then completely condensed, care being taken to ensure that the liquid air level was at the fiducial mark. Stopcock, S, was then

re-opened, the manometer relevelled to its original position and the final pressure, P_2 , recorded.

The amount of oxygen consumed was then calculated from the relation

$$O_2 = \frac{(P_1 - P_2)}{R} \left(\frac{V_A}{T_A} + \frac{V_B}{T_B} \right)$$

where T_A = temperature of V_A = ambient temperature.

T_B = temperature of liquid air.

Since a temperature gradient must exist between V_A and V_B , this expression is not completely accurate. However, by making the diameter of the connecting tube small compared with that of V_B , the volume of gas at the unknown transition temperature is minimized. To reduce the error further, the temperature, T_B , was replaced by an effective temperature obtained by measuring the pressure exerted by a known amount of gas under the same conditions. It is of interest to note that this effective temperature was always within 2°K of the actual liquid air temperature.

It is apparent from the oxidation reaction that 1 mole of oxygen is equivalent to two moles of N_2O_3 (or NO) and hence to two moles of oxygen atoms. The calculation of the molar flow rate of atomic oxygen follows immediately.

Verification of the stoichiometry
of the N - NO reaction

Although the stoichiometry of this reaction has been fairly well established, the direct equivalent of the oxygen atoms produced and the nitric oxide consumed has not been

demonstrated. To do this the following experiment was performed.

With the system running at the end-point, an excess of nitrogen dioxide was added to the gas stream a few centimetres below the titration jet, J_1 , by means of the movable jet, J_3 . The end-point was then readjusted if necessary and the system allowed to stabilize. After this was achieved a liquid air bath was placed around trap, T_3 , at time $t = 0$. After a time, t , the gas stream was made to bypass the trap by manipulation of stopcocks S_6 and S_4 . The N_2O_3 was then distilled out into bulb, V_B . The procedure was then repeated but with the discharge turned off.

In the first case it is apparent that the nitric oxide trapped out per unit time is equal to the molar flow rate of oxygen atoms at the position of jet, J_3 .

In the second case the nitric oxide issuing from J_1 will not be consumed and, after mixing with the nitrogen dioxide from J_3 , will be trapped out. Provided that the stoichiometry of the $N - NO$ reaction is correct, this molar flow rate will be equal to the oxygen atom flow at J_1 in the first case. Thus, if there is negligible recombination in the interval between J_1 and J_3 , the nitric oxide trapped out per unit time will be independent of whether the discharge is on or off.

This can be summarized as follows.

Case (1) - Discharge ON:

At J_1 a flow of nitric oxide $(NO)_1$ is converted to

an equivalent oxygen atom flow $(O)_1$. At J_3 the oxygen atom flow $(O)_3$ is converted to an equivalent flow of nitric oxide $(NO)_3$. Provided the stoichiometry of the N - NO reaction is correct $(NO)_1 = (O)_1$. If negligible recombination occurs between J_1 and J_3 , then $(O)_3 = (O)_1$ and $(NO)_3 = (O)_3 = (O)_1 = (NO)_1$.

Case (2) - Discharge OFF:

This is simply a determination of $(NO)_1$.

The results of such as experiment are shown in

Table I.

Table I

| Expt. No. | N ₂ flow rate micro moles sec ⁻¹ | Pressure mm Hg | Reaction time J ₁ - J ₃ milliseconds | NO trapped in T ₃ micro moles sec ⁻¹ | Discharge |
|-----------|--|-------------------|--|---|-----------|
| 8a | 240 | 3.0 | 36 | 1.76 ± 0.03 | ON |
| 8b | 240 | 3.0 | 36 | 1.75 ± 0.03 | OFF |
| 9a | 108 | 1.55 | 41 | 1.13 ± 0.03 | ON |
| 9b | 108 | 1.55 | 41 | 1.13 ± 0.03 | OFF |
| 10a | 74 | 1.25 | 48 | 1.06 ± 0.03 | ON |
| 10b | 74 | 1.25 | 48 | 1.07 ± 0.03 | OFF |

It is apparent that for a variety of conditions the nitric oxide trapped out per unit time is independent of whether the discharge is on or off. As seen previously, the

rate constant for recombination is not expected to be much larger than $10^{15} \text{ cm}^6 \text{ mole}^{-2} \text{ sec}^{-1}$. Even including heterogeneous recombination, the recombination between J_1 and J_3 will not be more than about 1% under the conditions of this experiment. Inspection of Table I shows that this is within experimental error of the determination.

It can therefore be safely concluded that the stoichiometry of the N - NO reaction is indeed correct within approximately 3%. Alternatively, assumption of the stoichiometry of the N - NO reaction justifies the validity of the NO_2/O reaction as a quantitative method of determining oxygen-atom concentrations.

Additional confirmation of the stoichiometry of the N - NO reaction will be presented in Part II of this thesis.

Alternative method for determining the oxygen-atom concentration

The method outlined above for determining the oxygen-atom concentration has a number of disadvantages when used in the present system.

- (a) It is apparent from the previous results that the O-atom concentration gradient along the reaction tube was quite small. The NO trapping technique was found to have an accuracy insufficient to determine this concentration gradient with the required precision.
- (b) This method was also found to be extremely time consuming, each individual determination taking

approximately twenty minutes. Thus, to obtain say, nine points on the concentration/distance curve would require at least three hours. It was found that the system could not be maintained at the end-point for this length of time without adjustment.

(c) The major disadvantage, however, arose from the necessity of having the gas stream bypass trap T_3 to allow removal of the N_2O_3 for analysis. Since the pumping speed of the two paths was necessarily different, the resulting pressure change disturbed the system from the end-point. Even when the gas was reverted to the original flow path, the system seldom returned exactly to the original end-point.

It was obvious therefore that this method was impracticable for obtaining kinetic data.

The following rapid methods were therefore examined.

Kaufman⁽³²⁾ has shown that nitric oxide and oxygen atoms react relatively slowly by the light emitting step



followed by the much faster regeneration step



The concentration of nitric oxide therefore remains constant, the net reaction being a recombination of oxygen atoms. The intensity of the emitted afterglow at any point in the flow stream will thus be directly proportional to the oxygen-atom concentration.

In the present system the addition of a slight excess of nitric oxide was easily obtained by slightly reducing the discharge power so that the nitric oxide issuing from J_1 was not completely consumed. The ratio of the oxygen-atom concentration at any two points, x and y , in the reaction tube could then be obtained directly from the ratio of the emitted light intensity as measured by the photomultiplier tube (P.M. Fig. 1), i.e.

$$\frac{(O)_x}{(O)_y} = \frac{I_x}{I_y}$$

This measurement can then be repeated for diminishing amounts of excess nitric oxide by increasing the input power to the discharge.

A plot of I_x/I_y as (NO) , and hence I is varied, should enable I_x/I_y to be extrapolated to $(NO) = 0$, i.e. $I = 0$. This limiting ratio then gives the relative oxygen-atom concentration at the points, x and y , in the absence of excess nitric oxide, i.e. the relative concentration change due to natural recombination between these points. By varying the position, y , and repeating the procedure, a complete curve of relative oxygen-atom concentration as a function of distance could thus be obtained. This curve could then be put on an absolute basis by determining the oxygen-atom flow rate at $y = 0$, i.e. by measuring the titration flow rate of nitric oxide at J_1 .

Unfortunately the monitoring reactions are

considerably faster than the natural recombination and the intercepts at $I = 0$ were consequently insufficiently accurate to determine the concentration distance curve with the required precision.

The alternative method which was examined did not suffer from this defect. In this case a small amount of nitric oxide was introduced into the flow stream through the movable jet, J_3 . The intensity of the emitted light at J_3 will therefore be directly proportional to the oxygen-atom concentration at this point. This eliminates the effect of the accelerated recombination, since no nitric oxide is present between J_1 and J_3 . Therefore, by moving J_3 and the photomultiplier tube simultaneously along the reaction tube, a plot of relative oxygen-atom concentration is obtained directly. As before, this relative plot can then easily be put on an absolute basis by a determination of the oxygen-atom flow rate at J_1 .

Using this method, a complete scan of the concentration/distance curve could be made in a matter of minutes.

Integrated rate expressions for oxygen-atom recombination in the absence of O_2

The kinetics of oxygen-atom recombination have been discussed previously. In the present system the elimination of oxygen molecules, however, eliminates the participation of reactions (1) and (2). The mechanism of recombination therefore can be described by reactions



The rate of disappearance of oxygen atoms is therefore given by

$$-\frac{d(O)}{dt} = 2k_4^M [M] [O]^2 + k_5 [O]$$

In this system the oxygen-atom concentration is only about 1% of the total molar concentration. Hence the concentration of M can be regarded as constant and equal to the concentration of nitrogen.

The integrated rate expression then becomes

$$k_5 = \frac{1}{t} \ln \frac{[O]_o}{[O]_t} + \frac{1}{t} \ln \frac{k_5 + 2k_4^{N_2} [N_2] [O]_t}{k_5 + 2k_4^{N_2} [N_2] [O]_o} \quad \dots\dots\dots (11)$$

Obviously such an expression does not readily lend itself to a separate determination of k_4 and k_5 . However, it will be seen that as $[N_2] \rightarrow 0$, i.e. as the pressure approaches zero, equation 11 approaches $\frac{1}{t} \ln \frac{[O]_o}{[O]_t}$.

This immediately suggests a means of determining k_5 . An experimental first order rate constant, k_5' , can be defined by

$$k_5' = \frac{1}{t} \ln \frac{[O]_o}{[O]_t}$$

The rate constant k_5' , defined as above, will obviously be a function both of pressure and of the degree of recombination because of the neglect of the last term in equation (11).

However, a plot of k_5' against $[N_2]$ or P_{N_2} , while obviously not linear, should enable an approximate extrapolation to zero pressure to be made. This intercept can then be identified with k_5 .

Equation (11) can be rearranged to yield

$$k_4^{N_2} = \frac{k_5 \left(\frac{[O]_t}{[O]_o} e^{k_5 t} - 1 \right)}{2 [N_2] [O]_t (1 - e^{k_5 t})} \dots\dots\dots (12)$$

Inspection of the differential rate equation shows that the rate of recombination increases as $[N_2]$ increases. Thus for a given degree of recombination $t \rightarrow 0$ as $[N_2] \rightarrow \infty$.

As t becomes very small, equation (12) reduces to

$$k_4^{N_2} = \left(\frac{1}{[O]_t} - \frac{1}{[O]_o} \right) \frac{1}{2 [N_2] t}$$

Thus, as before, an experimental third order rate constant, $k_4'^{N_2}$ can be defined by

$$k_4'^{N_2} = \left(\frac{1}{[O]_t} - \frac{1}{[O]_o} \right) \frac{1}{2 [N_2] t}$$

A plot of $k_4'^{N_2}$ against $[N_2]$ or P_{N_2} should therefore approach $k_4^{N_2}$ at very high pressures.

VII RESULTS

(i) Using ostensibly 'bone' dry nitrogen
without further water vapour removal

Determination of k_5 :

With the system running at the end-point, a relative oxygen-atom concentration versus distance curve was obtained using the technique described on P.71

The results of such an experiment are shown in Table II and Fig. 5 (pp. 75 and 76 respectively).

As can be seen, under the conditions of this experiment, the oxygen-atom decay can be described by a pseudo first order rate constant of 1.32 sec^{-1} . This, of course, does not imply that the decay is actually first order, since the recombination is small enough that both first and second order plots are linear within the experimental error.

The results of a number of such experiments performed under varying pressure conditions are shown in Table III and Fig. 6 (pp. 77 and 78 respectively). The preceding analysis has shown that there is no simple functional relationship between k_5' and pressure. However, it is apparent from Fig. 6 that a simple linear extrapolation to zero pressure fixes the value of k_5 between about 0.35 and 0.45 sec^{-1} .

Table II

Pressure = 4.25 mm Hg

Temperature = 20°C

Nitrogen Flow = 178 micromoles sec⁻¹

Linear velocity = 145 cms sec⁻¹

| d cms | t msecs | I | ln I |
|----------|------------|------------|-------|
| 7 | 48.3 | 57.5 ± 0.5 | 4.052 |
| 10 | 69.0 | 55.6 ± 0.5 | 4.018 |
| 15 | 103.5 | 53.1 ± 0.5 | 3.972 |
| 19 | 131.0 | 51.5 ± 0.5 | 3.942 |
| 23 | 159.0 | 49.4 ± 0.5 | 3.900 |
| 27 | 186.0 | 48.0 ± 0.5 | 3.871 |
| 30 | 207.0 | 46.5 ± 0.5 | 3.839 |

Figure 5

PLOT OF RELATIVE OXYGEN-ATOM CONCENTRATION

(Data from Table II)

● - Light intensity, I , as a
function of time

○ - $\ln I$ as a function of time

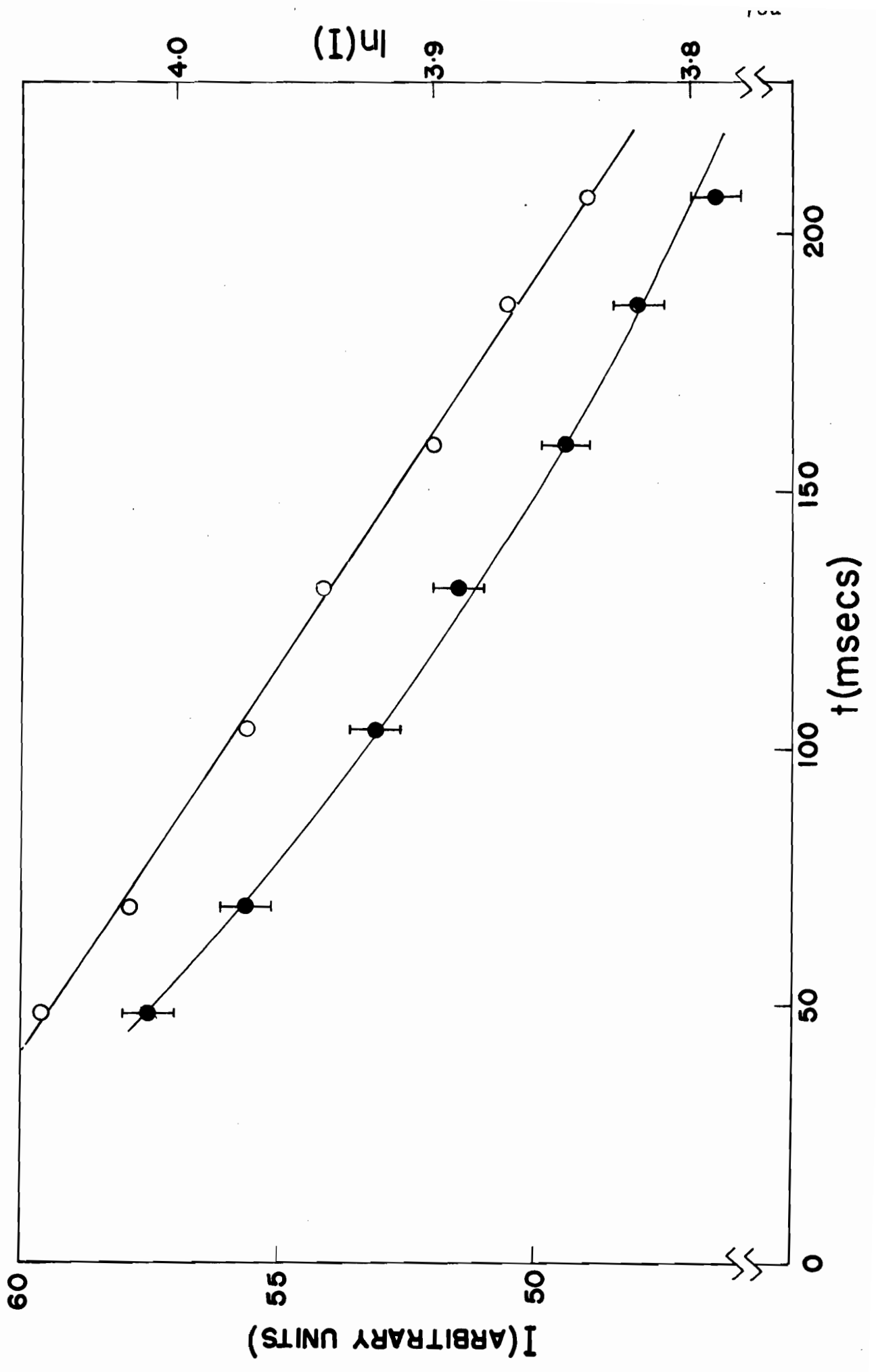


Table III

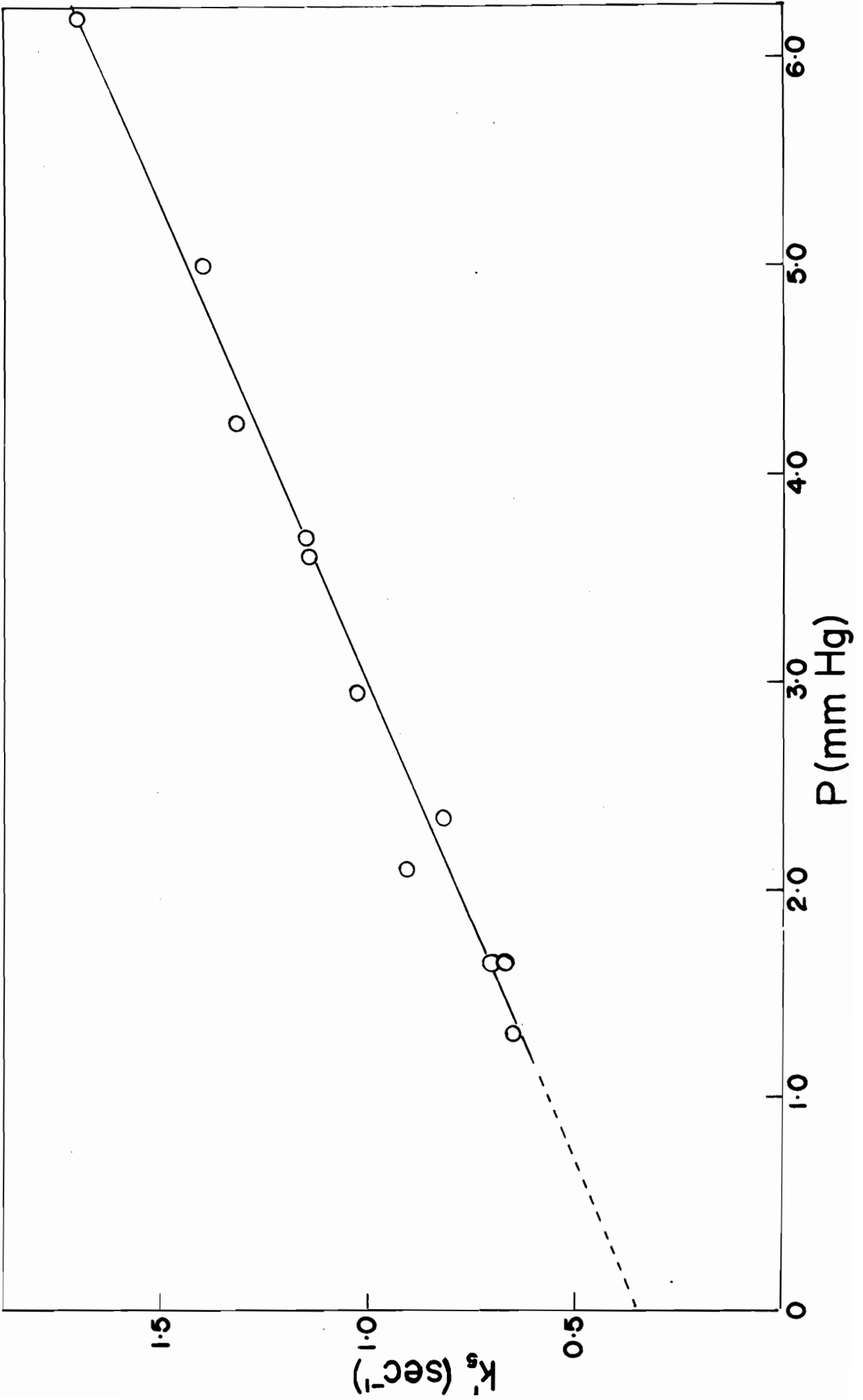
VARIATION OF k_5' WITH TOTAL PRESSURE

| Temperature = 20°C | | | | |
|--------------------|------------|-----------------------|------------|---|
| Expt. No. | P mm Hg | $\frac{[O]_o}{[O]_t}$ | t msecs | $k_5' = \frac{1}{t} \ln \frac{[O]_o}{[O]_t}$ sec ⁻¹ |
| 39a | 1.3 | 1.135 | 192 | 0.65 |
| 39b | 1.65 | 1.150 | 201 | 0.70 |
| 40a | 1.65 | 1.130 | 181 | 0.68 |
| 39c | 2.10 | 1.195 | 197 | 0.91 |
| 40b | 2.35 | 1.175 | 196 | 0.82 |
| 39d | 2.95 | 1.260 | 225 | 1.03 |
| 40c | 3.6 | 1.270 | 210 | 1.14 |
| 39e | 3.7 | 1.285 | 217 | 1.15 |
| 40d | 4.25 | 1.320 | 207 | 1.32 |
| 39f | 5.0 | 1.465 | 272 | 1.40 |
| 40e | 6.2 | 1.700 | 313 | 1.70 |

Figure 6

VARIATION OF k'_5 WITH TOTAL PRESSURE

(Data from Table III)



Determination of $k_4^{N_2}$:

The procedure in this case was similar to that used in determining k_5 . Recombination curves of oxygen-atom concentration against time were obtained for pressures in the range of 2 - 7 mm Hg. These results were then calculated to yield a pressure dependent third order rate constant $k_4^{N_2}$. The variation of $k_4^{N_2}$ with pressure is clearly shown in Table IV and Fig. 7 (pp. 80 and 81).

The required extrapolation (to infinite pressure) to yield $k_4^{N_2}$ is rather more difficult in this case. However, it is apparent that the curve is rapidly levelling off in the neighbourhood of $1.5 \times 10^{15} \text{ cm}^6 \text{ mole}^{-2} \text{ sec}^{-1}$, although the final value cannot be obtained too precisely. More accurate estimates of $k_4^{N_2}$ and k_5 were made in the following manner.

Values of k_5 in the range $0.3 - 0.5 \text{ sec}^{-1}$ were inserted into equation (12) and the constancy of $k_4^{N_2}$ with pressure was examined. Table V (p. 82) shows the evaluation of $k_4^{N_2}$ for values k_5 of 0.3, 0.4, and 0.5 sec^{-1} .

With $k_5 = 0.5 \text{ sec}^{-1}$, $k_4^{N_2}$ increases with pressure, while a choice of $k_5 = 0.3 \text{ sec}^{-1}$ leads to values of $k_4^{N_2}$ which decrease with pressure. However, for $k_5 = 0.40 \text{ sec}^{-1}$, $k_4^{N_2}$ remains approximately constant over the whole pressure range.

This procedure leads to the following values of the two rate constants.

$$k_5 = 0.40 \text{ sec}^{-1}$$

$$k_4^{N_2} = 1.47 \pm 0.05 \times 10^{15} \text{ cm}^6 \text{ mole}^{-2} \text{ sec}^{-1}$$

Table IV

| Expt. No. | P mm Hg | T °C | $[N_2] \times 10^7$ moles cm ⁻³ | $[O]_o \times 10^9$ moles cm ⁻³ | $[O]_t \times 10^9$ moles cm ⁻³ | t secs | $k_4^{N_2} \times 10^{-15}$ cm ⁶ mole ⁻² sec ⁻¹ |
|-----------|---------|------|--|--|--|-----------|--|
| 18 | 2.3 | 5 | 1.33 | 1.03 | 0.926 | 0.145 | 2.83 |
| 20 | 2.5 | 6 | 1.435 | 1.5 | 1.31 | 0.138 | 2.45 |
| 21 | 2.75 | 6 | 1.58 | 1.37 | 1.205 | 0.135 | 2.35 |
| 22 | 3.10 | 6 | 1.78 | 1.40 | 1.182 | 0.162 | 2.29 |
| 23 | 3.45 | 6 | 1.98 | 1.56 | 1.25 | 0.177 | 2.20 |
| 17 | 3.45 | 5 | 1.985 | 1.83 | 1.41 | 0.196 | 2.10 |
| 19 | 4.60 | 5 | 2.65 | 1.84 | 1.21 | 0.267 | 2.00 |
| 26 | 5.28 | 6.5 | 3.03 | 2.06 | 1.08 | 0.359 | 1.95 |
| 28 | 5.78 | 8 | 3.30 | 2.51 | 1.18 | 0.366 | 1.87 |
| 27 | 7.06 | 7.5 | 4.05 | 3.07 | 1.093 | 0.408 | 1.78 |

$k_4^{N_2}$ calculated from

$$k_4^{N_2} = \frac{[O]_o - [O]_t}{2[O]_o[O]_t[N_2]_t} \text{ cm}^6 \text{ mole}^{-2} \text{ sec}^{-1}$$

Figure 7

VARIATION OF $k_4^{N_2}$ WITH TOTAL PRESSURE

(Data from Table IV)

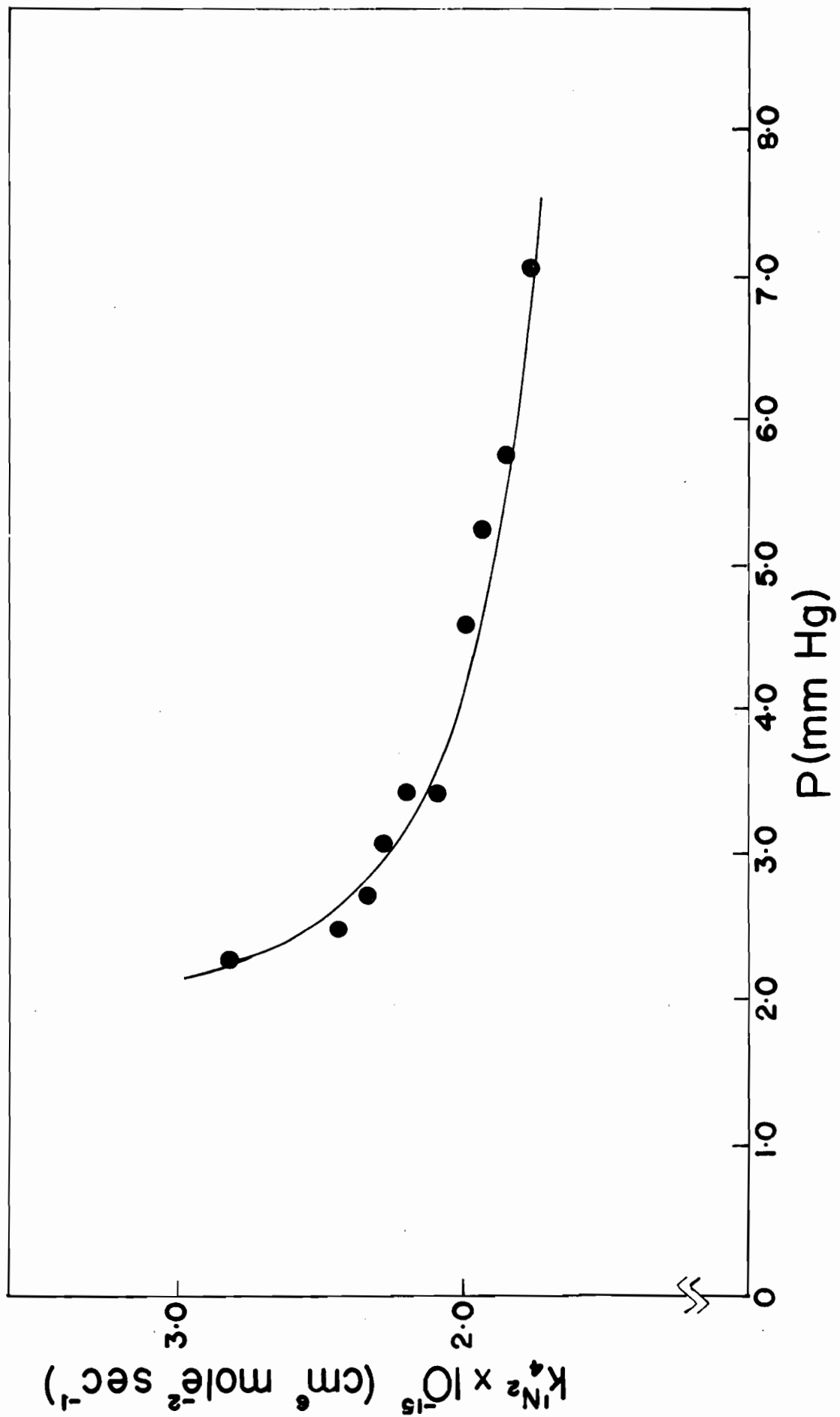


Table V

| Expt. No. | P mm Hg | $[N_2] \times 10^7$ moles cm^{-3} | $[O]_t \times 10^9$ moles cm^{-3} | $[O]_t/[O]_0$ | t secs | $k_4^{N_2} \times 10^{-15}$ $cm^6 \text{ mole}^{-2} \text{ sec}^{-1}$ | | |
|--------------|------------|--|--|---------------|-----------|--|-------------------------|-------------------------|
| | | | | | | k_6 = 0.3 sec^{-1} | k_6 0.4 sec^{-1} | k_6 0.5 sec^{-1} |
| 18 | 2.30 | 1.33 | 0.926 | 0.893 | 0.145 | 1.84 | 1.46 | 1.08 |
| 20 | 2.50 | 1.435 | 1.31 | 0.873 | 0.138 | 1.70 | 1.45 | 1.20 |
| 21 | 2.75 | 1.58 | 1.205 | 0.880 | 0.135 | 1.60 | 1.35 | 1.10 |
| 22 | 3.10 | 1.78 | 1.182 | 0.844 | 0.162 | 1.64 | 1.42 | 1.20 |
| 23 | 3.45 | 1.98 | 1.25 | 0.804 | 0.177 | 1.69 | 1.51 | 1.33 |
| 17 | 3.45 | 1.985 | 1.41 | 0.770 | 0.196 | 1.62 | 1.47 | 1.31 |
| 19 | 4.60 | 2.65 | 1.21 | 0.658 | 0.267 | 1.61 | 1.48 | 1.35 |
| 26 | 5.28 | 3.03 | 1.08 | 0.524 | 0.359 | 1.68 | 1.56 | 1.43 |
| 28 | 5.78 | 3.30 | 1.18 | 0.470 | 0.366 | 1.58 | 1.48 | 1.39 |
| 27 | 7.06 | 4.05 | 1.093 | 0.356 | 0.408 | 1.55 | 1.48 | 1.41 |

(ii) Effect of water vapour on the homogeneous recombination rate

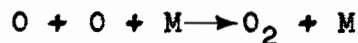
The previous results were obtained using nitrogen directly from the cylinder. Although this nitrogen was ostensibly 'bone dry', it was felt that the determination of $k_4^{N_2}$ should be repeated using nitrogen which had been dried by passage through two liquid air traps $\sqrt{T_1}$ and T_2 (Fig. 1)7.

The immediate effect of this treatment was to reduce significantly the degree of dissociation of the nitrogen. This decrease in atom concentration led inevitably to a much reduced rate of recombination. Consequently the pressure range over which measurements could be made extended only from about 3.5 - 7 mm Hg.

However, it is apparent from Table VI that the rate constant, $k_4^{N_2}$, has been markedly reduced. The average value of $k_4^{N_2}$ for this system is $1.03 \pm 0.05 \text{ cm}^6 \text{ mole}^{-2} \text{ sec}^{-1}$.

(iii) Efficiencies of various third bodies in the homogeneous recombination reaction

If a second gas, M, other than nitrogen, is added to the gas stream, the inclusion of the reaction



leads to the following integrated rate expression.

$$k_4^{N_2} [N_2] + k_4^M [M] = \frac{k_5 \left(\frac{[O]_t}{[O]_0} e^{k_5 t} - 1 \right)}{2 [O]_t (1 - e^{k_5 t})}$$

Table VI

| Expt. No. | P mm Hg | T °C | $[N_2] \times 10^7$ moles cm ⁻³ | $[O]_t \times 10^9$ moles cm ⁻³ | $\frac{[O]_t}{[O]_0}$ | t secs | $k_4^{N_2} \times 10^{-15}$ cm ⁶ mole ⁻² sec ⁻¹ |
|--------------|------------|---------|--|--|-----------------------|-----------|---|
| 226 | 3.45 | 21 | 1.89 | 1.48 | 0.860 | 0.150 | 1.01 |
| 225 | 4.12 | 21 | 2.25 | 1.47 | 0.821 | 0.165 | 1.09 |
| 224 | 4.53 | 20 | 2.48 | 1.425 | 0.820 | 0.166 | 1.02 |
| 227 | 5.30 | 21 | 2.90 | 1.39 | 0.769 | 0.195 | 1.01 |
| 223 | 5.50 | 20 | 3.01 | 1.30 | 0.765 | 0.202 | 1.04 |
| 222 | 6.77 | 20 | 3.71 | 1.22 | 0.682 | 0.250 | 1.04 |
| 221 | 7.10 | 20 | 3.88 | 1.19 | 0.660 | 0.271 | 0.98 |

$$\text{i.e. } k_4^{N_2} + \frac{[M]}{[N_2]} k_4^M = \frac{k_5 \left(\frac{[O]_t}{[O]_0} e^{k_5 t} - 1 \right)}{2 [N_2] (1 - e^{k_5 t})} \dots\dots\dots (13)$$

where $[N_2]$ and $[M]$ are the concentrations of N_2 and M respectively.

Thus a plot of the right-hand side of equation (13) against $[M]/[N_2]$ should yield a straight line of slope k_4^M and intercept $k_4^{N_2}$.

The particular gas being studied was added to the dissociated nitrogen stream through the jet, J_2 . Obviously the addition of an inert gas will increase the pressure in the flow tube. Since there is a pressure limit above which the discharge will not operate satisfactorily (≈ 8 mm Hg), large values of $[M]/[N_2]$ cannot be obtained unless $[N_2]$ is decreased. Decreasing $[N_2]$, however, leads to a concomitant decrease in $[O]$ with an associated decrease in recombination rate. In practice, the useful upper limit of $[M]/[N_2]$ was found to be about 0.5.

The results obtained with $M = N_2O, CO_2, He, Ar$ and SF_6 are shown in Table VII and Fig. 8 (pp. 86 - 88 inclusive).

The slopes of the plots of $k_4^{N_2} + k_4^M [M]/[N_2]$ obtained from Fig. 8 yield the following values:

| M | $k_4^{N_2}$ | k_4^M | $= k_4^M/k_4^{N_2}$ |
|--------|----------------------|-----------------------|---------------------|
| N_2O | 1.0×10^{15} | 1.37×10^{15} | 1.37 |
| CO_2 | 1.0×10^{15} | 3.3×10^{15} | 3.3 |
| He | 1.0×10^{15} | 0.33×10^{15} | 0.33 |
| Ar | 1.0×10^{15} | 0.3×10^{15} | 0.3 |
| SF_6 | 1.0×10^{15} | 3.3×10^{15} | 3.3 |

It will be noted that all of these plots extrapolate at $[M] = 0$ to a value of $k_4^{N_2}$ of $1.0 \times 10^{15} \text{ cm}^6 \text{ mole}^{-2} \text{ sec}^{-1}$, in agreement with the earlier determination.

It is also apparent from Fig. 8 that the experimental error associated with these data is such that efficiencies of less than about 0.3-0.4 relative to nitrogen cannot be determined with any precision. Both helium and argon fall into this category.

Table VII

A. $M = N_2O$

| Expt. No. | P mm Hg | $[M] \times 10^7$ moles cm^{-3} | $[N_2] \times 10^7$ moles cm^{-3} | $\frac{[M]}{[N_2]}$ | $[O]_t \times 10^9$ moles cm^{-3} | $\frac{[O]_t}{[O]_0}$ | t secs | $k_4^{N_2} + k_4^M \frac{[M]}{[N_2]}$ $\text{cm}^6 \text{ mole}^{-2} \text{ sec}^{-1}$ |
|-----------|---------|---|---|---------------------|---|-----------------------|-----------|---|
| 208 | 6.30 | 0.988 | 2.45 | 0.404 | 1.172 | 0.776 | 0.178 | 1.57 |
| 209 | 5.50 | 0.762 | 2.25 | 0.339 | 1.205 | 0.806 | 0.170 | 1.44 |
| 210 | 5.56 | 0.596 | 2.44 | 0.244 | 1.11 | 0.766 | 0.218 | 1.33 |
| 211 | 5.25 | 0.285 | 2.59 | 0.110 | 1.205 | 0.788 | 0.197 | 1.15 |

B. $M = CO_2$

| | | | | | | | | |
|-----|------|-------|------|-------|------|-------|-------|------|
| 235 | 6.44 | 1.25 | 2.27 | 0.55 | 0.92 | 0.730 | 0.186 | 2.64 |
| 236 | 6.20 | 1.02 | 2.36 | 0.432 | 0.99 | 0.717 | 0.197 | 2.34 |
| 237 | 6.34 | 0.787 | 2.78 | 0.283 | 1.08 | 0.671 | 0.223 | 1.91 |
| 238 | 6.76 | 0.75 | 2.96 | 0.253 | 1.11 | 0.665 | 0.238 | 1.64 |
| 239 | 5.47 | 0.31 | 2.68 | 0.116 | 1.30 | 0.732 | 0.208 | 1.35 |

Table VII (Contd.)

C. M = He

| Expt. No. | P mm Hg | $[M] \times 10^7$ moles cm^{-3} | $[N_2] \times 10^7$ moles cm^{-3} | $\frac{[M]}{[N_2]}$ | $[O]_t \times 10^9$ moles cm^{-3} | $\frac{[O]_t}{[O]_0}$ | t secs | $k_4^{N_2} + k_4^M \frac{[M]}{[N_2]}$ $\text{cm}^6 \text{mole}^{-2} \text{sec}^{-1}$ |
|-----------|---------|---|---|---------------------|---|-----------------------|-----------|---|
| 240 | 6.30 | 1.185 | 2.245 | 0.528 | 1.105 | 0.832 | 0.178 | 1.18 |
| 241 | 6.08 | 0.995 | 2.30 | 0.433 | 1.11 | 0.822 | 0.192 | 1.10 |
| 242 | 6.48 | 0.745 | 2.77 | 0.269 | 1.18 | 0.760 | 0.221 | 1.10 |
| 243 | 6.85 | 0.63 | 3.09 | 0.204 | 1.20 | 0.730 | 0.236 | 1.07 |

D. M = Ar

| | | | | | | | | |
|-----|------|-------|------|-------|------|-------|-------|------|
| 230 | 7.45 | 1.185 | 2.87 | 0.414 | 1.12 | 0.75 | 0.252 | 1.00 |
| 231 | 7.06 | 0.865 | 3.00 | 0.288 | 1.17 | 0.74 | 0.245 | 1.07 |
| 233 | 6.19 | 0.442 | 2.91 | 0.152 | 1.12 | 0.758 | 0.236 | 1.03 |

E. M = SF₆

| | | | | | | | | |
|-----|------|-------|------|-------|-------|-------|-------|------|
| 245 | 8.71 | 1.32 | 3.38 | 0.392 | 0.75 | 0.582 | 0.291 | 2.21 |
| 246 | 7.05 | 0.965 | 2.85 | 0.338 | 0.84 | 0.636 | 0.286 | 1.98 |
| 247 | 6.55 | 0.554 | 2.98 | 0.186 | 1.068 | 0.668 | 0.252 | 1.55 |
| 248 | 6.11 | 0.321 | 2.97 | 0.108 | 1.25 | 0.698 | 0.234 | 1.28 |

Figure 8

PLOTS OF $k_4^{N_2} + k_4^M M / N_2$ AS A

FUNCTION OF M

(Data from Table VII)

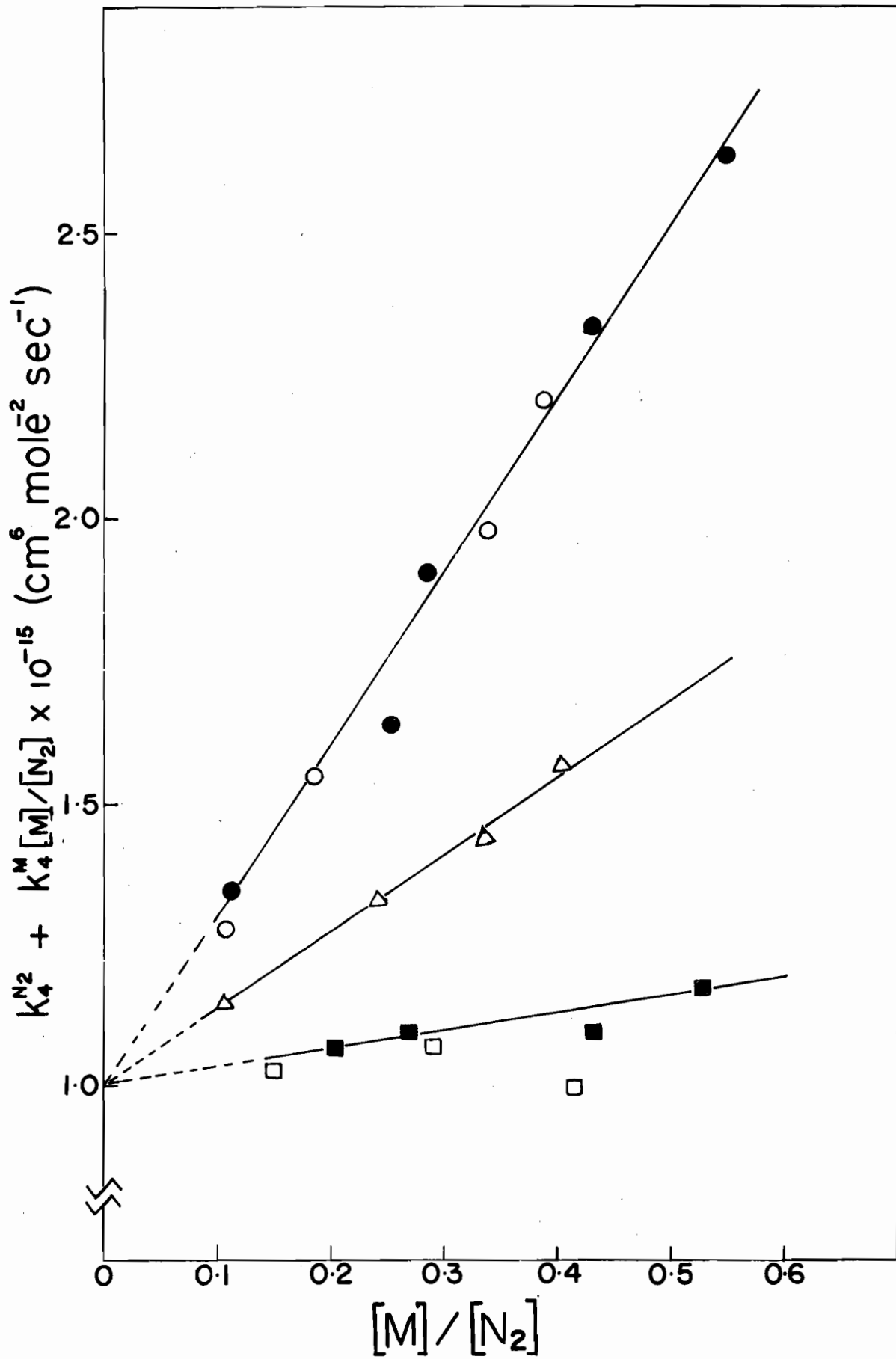
△ - M = N₂O

● - M = CO₂

■ - M = He

□ - M = Ar

○ - M = SF₆



VIII DISCUSSION

Heterogeneous recombination

The value of 1.65×10^{-5} for the recombination coefficient of atomic oxygen on pyrex obtained in this work can be compared with the previously published values which appear on P.29

For untreated pyrex, the following values have been reported.

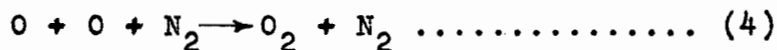
- 2×10^{-5} (32) Kaufman
- 1.1×10^{-4} (43) Herron and Schiff
- 7.7×10^{-5} (41) Elias, Ogryzlo and Schiff

It is obvious that, except for the value of 2×10^{-5} obtained by Kaufman, the present result is considerably lower than those obtained by other workers. The reason for this is not clear, unless the presence of O_2 in the above systems leads to an accelerated surface recombination due to a more rapid replenishment of the chemisorbed oxygen on the recombining surface.

On the other hand, the rate of heterogeneous recombination in different pieces of apparatus is so sensitive to the history of the surface that quantitative comparison in any case is rather difficult. The value obtained here may be simply a reflection of this surface variation.

Homogeneous recombination

The experimental results obtained in this investigation for the rate constant of the process



yielded two significantly different values depending upon the treatment accorded to the nitrogen.

Using nitrogen directly from the cylinder resulted in a value for $k_4^{N_2}$ (undried) of $1.5 \times 10^{15} \text{ cm}^6 \text{ mole}^{-2} \text{ sec}^{-1}$. This value, however, dropped to $1.0 \times 10^{15} \text{ cm}^6 \text{ mole}^{-2} \text{ sec}^{-1}$ consequent to removal of condensable impurity in the nitrogen by passage through two liquid air traps. This impurity was found to be mainly water vapour.

There are two possible ways in which this water vapour could affect the measured rate constant:

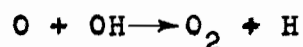
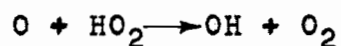
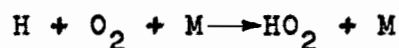
- (a) by acting as a very efficient third body, or
- (b) by effecting a catalyzed recombination of the atomic oxygen.

Although not measured quantitatively, the concentration of water vapour present in the nitrogen was estimated at less than 0.5 mole per cent. For this small amount of water vapour to produce a significant change in $k_4^{N_2}$ by alternative (a) would require a very high efficiency for H_2O in comparison with N_2 . A lower limit for this efficiency can be estimated. It is apparent from equation (13) that

$$k_4^{N_2} + \frac{[H_2O]}{[N_2]} k_4^{H_2O} = k_4^{N_2} \text{ (undried)}$$

If the value of $k_4^{N_2}$ is taken as $1.0 \times 10^{15} \text{ cm}^6 \text{ mole}^{-2} \text{ sec}^{-1}$, $k_4^{H_2O}$ can be evaluated as $1 \times 10^{17} \text{ cm}^6 \text{ mole}^{-2} \text{ sec}^{-1}$. Thus, for water vapour in these low concentrations to have the observed effect requires it to be at least one hundred times as efficient as N_2 as a third body in reaction (4). This would appear to be rather unlikely, particularly since the other molecular species examined in this work have efficiencies of the same order of magnitude as nitrogen.

Since the water vapour in the nitrogen has passed through the discharge, this effect could be the result of a catalyzed recombination by the dissociated fragments of H_2O . Such a mechanism has indeed been postulated by Kaufman⁽³²⁾ consisting of the following reactions:



There is, however, one further important possibility which cannot be ignored. It was found that elimination of water vapour from the nitrogen led to the production of a substantial quantity of vibrationally excited N_2 . This species has been more fully examined in Part II of this thesis. It could well be argued that the reduction in recombination rate might be due to the inefficiency of vibrationally excited N_2 as a third body. However, it will be shown later that nitrous oxide is very efficient in

deactivating this species. Experiments in which N_2O was added downstream from the discharge resulted in rapid and complete removal of vibrationally excited N_2 . The rate constants obtained in the presence of varying amounts of N_2O extrapolated smoothly to a value of $1.0 \times 10^{15} \text{ cm}^6 \text{ mole}^{-2} \text{ sec}^{-1}$ at zero concentration of N_2O (Fig. 8). Since vibrationally excited nitrogen is not present in these experiments, it can reasonably be concluded that the presence of vibrationally excited N_2 does not materially affect the recombination rate. Thus the value of $1.0 \times 10^{15} \text{ cm}^6 \text{ mole}^{-2} \text{ sec}^{-1}$ can be confidently ascribed to $k_4^{N_2}$.

Efficiencies of third bodies

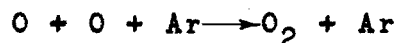
Except for argon, there are no published values for the recombination rate in the presence of the third bodies investigated in this work. It would appear that the molecules used in this study, ranging from monatomic inert gases to bulky polyatomic molecules like SF_6 , yield rate constants which do not differ by more than a factor of ten. Neglecting the inert gases reduces this to a factor of about three.

The difference in efficiency of quite different types of polyatomic molecules does not therefore appear to be very large.

Since the high temperature shock tube studies have yielded values for k_4^M of the same order of magnitude, it would appear that the temperature dependence of the recombination rate is quite small.

The only comparison which can be made with

previously published results is with the value for k_4^{Ar} obtained by Harteck et al. (48). These workers estimate the rate constant for the process



to be $0.97 \times 10^{15} \text{ cm}^6 \text{ mole}^{-2} \text{ sec}^{-1}$ which can be compared with the value obtained in the present work of $\leq 0.3 \times 10^{15} \text{ cm}^6 \text{ mole}^{-2} \text{ sec}^{-1}$. However, Harteck et al. assumed that heterogeneous recombination was negligible ($\gamma < 10^{-6}$).

Unless the walls of their reaction vessel were poisoned, which is not explicitly stated in their publication, this estimate of the heterogeneous recombination coefficient would appear to be too low. Examination of their data shows that their value for k_4^{Ar} is not completely pressure independent. This can be ascribed to an appreciable contribution from wall recombination which becomes increasingly important at the lower pressures, and this is precisely where the lack of constancy in their rate constant appears.

A recalculation of their data, assuming a value for γ_{pyrex} of 1.65×10^{-5} does indeed largely remove this pressure dependence and leads to a value of k_4^{Ar} quite close to the one found in this investigation. Whether this recalculation can be justified in view of the variation of γ from surface to surface is difficult to assess. It would appear, however, that the two sets of data are not necessarily inconsistent.

Conclusion

It is readily apparent from the results obtained in this thesis that the second order recombination of atomic oxygen is probably faster than was previously assumed by some workers. As was noted earlier, both Elias, Ogryzlo and Schiff⁽⁴¹⁾ and Kretschmer and Petersen⁽⁷⁴⁾ put upper limits on $k_4^{O_2}$ of $4 \times 10^{14} \text{ cm}^6 \text{ mole}^{-2} \text{ sec}^{-1}$ and $2 \times 10^{14} \text{ cm}^6 \text{ mole}^{-2} \text{ sec}^{-1}$ respectively based on the linearity of logarithmic plots of oxygen-atom concentration as a function of time. Unfortunately, since $k_4^{O_2}$ has not been determined in this investigation, these values cannot be completely ruled out. However, the criteria used to obtain them can be criticized.

The insensitivity of this procedure is adequately demonstrated in Fig. 9. The points on this graph represent the calculated variation of oxygen-atom concentration as a function of time under two typical operating conditions employed by Elias, Ogryzlo and Schiff.

The filled circles were calculated solely on the basis of the ozone mechanism, i.e. with $k_4^{O_2} = 0$.

The open circles were calculated with the inclusion of the second order mechanism, using $k_4^{O_2} = 1 \times 10^{15} \text{ cm}^6 \text{ mole}^{-2} \text{ sec}^{-1}$ and a corresponding decrease in k_1 from $1 \times 10^{14} \text{ cm}^6 \text{ mole}^{-2} \text{ sec}^{-1}$ to approximately $0.6 \times 10^{14} \text{ cm}^6 \text{ mole}^{-2} \text{ sec}^{-1}$. It is apparent that both sets of calculated points can be fitted by the same pair of straight lines. The departure from linearity of the mixed order mechanism is negligible.

The upper limit of $4 \times 10^{14} \text{ cm}^6 \text{ mole}^{-2} \text{ sec}^{-1}$, quoted by Elias, Ogryzlo and Schiff, cannot therefore be justified. It would appear that the published values for the rate constants in the ozone mechanism probably need revision.

Figure 9

CALCULATED PLOTS OF OXYGEN-ATOM DECAY
EXCLUDING AND INCLUDING REACTION (4)

● - Calculated using the data of Ref. (41)

$$k_5 = 1.87 \text{ sec}^{-1}$$

$$k_1 = 1 \times 10^{14} \text{ cm}^6 \text{ moles}^{-2} \text{ sec}^{-1}$$

$$k_4 = 0$$

○ - Calculated from equation (12) using:

$$k_5 = 1.87 \text{ sec}^{-1}$$

$$k_1 = 0.6 \times 10^{14} \text{ cm}^6 \text{ moles}^{-2} \text{ sec}^{-1}$$

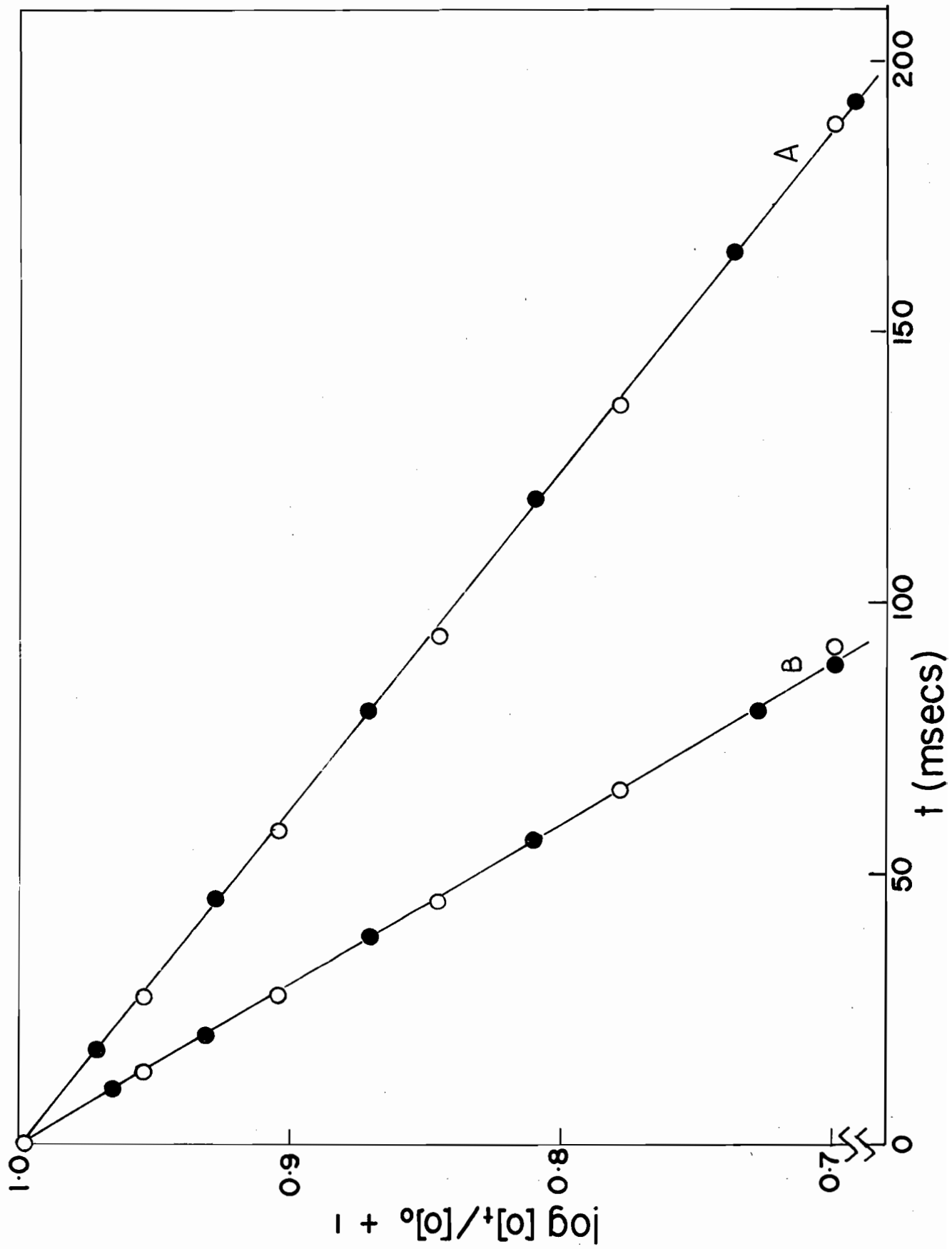
$$k_4 = 1 \times 10^{15} \text{ cm}^6 \text{ moles}^{-2} \text{ sec}^{-1}$$

Curve A : $[M] = [O_2] = 1.0 \times 10^{-7} \text{ moles cm}^{-3}$

$$[O]_0 = 5\% [O_2] = 0.5 \times 10^{-8} \text{ moles cm}^{-3}$$

Curve B : $[M] = [O_2] = 1.732 \times 10^{-7} \text{ moles cm}^{-3}$

$$[O]_0 = 5\% [O_2] = 0.866 \times 10^{-8} \text{ moles cm}^{-3}$$



BIBLIOGRAPHY

1. D.R. Bates, 'The Earth as a Planet', pp. 576-591.
Edited by G.P. Kuiper, University of
Chicago Press (1954).
2. H.W. Ford and N. Endow, J. Chem. Phys., 27, 1156 (1957).
Ibid. 27, 1277 (1957).
3. G.B. Kistiakowski, J. Am. Chem. Soc., 37, 417 (1915).
4. W.D. McGrath and R.G. Norrish, Proc. Roy. Soc.,
A242, 265 (1957).
- 4a. W.D. McGrath and R.G. Norrish, Proc. Roy. Soc.,
A254, 317 (1960).
5. J.Y. McDonald, J. Chem. Soc., p. 1 (1928).
6. W.A. Noyes, Jr., J. Chem. Phys., 2, 807 (1937).
7. F.C. Henriques, A.B.F. Duncan and W.A. Noyes, Jr.,
J. Chem. Phys., 6, 518 (1938).
8. R.J. Cvetanovic, J. Chem. Phys., 23, 1203 (1955).
9. R. Glissman and H.J. Schumacher, Z. Phys. Chem.
B21, 323 (1933).
10. S.W. Benson and A.E. Axworthy, J. Chem. Phys., 26, 1718 (1957)
11. J.A. Zaslowsky, H.B. Urbach, F. Leighton, R.J. Wnuk
and J.A. Wojtowicz, J. Am. Chem. Soc., 82, 2682 (1960).
- 11a. J.A. Zaslowsky, H.B. Urbach, F. Leighton, R.J. Wnuk
and J.A. Wojtowicz, Abstracts 135th Meeting Am. Chem.
Soc., p. 23R (1959).
- 11b. J.A. Zaslowsky, H.B. Urbach, F. Leighton, R.J. Wnuk
and J.A. Wojtowicz, Abstracts 136th Meeting Am. Chem.
Soc., p. 46S, p. 47S (1959)
12. W.M. Jones and N. Davidson, Abstracts 135th Meeting
Am. Chem. Soc., p. 37R (1959).
13. L. Elias, Private communication.
14. H.S. Glick, J.J. Klein and W. Squire, J. Chem. Phys.,
27, 850 (1957).
15. H.S. Glick and W.H. Wurster, J. Chem. Phys., 27, 1224 (1957).

16. R.A. Strenlow and A. Cohen, *J. Chem. Phys.*, 30, 257 (1959).
17. D.L. Matthews, *Phys. Fluids*, 2, 170 (1959).
18. S.R. Byron, *J. Chem. Phys.*, 30, 1380 (1959).
19. M. Camac and A. Vaughan, *J. Chem. Phys.*, 34, 460 (1961).
20. J.P. Rink, H.T. Knight and R.E. Duff, *J. Chem. Phys.*,
34, 1942 (1961).
21. H.S.W. Massey and L.H.S. Burhop, 'Electronic and Ionic
Impact Phenomena', Oxford University Press,
London and New York (1952).
22. R.W. Wood, *Phil. Mag.*, 44, 538 (1922).
23. G.C. Fryburg, *J. Chem. Phys.*, 24, 175 (1956).
24. J.H. Greenblatt and C.A. Winkler, *Can. J. Chem.*,
27B, 721 (1949).
25. M.A. Heald and R. Beringer, *Phys. Rev.*, 96, 645 (1954).
26. A.G. Prodel and P. Kusch, *Phys. Rev.*, 106, 87 (1957).
27. H.L. Garvin, T.M. Green and E. Lidworth, *Phys. Rev.*,
111, 534 (1958).
28. D.E. Nagle, R.J. Julian and J.R. Zacharias, *Phys. Rev.*,
72, 971 (1947).
29. H.P. Broida and J.W. Moyer, *J. Opt. Soc. Am.*, 42, 37 (1952).
30. H.P. Broida and J.R. Pellam, *Phys. Rev.*, 95, 845 (1954).
Ibid. 23, 409 (1955).
31. H.P. Broida and M.W. Chapman, *Anal. Chem.*, 30, 2049 (1958).
32. F. Kaufman, *Proc. Roy. Soc.*, A247, 123 (1958).
J. Chem. Phys., 28, 978 (1958).
33. P. Harteck and V. Kopsch, *Z. Phys. Chem.*, B12, 327 (1931).
34. J.W. Linnett and D.G.H. Marsden, *Proc. Roy. Soc.*,
A234, 489, 504 (1956).
35. J.C. Greaves and J.W. Linnett, *Trans. Faraday Soc.*,
54, 1323 (1958).
36. D.G.H. Marsden and J.W. Linnett, p. 685, 5th Comb. Symp.,
Reinhold, New York (1955).

37. J.C. Greaves and J.W. Linnett, *Trans. Faraday Soc.*, 55, 1338 (1959).
38. P. Harteck, *Z. Phys. Chem.*, A139, 98 (1928).
39. E. Wrede, *Z. Instrumentenkunde*, 48, 201 (1928).
40. E.L. Tollefson and D.J. Le Roy, *J. Chem. Phys.*, 16, 1057 (1948).
41. L. Elias, E. Ogryzlo and H.I. Schiff, *Can. J. Chem.*, 37, 1680 (1959).
42. S.N. Foner and R.L. Hudson, *J. Chem. Phys.*, 25, 601 (1956).
43. J.T. Herron and H.I. Schiff, *Can. J. Chem.*, 36, 1159 (1958).
- 43a. D.S. Jackson and H.I. Schiff, *J. Chem. Phys.*, 23, 233 (1955).
44. H.D. Beckey and P. Warneck, *Z. Naturforsch.*, 10a, 62 (1955).
45. W. Groth and P. Warneck, *Z. Phys. Chem.*, 10, 323 (1957).
46. R.A. Sharpless, K.C. Clarke and R.A. Young, *Rev. Scient. Instr.*, 32, 532 (1961).
47. M.L. Spealman and W.H. Rodebush, *J. Am. Chem. Soc.*, 57, 1474 (1936).
48. R.R. Reeves, G. Manella and P. Harteck, *J. Chem. Phys.*, 32, 632 (1960).
49. S. Krongelb and M.W.P. Strandberg, *J. Chem. Phys.*, 31, 1196 (1959).
50. E.S. Campbell and C. Nudelman, U.S. AFOSR TN-60-502.
51. D.L. Chapman and H.E. Jones, *J. Chem. Soc.*, 97, 2463 (1910).
52. H.E. Clarke and D.L. Chapman, *J. Chem. Soc.*, 93, 1638 (1908).
53. J.K. Clement, *Ann. Physik.*, 14, 334 (1904).
54. R.O. Griffith and A. McKeon, *J. Chem. Soc.*, 127, 2086 (1925).
55. S. Jahn, *Z. Anorg. Chem.*, 48, 26 (1906).
56. E.P. Perman and R.H. Greaves, *Proc. Roy. Soc.*, A80, 353 (1908).
57. E. Warburg, *Ann. Physik*, 9, 1286 (1902).
58. A. Glissman and H.J. Schumacher, *Z. Physik. Chem.*, 821, 323 (1933).
- 58a. H.J. Schumacher, *Proc. Roy. Soc.*, A150, 220 (1935).

59. M. Ritchie, Proc. Roy. Soc., A146, 848 (1934).
60. H.J. Schumacher, Z. Physik. Chem., B17, 405 (1932).
61. U. Beretta and H.J. Schumacher, Z. Physik. Chem.,
B17, 417 (1932).
- 61a. S. Ya Pshezhetskii, N.M. Morozov, S.A. Kamenetskaya,
V.N. Siryatskaya and E.I. Gribova, Zhur. Fiz. Chim.,
23, 2306 (1959).
- 61b. L.F. Phillips and H.I. Schiff, J. Chem. Phys., 37, 924 (1962).
62. H.J. Schumacher, J. Chem. Phys., 33, 938 (1960).
- 62a. H.J. Schumacher, J. Chem. Phys., 36, 2238 (1962).
63. S.W. Benson, J. Chem. Phys., 33, 939 (1960).
64. J.C. Greaves and J.W. Linnett, Trans. Faraday Soc.,
55, 1346 (1959).
65. J.C. Greaves and J.W. Linnett, Trans. Faraday Soc.,
55, 1355 (1959).
66. W.V. Smith, J. Chem. Phys., 11, 110 (1943).
67. V.V. Veovodskii and G.K. Lavrovskaya, Chem. Abs.,
43, 1635d (1949).
46, 2893c (1952).
68. F. Kaufman, 'Progress in Reaction Kinetics', Vol. I,
Pergamon Press (1961).
69. P. Harteck, R.R. Reeves and G. Manella, J. Chem. Phys.,
29, 1333 (1958).
70. C.B. Kretschmer, U.S. AFOSR-TR-59-62.
71. D.S. Hacker, S.A. Marshall and M. Steinberg,
J. Chem. Phys., 35, 1788 (1960).
72. P.G. Dickens, R.D. Gould, J.W. Linnett and A. Richmond,
Nature, 187, 686 (1960).
73. P. Harteck and R.R. Reeves, U.S. AFOSR-TR-57-50.
74. C.B. Kretschmer and H.L. Petersen, J. Chem. Phys.,
33, 948 (1960).
75. L.F. Phillips and H.I. Schiff, J. Chem. Phys.,
36, 1509 (1962).

76. R.H. Fowler and E.A. Guggenheim, 'Statistical Thermodynamics', pp. 505 et seq, Cambridge University Press (1939).
77. E.P. Wigner, J. Chem. Phys., 5, 720 (1937).
Ibid. 7, 616 (1939).
78. P. Brix and G. Herzberg, J. Chem. Phys., 28, 978 (1958).
79. J.A. Golden and A.L. Myerson, J. Chem. Phys., 28, 978 (1958).
80. F.A. Jenkins, H.A. Barton and R.S. Mulliken,
Phys. Rev., 30, 150 (1927).
81. Y. Tanaka, J. Chem. Phys., 22, 2045 (1954).
82. A.G. Gaydon, Proc. Roy. Soc., 56, 95, 160 (1944).
83. B.M. Anand, P.N. Kalia and Mela Ram, Ind. J. Phys.,
17, 69 (1943).
84. H.P. Knaus, Phys. Rev., 54, 176 (1938).
85. F. Kaufman and J.R. Kelso, J. Chem. Phys., 27, 1209 (1957).
86. F. Kaufman and J.R. Kelso, 7th Combustion Symposium,
2, 53 (1958).
87. G.B. Kistiakowsky and G.G. Volpi, J. Chem. Phys.,
27, 1141 (1957).
88. G.B. Kistiakowsky and G.G. Volpi, J. Chem. Phys.,
28, 665 (1958).
89. M.A.A. Clyne and B.A. Thrush, Proc. Roy. Soc.,
A261, 259 (1961).
90. L.F. Phillips and H.I. Schiff, J. Chem. Phys.,
36, 1509 (1962).
91. J.T. Herron, J. Chem. Phys., 35, 1138 (1961).
92. G.J. Verbeke and C.A. Winkler, J. Phys. Chem., 64, 319 (1960).
93. J. Kaplan, W.J. Schade, C.A. Barth and A.F. Hildebrant,
Can. J. Chem., 38, 1688 (1960).
94. G.M. Harris, J. Phys. and Colloid Chem., 51, 505 (1947).
95. K.G. Denbigh, Trans. Faraday Soc., 40, 352 (1944).
Ibid. 44, 479 (1948).

96. B. Stead, F.M. Page and K.G. Denbigh, *Disc. Faraday Soc.*,
2, 263 (1947).
97. O.A. Hougen and K.M. Watson, *Chem. Process Principles*,
Part III, p. 834, John Wiley & Sons,
New York (1947).
98. F. Kaufman, Private communication.

PART II

A STUDY OF VIBRATIONALLY EXCITED NITROGEN
PRODUCED BY A MICROWAVE DISCHARGE AND
BY CHEMICAL REACTION

I. INTRODUCTION

Vibrational excitation of diatomic molecules

The classical treatment of energy distribution among the various degrees of freedom of a molecule ascribes a contribution of $\frac{1}{2}kT$ to each square term.

For a gaseous diatomic molecule with three translational degrees of freedom (three square terms) two rotational degrees of freedom (two square terms) and one vibrational degree of freedom (two square terms) the total energy, excluding electronic contributions, would be expected to be $\frac{3}{2} kT + kT + kT = \frac{7}{2} kT$ per molecule or $\frac{7}{2} RT$ per mole. This would correspond to a heat capacity at constant volume of

$$C_v = \left(\frac{dE}{dT} \right)_v = \frac{7}{2} R \text{ per degree per mole.}$$

The observed fact that most diatomic gases at room temperature have a molar heat capacity of approximately $\frac{5}{2} R$ would indicate that either the rotational or vibrational degrees of freedom are inoperative.

The quantum mechanical explanation of this is simple. All of these terms of energy are quantized, but the translational and to a lesser extent the rotational energy levels are sufficiently closely spaced to allow a virtually continuous increase of energy with temperature. They can therefore be treated classically and can be expected to contribute $\frac{1}{2}RT$ per square term per mole to the total energy.

On the other hand, the vibrational levels are sufficiently widely spaced that excitation even to the first level is negligible, in most cases, at room temperature, and the vibrational energy reaches the classical value only at very high temperatures.

This is shown clearly by the following brief description of the statistical treatment of the vibrational energy of a harmonic oscillator⁽¹⁾.

The Maxwell-Boltzman law governing the statistical distribution of a number of molecules among a range of available energy levels has the form

$$N_i = \frac{N_0}{g_0} g_i e^{-\epsilon_i/kT} \dots\dots\dots (1)$$

where N_i = number of molecules in the i^{th} level.

N_0 = number of molecules in the 0^{th} level.

ϵ_i = energy of the i^{th} level with respect to the 0^{th} level.

g_i and g_0 are the degeneracies of the i^{th} and 0^{th} levels respectively and are introduced to allow for the possibility that there may be more than one level with an energy equal (or close to) ϵ_i .

The total number of molecules, N , is then given by

$$N = \sum_{i=0}^{\infty} N_i = \frac{N_0}{g_0} \sum_{i=0}^{\infty} g_i e^{-\epsilon_i/kT} = \frac{N_0}{g_0} Q \dots\dots\dots (2)$$

This equation defines the 'partition function', Q .

The total energy in excess of the zero point energy is therefore

$$E = \sum_{i=0}^{\infty} n_i \epsilon_i \quad \text{with } \epsilon_0 = 0.$$

Replacing $\frac{N_0}{g_0}$ in (1) by $\frac{N}{Q}$ from (2) yields

$$E = \frac{N}{Q} \sum_{i=0}^{\infty} \epsilon_i g_i e^{-\epsilon_i/kT}$$

Now

$$\frac{dQ}{dT} = \frac{1}{kT^2} \sum_{i=0}^{\infty} \epsilon_i g_i e^{-\epsilon_i/kT}$$

Therefore

$$E = \frac{NkT^2}{Q} \frac{dQ}{dT} = RT^2 \frac{d \ln Q}{dT} \quad \text{per mole} \dots (3)$$

For a harmonic oscillator, it can be shown that the energy of the v^{th} level is given by

$$\epsilon_v = (v + \frac{1}{2}) hc\omega$$

where v is integral and $hc\omega$ is the energy spacing between adjacent levels.

Since it is only necessary to consider the energy of a particular level with respect to the zeroth level, it can be seen that the energy term to be used in evaluating Q is given by

$$\epsilon_i = ihc\omega$$

Furthermore, these levels are non-degenerate, i.e. the g_i 's are all equal to unity.

$$\text{Therefore } Q = \sum_{i=1}^{\infty} e^{-ix} \quad \text{where } x = \frac{hc\omega}{kT}$$

$$= (1 - e^{-x})^{-1}$$

Differentiation with respect to T and substitution in (3) then yields

$$E_{\text{vib}} = RT \frac{x}{(e^x - 1)}$$

For a nitrogen molecule $\omega = 2352 \text{ cm}^{-1}$ (2)

Therefore at $T = 300$

$$x = 11.28$$

Thus the vibrational energy of a nitrogen molecule is effectively zero at room temperature.

Alternatively, Equation (1) shows that

$$\frac{N_1}{N_0} = e^{-x} \approx 1.3 \times 10^{-5}$$

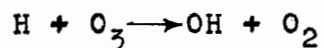
It is therefore apparent that any appreciable population of the levels above the zeroth in a gaseous system kinetically at room temperature will correspond to an extreme non-equilibrium system.

However, such systems have been produced both as the result of chemical reaction and also of electrical discharge. Vibrational energies in some cases of more than 30 kcal mole⁻¹ have been observed. This corresponds to vibrational temperatures in excess of 15,000°K. In such systems both the distribution of the energy among the vibrational levels and the rate of relaxation are of considerable interest.

Vibrational excitation produced by
chemical reaction

The first authenticated reaction shown to produce vibrational excitation of the products involved the reaction

of hydrogen atoms with ozone. Garvin et al.^(3,4) found that the reaction



which is exothermic to the extent of 77 kcal mole⁻¹ produced vibrationally excited hydroxyl radicals. The highest vibrational level observed was that with $v'' = 9$, corresponding to an energy of 75 kcal mole⁻¹. This reaction has been the subject of later study, and Garvin, Broida and Kostkowski⁽⁵⁾ observed significant concentrations in all the levels up to and including the ninth.

The problem of whether the initial distribution is a delta function at $v'' = 9$ followed by rapid relaxation, as contrasted with simultaneous production in all levels with $v'' \leq 9$, has not yet been resolved, although the above authors favour the latter on the basis of the kinetics of the relaxation.

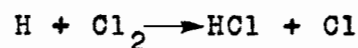
Lipscombe, Norrish and Thrush⁽⁶⁾ have observed vibrationally excited oxygen with energies up to 34 kcal mole⁻¹ ($v'' = 8$) formed in the reactions:



The excited O_2 was observed spectroscopically, and these authors found that the rate of decay from the sixth level was faster than that from either adjacent level. This has been argued in favour of an initial non-equilibrium distribution, but a lack of knowledge of the detailed

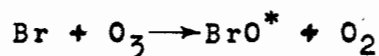
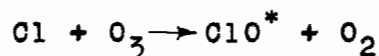
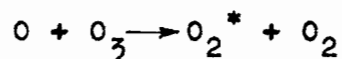
kinetics of the relaxation makes this argument somewhat less than compelling.

However, Cashion and Polanyi⁽⁷⁾ have shown that vibrationally excited HCl produced in the reaction



behaves qualitatively like a system relaxing from an initially sharp energy distribution.

Vibrationally excited O₂, ClO and BrO have also been observed by McGrath and Norrish⁽⁸⁾ in the following reactions



where the asterisk both here and subsequently is used to denote an excited state.

A series of reactions of the type



have been investigated by Basco and Norrish^(9,10) where HR was H₂, HCl, H₂O, NH₃ and CH₄.

In all cases vibrationally excited OH was found in the first and second vibrational levels. It was also found necessary to use ¹D oxygen atoms, since ground state (³P) atoms led to endothermic reactions. These reactions are significant in that they demonstrate a direct conversion of electronic to vibrational energy.

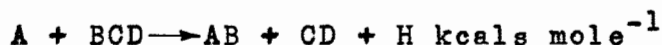
Numerous other examples of the formation of

vibrationally excited products have been investigated by Cashion and Polanyi^(11,12).

Two facts are very evident from the foregoing examples:

- (i) All of these reactions are considerably exothermic.
- (ii) The vibrational excitation appears to be located exclusively in the newly-formed bond.

Basco and Norrish⁽¹⁰⁾ have formulated, as a general principle, that a reaction of the type



leads to the accumulation of most of the exothermicity, H, in the newly-formed bond, AB, as vibrational energy. The fact that no reaction has yet been found in which all of the exothermicity enters the newly-formed bond has been regarded by these authors as a failure of experimental technique.

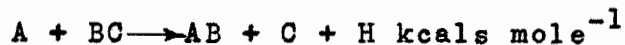
Simons⁽¹³⁾ has postulated the following model for the reaction



- (i) A approaches BCD with sufficient velocity that A is brought to rest very close to B with an inter-nuclear separation much less than the equilibrium separation in the isolated molecule.
- (ii) The bond, AB, must be strong relative to BC so that the complex dissociates readily and little of the impact of A is transferred to CD.
- (iii) There must be an attractive force between A and B strong enough to overcome the mutual repulsion of non-interacting particles.

The value of this model is somewhat doubtful, since the postulated requirements are to a large extent implicit in the required exothermicity of the reaction.

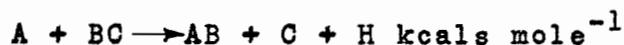
Polanyi⁽¹⁴⁾ has also examined this problem and has set up a valence bond model for the simpler three-body case



He arrived at the conclusion that the maximum energy that can be located in the bond, AB, is equal to $H + (E_{\text{act}} - E)$ where E_{act} = activation energy of the transition state complex.

E = small amount of energy which must be lost to stabilize the complex.

The most successful theoretical approach to estimating the maximum energy which can be located in the bond, AB, is that due to Smith⁽¹⁵⁾. For the reaction

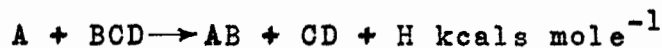


Smith has calculated a kinematic factor which limits the energy in the bond, AB, to $H \text{ Sin}^2 \beta$ where β is the angle of rotation required to take a co-ordinate system suitable for expressing the reactants into one suitable for expressing the products.

For the three-body case above, he finds

$$\text{Tan}^2 \beta = \frac{M_B}{M_A} + \frac{M_B}{M_C} + \frac{M_B^2}{M_A M_C}$$

For the four-body case



The energy located in the bond, AB, lies between $H \text{ Sin}^2 \beta$ and

$H \sin^2 \beta'$ where β is as defined above and β' is given by

$$\tan^2 \beta' = \frac{M_B}{M_A} + \frac{M_B}{M_C + M_D} + \frac{M_B^2}{M_A(M_A + M_C)}$$

According to Smith, this model predicts quite accurately the published experimental results.

However, Basco and Norrish⁽¹⁰⁾ have reported subsequent experimental results which do not agree with this treatment.

Vibrational excitation produced by electrical discharge

The production of vibrationally excited nitrogen molecules by electrical discharges has received comparatively little attention.

However, evidence has been reported in the literature for the presence in discharged nitrogen of an energetic species other than ground state atoms.

For example, Kaufman and Kelso⁽¹⁶⁾ have shown that introduction of nitrous oxide into a stream of discharged nitrogen resulted in a marked temperature rise in the neighbourhood of the inlet jet. They were also able to show that this energy release was not due to an accelerated recombination of nitrogen atoms and ascribed it to deactivation of vibrationally excited nitrogen molecules by the nitrous oxide. While the experiment was essentially qualitative in nature, they estimated the energy release as being of the order of 2 kcals per mole of total nitrogen. By introducing the nitrous oxide at a second point downstream

they estimated, from the difference in temperature rise, a half-life for the excited species of approximately 50 msec.

Subsequently Dressler⁽¹⁷⁾ examined discharged nitrogen spectroscopically and confirmed the presence of vibrationally excited nitrogen but observed no excitation beyond the first vibrational level. From the space average concentration over the observed length of the reaction tube, he was able to establish a lower limit for the half-life of 10 msec.

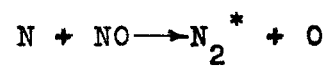
The present problem

The use of calorimetric probes to measure atom concentrations has been widespread.

Such probes measure either the temperature rise^(18,19) or the energy release^(20,21) resulting from atomic recombination on the probe surface. As was noted in Part I of this thesis, the possibility of a concomitant deactivation of other energetic species can lead to a lack of specificity which considerably reduces the utility of these probes in determining absolute atom concentrations.

If an independent method of determining the atom concentration is available, the energy release due to atom recombination can be calculated and compared with the experimentally observed value. Any discrepancy between these two values can thus be attributed to the simultaneous deactivation of species other than atoms on the probe surface. This has been utilized in the present investigation to study both the vibrationally excited nitrogen originating in the

discharge and also that originating from the reaction



which is exothermic to the extent of 75 kcals.

II. EXPERIMENTAL

Apparatus

The apparatus and materials were as described in Part I with the exception that the movable jet assembly, J_3 , (Fig. 1, Part I, p. 48) was replaced by a movable isothermal catalytic detector (referred to subsequently as the 'detector').

Detector Assembly:

The detector used in this work was similar to that described by Elias, Ogryzlo and Schiff⁽²¹⁾. Details of the detector and associated circuitry are shown in Figs. 1 and 2.

Essentially it consists of a filament, F, made from approximately 100 cms of 27 B & S gauge platinum wire with a resistance at room temperature of about 1Ω . This filament could be located at any desired position in the reaction tube by means of the rack and pinion gear. Flexible leads from the filament were taken out through tungsten-nonex seals and allowed the filament to be connected into one arm of the Wheatstone bridge shown in Fig. 2.

Operation of detector

The method of operation of the detector was as follows.

Current from the six-volt storage battery, B, was fed to the filament through the variable resistance network R_1 , R_2 , R_3 and R_4 . The values chosen for these resistors were such that the filament current could be controlled between

Figure 1

MOVABLE DETECTOR ASSEMBLY

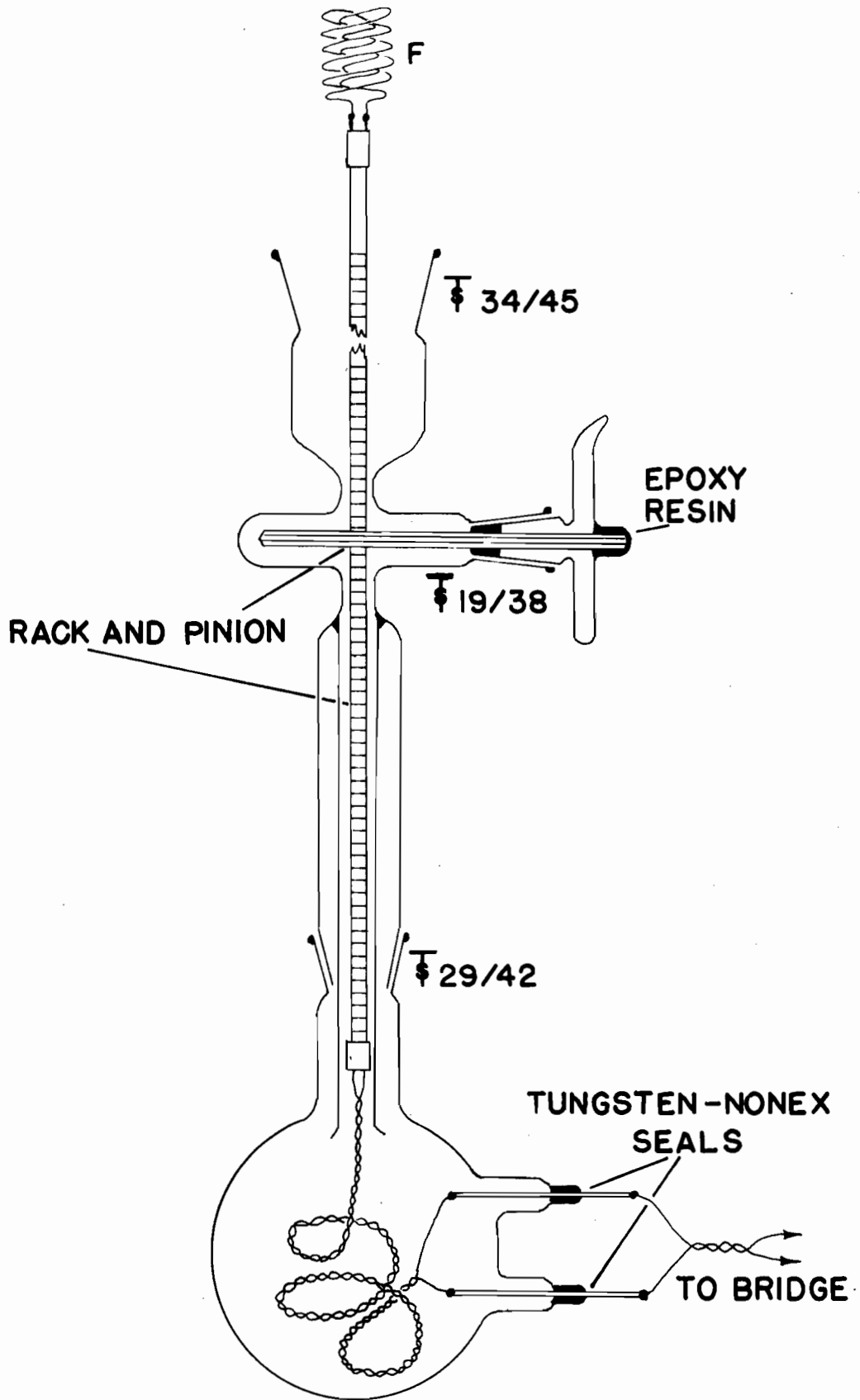
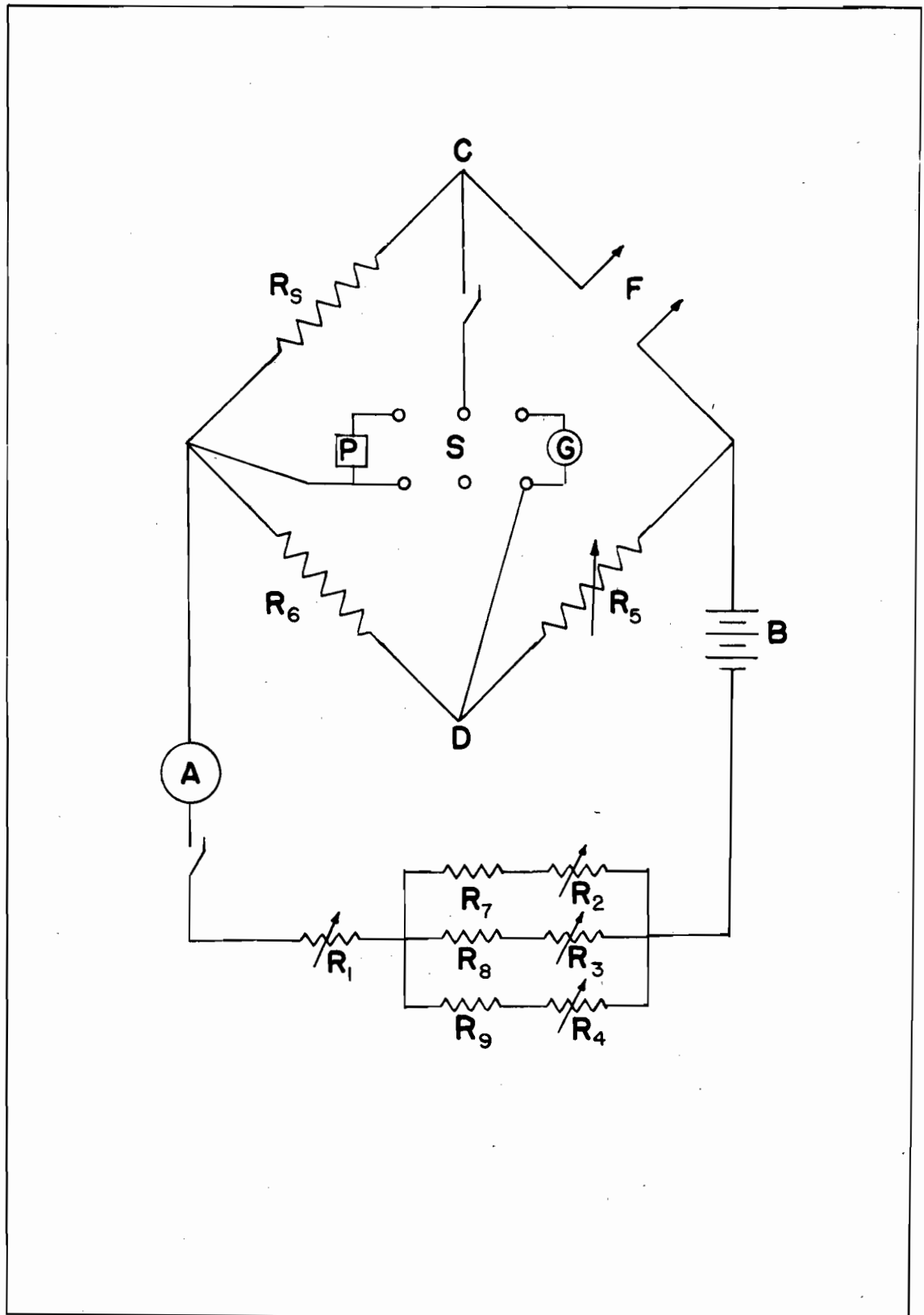


Figure 2

BRIDGE CIRCUIT FOR DETECTOR

- R_s - Standard 1.00 Ω resistor
- F - Leads to detector
- P - Potentiometer
- G - Galvanometer
- S - Double-pole double-throw switch
- R₁ - 0 - 1K Ω variable resistor
- R₂ - 0 - 20 Ω variable resistor
- R₃ - 0 - 50 Ω variable resistor
- R₄ - 0 - 250 Ω variable resistor
- R₅ - 0 - 10K Ω decade resistance
- R₆ - 1K Ω
- R₇ - 5 Ω
- R₈ - 50 Ω
- R₉ - 250 Ω
- A - Ammeter
- B - 6 volt storage battery



0 - 1 amp with an accuracy of better than one milliamp. The double pole double throw switch, S, allowed either a potentiometer, P, to be connected across the standard 1Ω resistor, R_s , or a galvanometer, G, across the points C,D.

The decade resistor, R_5 , was then set to some predetermined value and the current through R_s and F adjusted until the bridge was balanced as indicated by the galvanometer.

This balanced condition implies that the temperature of F was such that its resistance was equal to $R_5/1000$.

The potentiometer was then connected into the circuit by means of the switch, S, and the potential drop, E_o , determined across R_s . In this way the resistance of the filament, R_F , and the current flow can be accurately measured.

The power dissipated by the filament was then calculated as follows:

$$P_o = \frac{I_o^2 R_F}{4.186} \text{ cal sec}^{-1}$$

$$\text{where } I_o = \frac{E_o}{R_s}$$

$$R_F = \left(\frac{R_5}{1000} - \text{lead resistance of detector} \right)$$

If energy is now liberated on the filament by, for example, atomic recombination, the temperature, and hence the resistance, of the filament will increase causing an unbalance in the bridge. The bridge can be rebalanced,

however, by decreasing the current flowing through the filament to some value, I_f , such that the original temperature and resistance are restored. The electrical power supplied to the filament is now

$$P_f = \frac{I_f^2 R_f}{4.186} \text{ cal s}^{-1}$$

The change in electrical power, $(P_o - P_f)$, can then be equated to the rate of energy release to the filament due to atomic recombination, i.e.

heat released on the probe by atom recombination

$$= f \frac{D}{2} \text{ cal s}^{-1}$$

where f = atom flow rate.

D = dissociation energy of the parent diatomic molecule.

The atom flow rate can then be calculated from

$$f = \frac{2(I_o^2 - I_f^2)R}{4.186 D} \dots\dots\dots (1)$$

This equality is only valid provided:

(i) All the atoms reaching the probe surface are recombined.

(ii) The energy released in the probe is due only to atom recombination.

This first condition can be met by using an efficient surface of sufficient area such that the atom flow rate downstream from the probe is zero.

The second condition forms the basis of this investigation. Since in the system described in Part I f is known independently, any inequality in expression (1) can be attributed to deactivation on the probe of a species other than ground state atoms.

Preparation of the catalytic surface

(a) For use in the oxygen-atom system:

Elias, Ogryzlo and Schiff⁽²¹⁾ have found silver peroxide to be a very effective catalyst for oxygen-atom recombination.

In this work a silver coating was applied to the filament by electroplating from a dilute solution of carefully purified potassium silver cyanide. The adherent silver coating thus formed was then thoroughly washed with distilled water and dried in vacuo.

Exposure of the clean silver coating to a stream of atomic oxygen then rapidly converted the silver to black silver peroxide. It was found advisable not to use too thick a layer of silver otherwise, on conversion to oxide, it tended to flake off. Furthermore, care had to be taken to ensure that the silver was completely oxidized before the detector was used for quantitative studies, otherwise heat is released to the probe from continuing oxidation.

(b) For use in a nitrogen-atom system:

The catalytic surface prepared above was found to be unsatisfactory for recombining nitrogen atoms. However, an

electroplated layer of copper was found to be very efficient and terminated the discharged nitrogen afterglow very abruptly at the surface of the filament.

Unfortunately a copper surface appeared to liberate some volatile material under these conditions which resulted in contamination of the walls of the reaction tube. This contamination, if sufficiently great, was capable of terminating the afterglow even after the filament was withdrawn downstream. Less severe contamination resulted in a marked decrease in intensity of the afterglow and was accompanied by a greenish fluorescence on the walls of the reaction tube.

After examining several other surfaces, it was found that cobalt was quite effective and did not produce the wall contamination experienced with copper.

The cobalt was electroplated on to the clean platinum filament from a solution made up as follows.

To approximately 100 mls of a 1% solution of cobalt sulphate (hexahydrate) was added concentrated ammonia until the initial precipitate of cobalt hydroxide was just redissolved. It was found that a clear solution was not obtained immediately even in the presence of excess ammonia. However, the solution slowly cleared on standing to form a very dark reddish-brown liquid which was filtered before use. Alternatively, a clear solution could be obtained by the addition of about 1% ammonium chloride.

This solution was prepared freshly for each plating.

The greyish cobalt layer obtained by electrolysis from such a solution was then washed and dried as before.

III. RESULTS

An oxygen-atom system of known flow rate was produced as described in Part I.

With the detector at its lowest position in the reaction tube, the current through the filament, F , was adjusted to about 0.8 amps, as indicated by the ammeter, A , (Fig. 2). The resistance of R_5 was set to give an approximate balance of the Wheatstone bridge. Without further adjustment of R_5 the bridge was then accurately balanced by adjusting the current through the filament. The potential drop across R_5 ($= I_f$) was then determined and recorded. The detector was then moved upstream a few centimetres, the bridge rebalanced and the new value of I_f recorded. These measurements were repeated for decreasing values of d . The discharge was then turned off and the corresponding values of I_0 obtained. The results of such an experiment are shown in Table I and Fig. 3.

The first point on curve A in Fig. 3 represents the calculated heat release to the filament based on the known flow rate of oxygen atoms, i.e. $H_{\text{calc}}(t = 0) = f_{(0)} \frac{D}{2}$ where $D = 119 \text{ kcal mol}^{-1}$. With $f_{(0)}$ in units of micromoles sec^{-1} and D_{O_2} in units of kcal mol^{-1} , H_{calc} is given directly by this relation in units of millicals sec^{-1} .

The variation of H_{calc} with t was then calculated from the rate constants for oxygen-atom recombination obtained in Part I.

Table I

$P = 3.80 \text{ mm Hg}$ $N_2 \text{ flow} = 164 \text{ micromoles sec}^{-1}$
 $T = 21^\circ\text{C}$ $NO \text{ flow} = 1.36 \text{ micromoles sec}^{-1} = 0 \text{ flow}$
 $R = 1.500\Omega$ $H_{\text{calc}}(t=0) = 1.36 \times 59.5 = 79.5 \text{ mcals sec}^{-1}$
 Lead resistance = 0.216Ω

| t msecs | I_o amps | I_f amps | H_{exp} mcals sec^{-1} | $\Delta H =$ $H_{\text{exp}} - H_{\text{calc}}$ mcals sec^{-1} | $\ln(\Delta H)$ |
|--------------|---------------|---------------|---|---|-----------------|
| 202 | 0.841 | 0.634 | 93 | 31.0 | 3.434 |
| 181.5 | 0.842 | 0.610 | 102 | 38.0 | 3.638 |
| 161 | 0.842 | 0.590 | 110 | 44.0 | 3.784 |
| 141 | 0.842 | 0.565 | 118 | 51.3 | 3.938 |
| 121 | 0.841 | 0.531 | 130 | 61.0 | 4.111 |
| 101 | 0.840 | 0.492 | 142 | 72.3 | 4.281 |
| 80.5 | 0.840 | 0.440 | 157 | 85.4 | 4.447 |
| 60.5 | 0.835 | 0.362 | 176 | 102.3 | 4.627 |
| 40.2 | 0.835 | 0.249 | 195 | 120.0 | 4.788 |

Figure 3

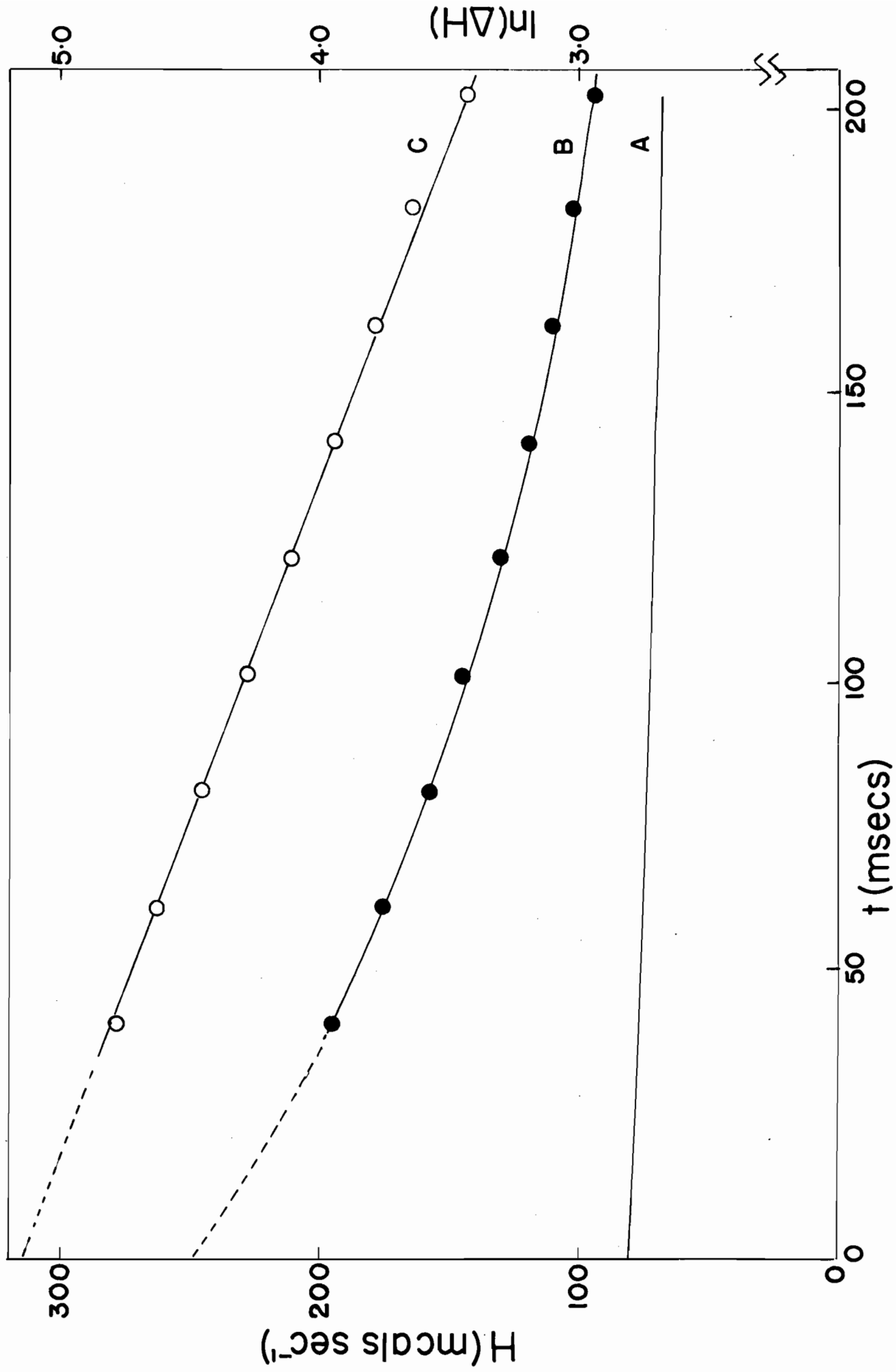
DETECTOR MEASUREMENTS IN AN OXYGEN-ATOM
SYSTEM PRODUCED BY TITRATION OF N-ATOMS WITH NO

(Data from Table I)

Curve A - Calculated heat release
to detector (H_{calc})

Curve B - Measured heat release
to detector (H_{exp})

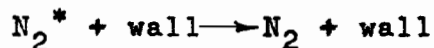
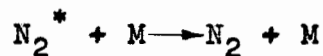
Curve C - Plot of $\ln(H_{\text{exp}} - H_{\text{calc}})$
= $\ln(\Delta H)$



Curve B, denoted by H_{exp} , was obtained from the measured heat release to the filament.

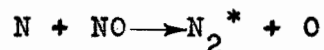
The discrepancy between these two curves is very apparent. However, it can be seen that H_{exp} approaches H_{calc} as t becomes very large. This is shown clearly by curve C which is a plot of $\ln \Delta H$ against t , where

$\Delta H = H_{\text{exp}} - H_{\text{calc}}$. The linearity of this plot shows that ΔH is decaying exponentially to zero. Furthermore, the energetic species responsible for ΔH must therefore be decaying by a first order reaction. If this species is denoted by N_2^* , the first order decay can be most simply explained by a collisional deactivation process such as



The identity and origin of the species denoted by N_2^* , however, is open to speculation.

From the preceding introductory remarks, it is possible that it could be vibrationally excited nitrogen molecules produced in the titration reaction



This reaction is exothermic to the extent of about 75 kcal/mole⁻¹ and therefore fulfils the postulated conditions for the production of vibrationally excited nitrogen.

The molar flow rate of N_2^* produced in this reaction, however, must obviously be equal to or less than

the oxygen-atom flow rate, i.e. $f(N_2^*)_{t=0} \leq 1.36 \mu\text{mole sec}^{-1}$ in this particular experiment. From Fig. 3 it can be seen that the corresponding value of $(\Delta H)_{t=0}$ is 170 mcals sec^{-1} . Therefore the energy content of N_2^* must be equal to or greater than 125 kcals mole^{-1} . Since the maximum excitation which can be produced by the titration reaction corresponds to an energy of 75 kcals mole^{-1} , it obviously cannot be the sole source of the excess energy measured by the detector.

One obvious alternative is that the energetic species is already present in the discharged nitrogen stream. To examine this possibility the following experiment was performed.

A discharged nitrogen stream was first titrated to the end-point with nitric oxide. The nitric acid flow rate was then measured and the nitric oxide flow discontinued. This resulted in a nitrogen-atom stream of known nitrogen-atom flow rate. Detector measurements were then made in this nitrogen-atom system, using a cobalt plated filament. The results of such an experiment are shown in Table II and Fig. 4.

As before, the first point on curve A represents the calculated heat release to the filament based on the known nitrogen-atom flow rate, i.e. $H_{\text{calc}}(t=0) = f(N)_0 \frac{D_{N_2}}{2}$ where D_{N_2} = dissociation energy of N_2
= 225 kcals mole^{-1} .

Table II

P = 1.65 mm Hg N₂ flow = 72 micromoles sec⁻¹
 T = 22.5°C NO flow = 0.5 micromoles sec⁻¹ = N flow
 R = 1.570Ω H_{calc}(t = 0) = 0.5 x 112.5 = 56.3 mcals sec⁻¹
 Lead resistance = 0.217Ω

| t | I _o | I _f | H _{exp} | H _{calc} | ΔH | ln(ΔH) |
|-------|----------------|----------------|-------------------------|-------------------------|-------------------------|--------|
| msecs | amps | amps | mcals sec ⁻¹ | mcals sec ⁻¹ | mcals sec ⁻¹ | |
| 166 | 0.803 | 0.6550 | 69.9 | 50.6 | 19.3 | 2.960 |
| 153 | 0.803 | 0.6500 | 72.0 | 51.0 | 21.0 | 3.045 |
| 139 | 0.803 | 0.6417 | 75.5 | 51.5 | 24.0 | 3.178 |
| 126 | 0.803 | 0.6340 | 78.7 | 52.0 | 26.7 | 3.285 |
| 113 | 0.803 | 0.6270 | 82.5 | 52.4 | 30.1 | 3.405 |
| 99.5 | 0.803 | 0.6190 | 85.6 | 52.9 | 32.7 | 3.487 |
| 86 | 0.803 | 0.6070 | 89.5 | 53.3 | 36.2 | 3.589 |
| 73 | 0.803 | 0.5940 | 94.6 | 53.6 | 41.0 | 3.714 |
| 59.6 | 0.803 | 0.5810 | 99.5 | 54.3 | 45.2 | 3.811 |
| 46.4 | 0.803 | 0.5640 | 106.0 | 54.7 | 51.3 | 3.938 |
| 33.2 | 0.803 | 0.5440 | 113.0 | 55.1 | 57.9 | 4.059 |

Figure 4

DETECTOR MEASUREMENTS IN A

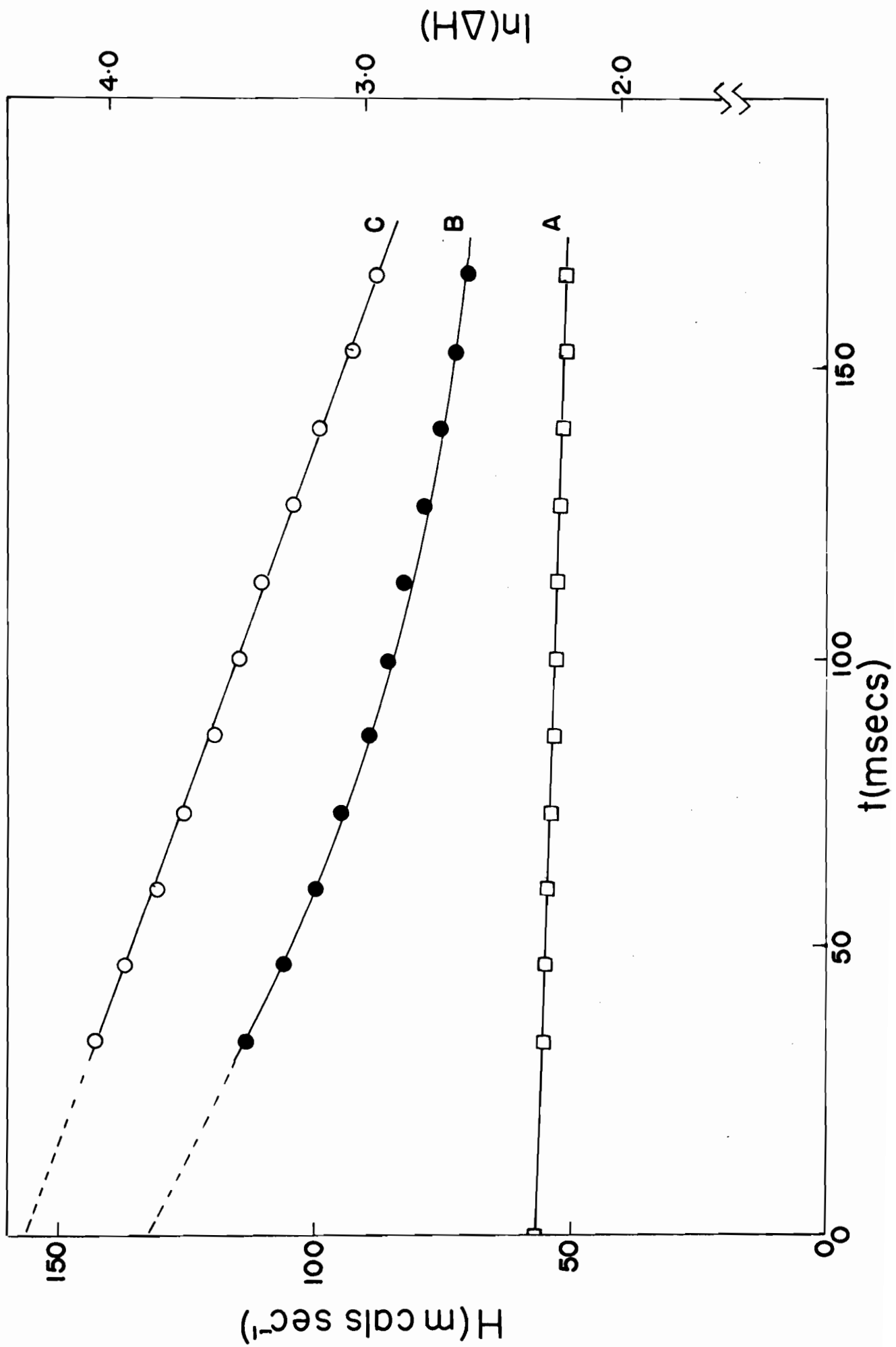
NITROGEN-ATOM SYSTEM

(Data from Table II)

Curve A - Calculated heat release
to detector (H_{calc})

Curve B - Measured heat release
to detector (H_{exp})

Curve C - Plot of $\ln(H_{\text{exp}} - H_{\text{calc}})$
= $\ln(\Delta H)$



The decrease of $f_{(N)}$ and hence H_{calc} with t was obtained from measurements of the nitrogen afterglow intensity with the photomultiplier tube. It has been shown⁽²²⁾ that this intensity is proportional to the square of the nitrogen-atom concentration, and thus curve A can be readily calculated.

Curves B and C are plots of H_{exp} and ΔH respectively, where $\Delta H = H_{exp} - H_{calc}$.

Since the discrepancy between H_{exp} and H_{calc} is still present, it is obvious that a major portion of the energetic species found in the oxygen-atom system must be attributed to an energetic species present in discharged nitrogen.

It was found, however, in subsequent experiments using a different tank of nitrogen that this discrepancy between H_{exp} and H_{calc} had disappeared. Although rather puzzling at first sight, this must be attributed to the presence of an impurity in one tank of nitrogen but not in the other.

The most likely impurity in the nitrogen is water vapour. It was found that removal of water vapour in the second case, by passage through two liquid air traps, resulted in the reappearance of the discrepancy between H_{exp} and H_{calc} . This treatment also resulted in the appearance of a localized bright pink glow about 10 cms downstream from the discharge. The normal yellow Lewis-Rayleigh afterglow was present both upstream and downstream from this region.

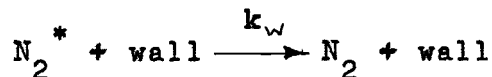
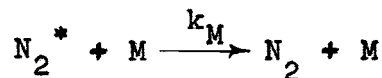
This phenomenon has been observed previously by Beale and Broida⁽²³⁾ who showed that it resulted from a transition between two states of N_2^+ . The upper state of this transition ($B^2 \sum_u^+$) has an energy of nearly 19 e.v. Although the mechanism of the production of this species has not yet been deduced, it is apparent that a large amount of energy must be available in discharged nitrogen. Since the energy of a ground state of nitrogen atom is 4.88 e.v., it is unlikely that nitrogen atoms are the immediate precursor of N_2^+ ($B^2 \sum_u^+$).

The disappearance of both N_2^+ and N_2^* on introduction of water vapour would suggest that these two species are intimately related. Whether N_2^* is the precursor of N_2^+ or vice versa cannot yet be answered.

In view of the sensitivity of N_2^* to traces of condensable impurity, all the subsequent experiments were performed using dried nitrogen.

Relaxation rate of N_2^*

The previously suggested collisional deactivation mechanism for N_2^*



leads to the following differential rate expression for the disappearance of N_2^*

$$-\frac{d[N_2^*]}{dt} = k_M [M] [N_2^*] + k_w [N_2^*]$$

Provided $[M]$ is constant, integration yields

$$- \ln [N_2]^* = (k_M [M] + k_W)t + C$$

Thus for a particular value of $[M]$ the slope of a plot of $\ln [N_2]^*$, [therefore $\ln(\Delta H)$], against t should yield a rate constant

$$k_{obs} = k_W + k_M [M].$$

A plot of k_{obs} against $[M]$ should then yield k_W and k_M from the intercept and slope respectively.

The results of such a series of experiments are shown in Table III.

Table III

| Expt. No. | P mm Hg | $[M] \times 10^7$ moles cm^{-3} | $k_{obs} = \frac{1}{t} \ln \frac{(\Delta H)_0}{(\Delta H)_t}$ sec^{-1} | $t_{\frac{1}{2}}$ msecs |
|-----------|------------|---|--|----------------------------|
| 250 | 2.3 | 1.24 | 8.73 \pm 0.2 | 79.5 |
| 251 | 2.95 | 1.60 | 8.70 \pm 0.2 | 79.5 |
| 252 | 4.10 | 2.22 | 8.73 \pm 0.2 | 79.5 |
| 253 | 5.84 | 3.14 | 9.10 \pm 0.2 | 76.1 |

DATA FOR TABLE III

Expt. No. 250

P = 2.3 mm Hg

N₂ flow = 132 μmoles sec⁻¹

T = 24°C

NO flow = 1.08 μmoles sec⁻¹

H_{calc}(t = 0) = 121.5 mcals sec⁻¹

| t | I _o | I _f | R | H _{exp} | H _{calc} | ΔH | ln(ΔH) |
|-------|----------------|----------------|-------|----------------------------|----------------------------|----------------------------|--------|
| msecs | amps | amps | ohms | mcals sec ⁻¹ | mcals sec ⁻¹ | mcals sec ⁻¹ | |
| 150 | 0.9995 | 0.6285 | 1.410 | 204 | 90 | 114 | 4.736 |
| 135 | 0.9965 | 0.5785 | 1.410 | 222 | 91.5 | 130 | 4.868 |
| 120 | 0.9940 | 0.5220 | 1.410 | 241 | 93.0 | 148 | 4.997 |
| 105 | 0.9930 | 0.4630 | 1.410 | 260 | 95.0 | 165 | 5.106 |
| 90 | 0.9915 | 0.3820 | 1.410 | 283 | 97.3 | 186 | 5.226 |
| 75 | 0.9900 | 0.1980 | 1.410 | 317 | 99.6 | 217 | 5.380 |
| 60 | 1.1000 | 0.5030 | 1.520 | 348 | 102.0 | 246 | 5.505 |
| 45 | 1.0950 | 0.3710 | 1.520 | 387 | 105.3 | 282 | 5.642 |
| 30 | 1.1090 | 0.1800 | 1.530 | 438 | 109.5 | 328 | 5.793 |

DATA FOR TABLE III

Expt. No. 251

P = 2.95 mm Hg

N₂ flow = 140 μmoles sec⁻¹

T = 24°C

NO flow = 1.085 μmoles sec⁻¹

H_{calc} (t = 0) = 122 mcals sec⁻¹

| t | I _o | I _f | R | H _{exp} | H _{calc} | ΔH | ln(ΔH) |
|-------|----------------|----------------|-------|----------------------------|----------------------------|----------------------------|--------|
| msecs | amps | amps | ohms | mcals sec ⁻¹ | mcals sec ⁻¹ | mcals sec ⁻¹ | |
| 182 | 0.9470 | 0.6190 | 1.360 | 168 | 89 | 79 | 4.369 |
| 163 | 0.9450 | 0.5680 | 1.360 | 185 | 90.5 | 94 | 4.543 |
| 145 | 0.9430 | 0.5360 | 1.360 | 202 | 93.0 | 109 | 4.691 |
| 127 | 0.9415 | 0.4590 | 1.360 | 222 | 95.4 | 127 | 4.844 |
| 109 | 0.9405 | 0.3485 | 1.360 | 248 | 98.3 | 150 | 5.011 |
| 91 | 0.9380 | 0.1995 | 1.360 | 273 | 101.0 | 172 | 5.142 |
| 72.5 | 1.0880 | 0.5650 | 1.500 | 309 | 104.0 | 205 | 5.323 |
| 54.5 | 1.0860 | 0.4620 | 1.500 | 350 | 108.0 | 242 | 5.489 |
| 36.4 | 1.0850 | 0.3220 | 1.500 | 385 | 112.0 | 273 | 5.609 |

DATA FOR TABLE III

Expt. No. 252

P = 4.10 mm Hg

N₂ flow = 148 μ moles sec⁻¹

T = 24°C

NO flow = 1.130 μ moles sec⁻¹

H_{calc} (t = 0) = 127 mcals sec⁻¹

| t | I _o | I _f | R | H _{exp} | H _{calc} | Δ H | ln(Δ H) |
|-------|----------------|----------------|-------|----------------------------|----------------------------|----------------------------|-----------------|
| msecs | amps | amps | ohms | mcals sec ⁻¹ | mcals sec ⁻¹ | mcals sec ⁻¹ | |
| 239 | 0.8910 | 0.6550 | 1.310 | 117 | 81.5 | 35.5 | 3.569 |
| 215 | 0.8880 | 0.6190 | 1.310 | 127 | 83.5 | 43.5 | 3.773 |
| 191 | 0.8865 | 0.5760 | 1.310 | 143 | 86.6 | 56.4 | 4.033 |
| 167 | 0.8870 | 0.5325 | 1.310 | 157 | 89.8 | 67.2 | 4.208 |
| 143 | 0.8840 | 0.4750 | 1.310 | 175 | 93.5 | 81.0 | 4.394 |
| 119 | 0.8835 | 0.3820 | 1.310 | 199 | 97.5 | 101.5 | 4.620 |
| 95.5 | 0.8810 | 0.2310 | 1.310 | 227 | 102.0 | 125.0 | 4.828 |
| 71.5 | 1.0635 | 0.6200 | 1.470 | 263 | 107.5 | 155.5 | 5.047 |
| 48 | 1.0620 | 0.5190 | 1.470 | 303 | 114.0 | 189.0 | 5.242 |
| 24 | 1.0610 | 0.3630 | 1.470 | 351 | 120.0 | 231.0 | 5.442 |

DATA FOR TABLE III

Expt. No. 253

P = 5.84 mm Hg

N₂ flow = 183 μmoles sec⁻¹

T = 25°C

NO flow = 1.27 μmoles sec⁻¹

H_{calc} (t = 0) = 143 mcals sec⁻¹

| t | I _o | I _f | R | H _{exp} | H _{calc} | ΔH | ln(ΔH) |
|-------|----------------|----------------|-------|----------------------------|----------------------------|----------------------------|--------|
| msecs | amps | amps | ohms | mcals sec ⁻¹ | mcals sec ⁻¹ | mcals sec ⁻¹ | |
| 274 | 0.8540 | 0.6530 | 1.270 | 95.0 | 70.0 | 25.0 | 3.218 |
| 246 | 0.8523 | 0.6150 | 1.270 | 105.8 | 74.0 | 31.8 | 3.460 |
| 219 | 0.8510 | 0.5740 | 1.270 | 120.0 | 78.0 | 42.0 | 3.738 |
| 192 | 0.8500 | 0.5230 | 1.270 | 136.3 | 82.5 | 54.0 | 3.990 |
| 164 | 0.8485 | 0.4560 | 1.270 | 156.0 | 86.7 | 69.0 | 4.234 |
| 137 | 0.8460 | 0.3510 | 1.270 | 180.0 | 93.0 | 87.0 | 4.477 |
| 110 | 0.8440 | 0.1400 | 1.270 | 210.0 | 99.0 | 111.0 | 4.709 |
| 82 | 1.0630 | 0.6300 | 1.450 | 254.0 | 106.8 | 147.0 | 4.990 |
| 55 | 1.0620 | 0.5080 | 1.450 | 303.0 | 115.0 | 188.0 | 5.236 |
| 27.4 | 1.0615 | 0.3125 | 1.450 | 358.0 | 125.0 | 233.0 | 5.451 |

Over the pressure range employed, k_{obs} can be seen to be independent of pressure within the experimental error. Therefore, when $M = N_2$, it appears that there is negligible gas phase deactivation, and k_{obs} can be identified with k_w . This rate constant can be expressed in terms of the efficiency of collisional deactivation. As seen previously, a first order wall decay rate constant can be related to the collisional efficiency, γ_{pyrex} , by

$$\gamma_{pyrex} = \frac{2k_w r}{\bar{c}}$$

where r = radius of cylindrical reaction tube,

\bar{c} = average velocity of colliding particle.

In the present work $r = 1.3$ cms and $k = 8.8 \pm 0.3 \text{ sec}^{-1}$

$$\bar{c} = 1.455 \times 10^4 \sqrt{T/M} \text{ cm sec}^{-1}$$

$$M = 28$$

$$T = 298$$

$$\text{Therefore } \gamma_{pyrex} = (4.8 \pm 0.2) \times 10^{-4}$$

Magnitude of the energy of N_2^*

The average energy of the discharged nitrogen in excess of that due to atomic nitrogen is obviously equal to $\Delta H/f(N_2)$, where $f(N_2)$ is the total molar flow of nitrogen. Since ΔH is a function of time, this expression is only meaningful if the time allowed for deactivation is also stated.

Of more significance is the value of $\Delta H/f(N_2)$ immediately after the discharge.

In all of the preceding experiments the zero point of the time scale is completely arbitrary, since it corresponds to the position of the titration jet. Even comparisons at this point are meaningless since the time interval between the discharge and the titration jet is dependent on the linear gas velocity.

Although a direct extrapolation could be made to the true time zero, this is difficult for two reasons:

- (a) The geometry of the apparatus is such that the time interval between the discharge and the titration jet is difficult to estimate with any accuracy.
- (b) The non-uniformity of this part of the apparatus will certainly lead to a varying deactivation rate constant.

A valid extrapolation can, however, be made in the following manner.

Since, as seen previously, the rate of deactivation of N_2^* is independent of pressure, plots of $\log (\Delta H/f_{(N_2)})$ against t have the same slope. However, if $\log (\Delta H/f_{(N_2)})$ is plotted against distance along the reaction tube, a change in time scale will produce a change in slope. Since the discharge is located at a constant distance from the reaction tube, these plots should intersect at the effective discharge position. It will be appreciated that this will not be a true geometrical position but rather a position defined in reaction tube co-ordinates. It will therefore take into account both geometrical variations and variations in the

deactivation rate constant due to non-uniformity. The results of such plots are shown in Table IV and Fig. 5.

It is apparent from Fig. 5 that this procedure accurately locates the discharge at an effective value of $d = -15$ cms. The value of $\log(\Delta H/f_{(N_2)})$ at this point is 0.78. Thus the excess energy carried by the nitrogen is 6.03 kcal mole⁻¹.

The quantitative validity of this value for the excess energy will depend on the efficiency of the detector in deactivating this species.

A separate experiment in which a coil of cobalt-plated platinum wire was inserted into the gas stream above the detector was performed to examine this point. It was found that, provided the first probe recombined all the nitrogen atoms, the detector picked up almost no heat downstream from this probe. The efficiency of the first probe was estimated from these results as being greater than 99%. Since the physical dimensions of both the first probe and the detector filament were similar (though not absolutely identical) it is probable that the detector was capable of making quantitative measurements of the energy associated with N_2^* .

Efficiency of molecules in deactivating N_2^*

If the species denoted by N_2^* is indeed vibrationally excited nitrogen, it is perhaps not too surprising that gas phase collisional deactivation by ground

TABLE IV

| | | $f_{(N_2)}$ micromoles sec^{-1} | | | | | | | | | | | |
|-----|-------------------------|--|-------|-------|-------|----------------------|-------|-------|-------|---------------------------------|--|--|--|
| | | 132 | 140 | 148 | 183 | | | | | | | | |
| d | ΔH | | | | | $\Delta H/f_{(N_2)}$ | | | | $\log [\Delta H/f_{(N_2)}] + 2$ | | | |
| cms | mcals sec^{-1} | | | | | kcal mole $^{-1}$ | | | | | | | |
| 30 | 114 79 36 25 | 0.865 | 0.565 | 0.240 | 0.137 | 1.937 | 1.752 | 1.380 | 1.135 | | | | |
| 27 | 130 94 44 32 | 0.985 | 0.671 | 0.294 | 0.174 | 1.994 | 1.827 | 1.468 | 1.241 | | | | |
| 24 | 148 109 56 42 | 1.120 | 0.780 | 0.382 | 0.230 | 2.049 | 1.892 | 1.582 | 1.361 | | | | |
| 21 | 165 127 67 54 | 1.250 | 0.908 | 0.454 | 0.295 | 2.097 | 1.958 | 1.657 | 1.470 | | | | |
| 18 | 186 150 81 69 | 1.410 | 1.070 | 0.548 | 0.377 | 2.149 | 2.029 | 1.739 | 1.576 | | | | |
| 15 | 217 172 102 87 | 1.645 | 1.230 | 0.686 | 0.476 | 2.216 | 2.090 | 1.831 | 1.678 | | | | |
| 12 | 246 205 125 111 | 1.865 | 1.465 | 0.845 | 0.602 | 2.271 | 2.166 | 1.927 | 1.779 | | | | |
| 9 | 282 242 156 147 | 2.140 | 1.730 | 1.050 | 0.804 | 2.330 | 2.238 | 2.021 | 1.905 | | | | |
| 6 | 328 273 189 188 | 2.490 | 1.950 | 1.277 | 1.028 | 2.396 | 2.290 | 2.106 | 2.012 | | | | |

Figure 5

PLOTS OF $\log(H/f_{N_2})$ AS A FUNCTION

OF d FOR VARIOUS PRESSURES

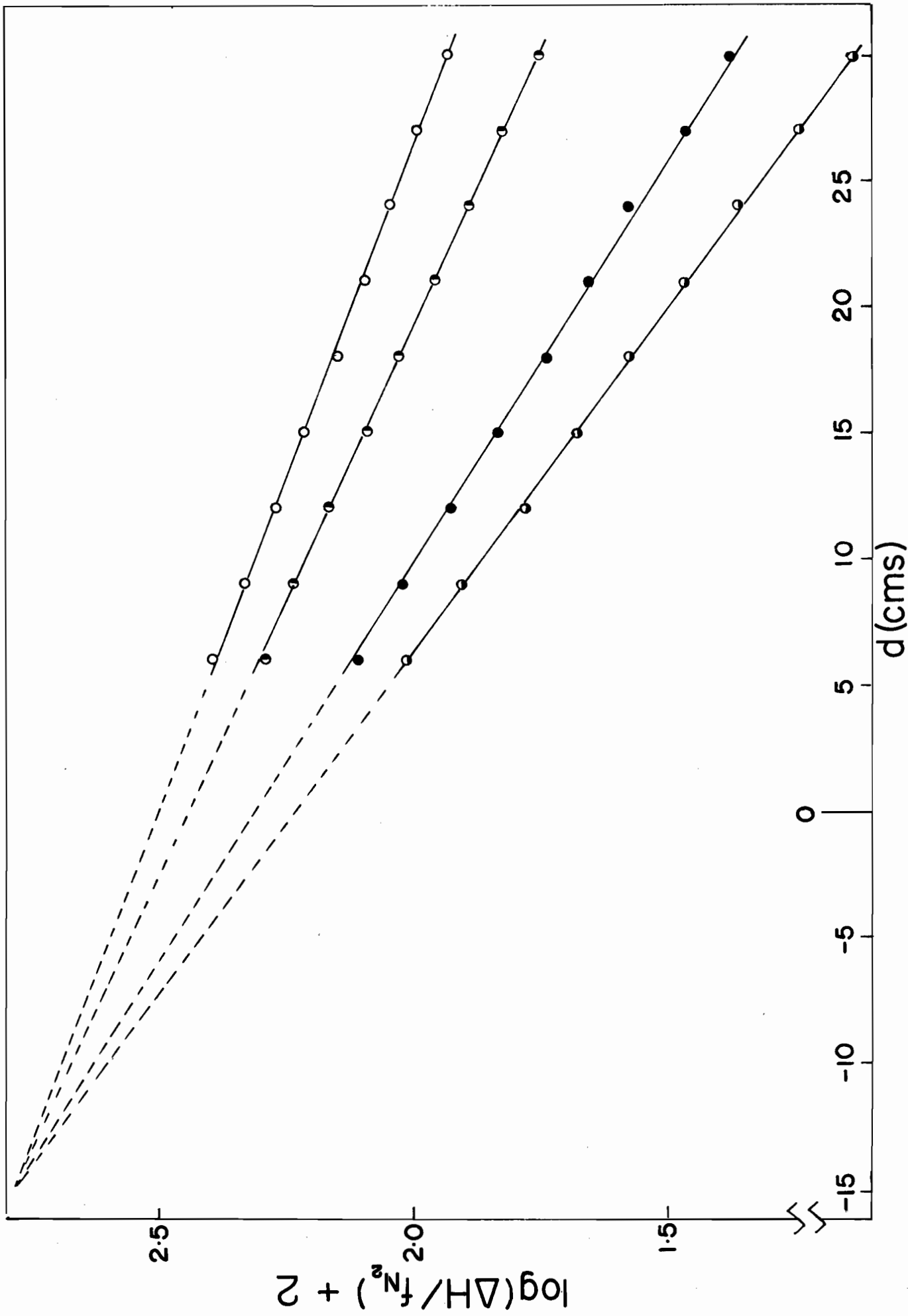
(Data from Tables III and IV)

○ - P = 2.3 mm Hg

◐ - P = 2.95 mm Hg

● - P = 4.10 mm Hg

◑ - P = 5.84 mm Hg



state nitrogen molecules is very inefficient (vide infra). However, this restriction should not apply to other collision partners. As mentioned previously, Kaufman et al. have found N_2O to be very effective in deactivating this species. To verify this, nitrous oxide was added in quite small amounts to a discharged nitrogen stream which was then examined, using a cobalt-plated detector.

The results of such an experiment are shown in Table V and Fig. 6. The remarkably good agreement between H_{calc} and H_{exp} under these conditions indicates that N_2O is indeed very efficient in deactivating N_2^* . This experiment also leads to two further important conclusions.

(i) It confirms the validity of the NO titration as a means of estimating nitrogen-atom flow rates.

(ii) It shows that the atomic nitrogen is almost exclusively in the ground (4S) state since the probe measurements were calculated using

$$D_{N_2} = 225 \text{ kcal/mole}^{-1}.$$

To make a quantitative estimate of the homogeneous deactivation rate of N_2^* by N_2O , it was obviously necessary to use much lower concentrations of nitrous oxide.

A typical experiment using approximately 2.5% N_2O is shown in Table VI and Fig. 7. The rapid approach of H_{exp} to H_{calc} is evident. Since $[N_2]$ has no effect on the decay rate of N_2^* , the slope of the $\ln(\Delta H)$ plot can be equated to k_{obs} where

$$k_{obs} = k_w + k_{N_2O} [N_2O]$$

TABLE V

$P = 4.17 \text{ mm Hg}$ $N_2 \text{ flow} = 162 \mu\text{moles sec}^{-1}$
 $T = 19^\circ\text{C}$ $N_2O \text{ flow} = 16 \mu\text{moles sec}^{-1}$
 $R = 1.490 \Omega$ $NO \text{ flow} = 1.53 \mu\text{moles sec}^{-1}$
 Lead resistance $H_{\text{calc}}(t = 0) = 172 \text{ mcals sec}^{-1}$
 $= 0.185 \Omega$

| t msecs | I_o amps | I_f amps | H_{exp} mcals sec ⁻¹ | H_{calc} mcals sec ⁻¹ |
|--------------|---------------|---------------|---|--|
| 206 | 0.9000 | 0.6375 | 126.5 | 127.0 |
| 185 | 0.9000 | 0.6280 | 129.5 | 129.0 |
| 165 | 0.8970 | 0.6170 | 132.0 | 132.0 |
| 144 | 0.8960 | 0.6060 | 136.0 | 136.0 |
| 123 | 0.8960 | 0.5935 | 140.8 | 140.0 |
| 103 | 0.8960 | 0.5835 | 144.5 | 143.3 |
| 82 | 0.8960 | 0.5705 | 149.0 | 148.0 |
| 62 | 0.8960 | 0.5575 | 153.5 | 153.0 |
| 41 | 0.8960 | 0.5410 | 159.3 | 158.0 |
| 21 | 0.8950 | 0.5250 | 164.0 | 164.0 |

Figure 6

DEACTIVATION OF N_2^* BY N_2O

(Data from Table V)

- - Calculated heat release to detector
- - Measured heat release to detector

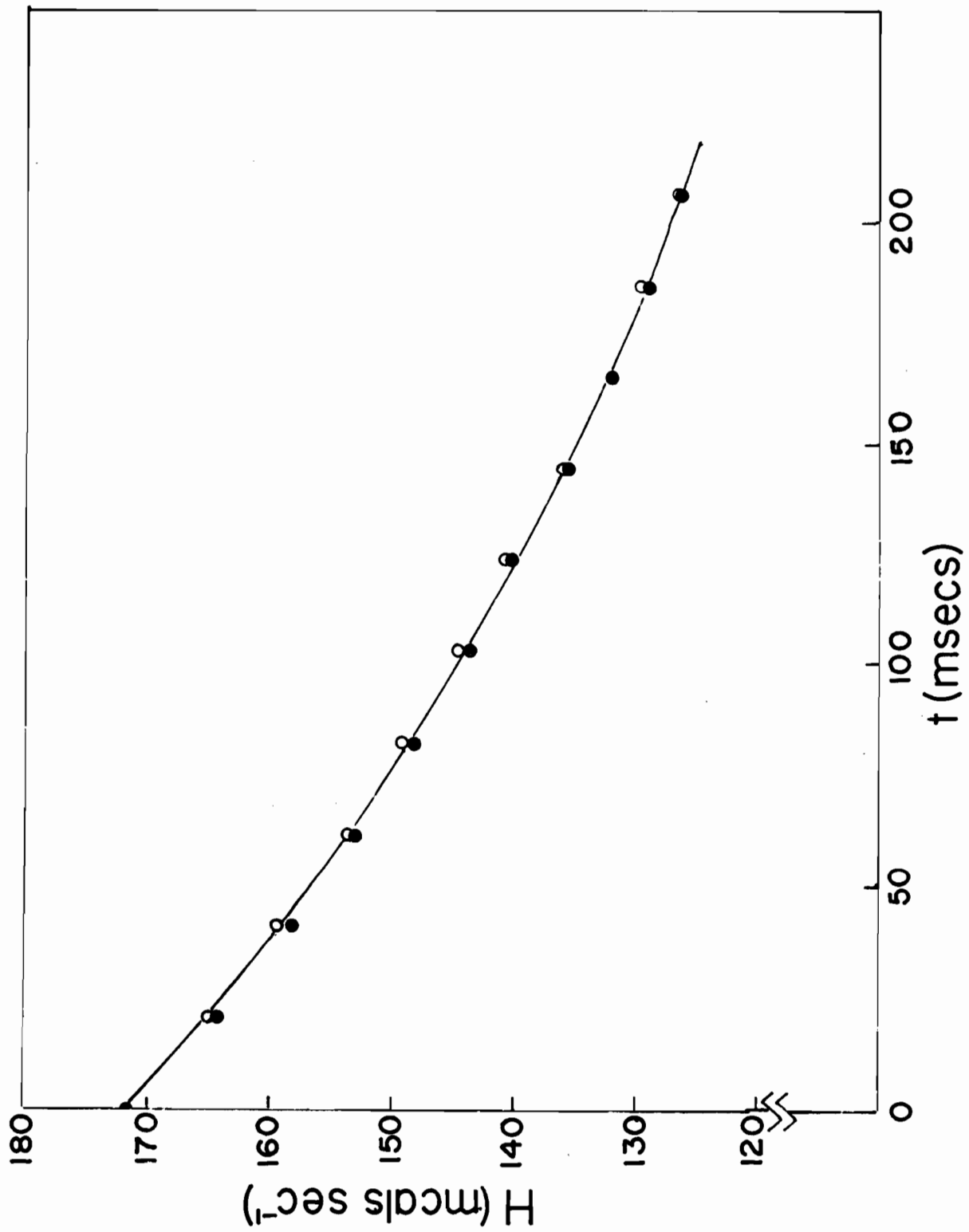


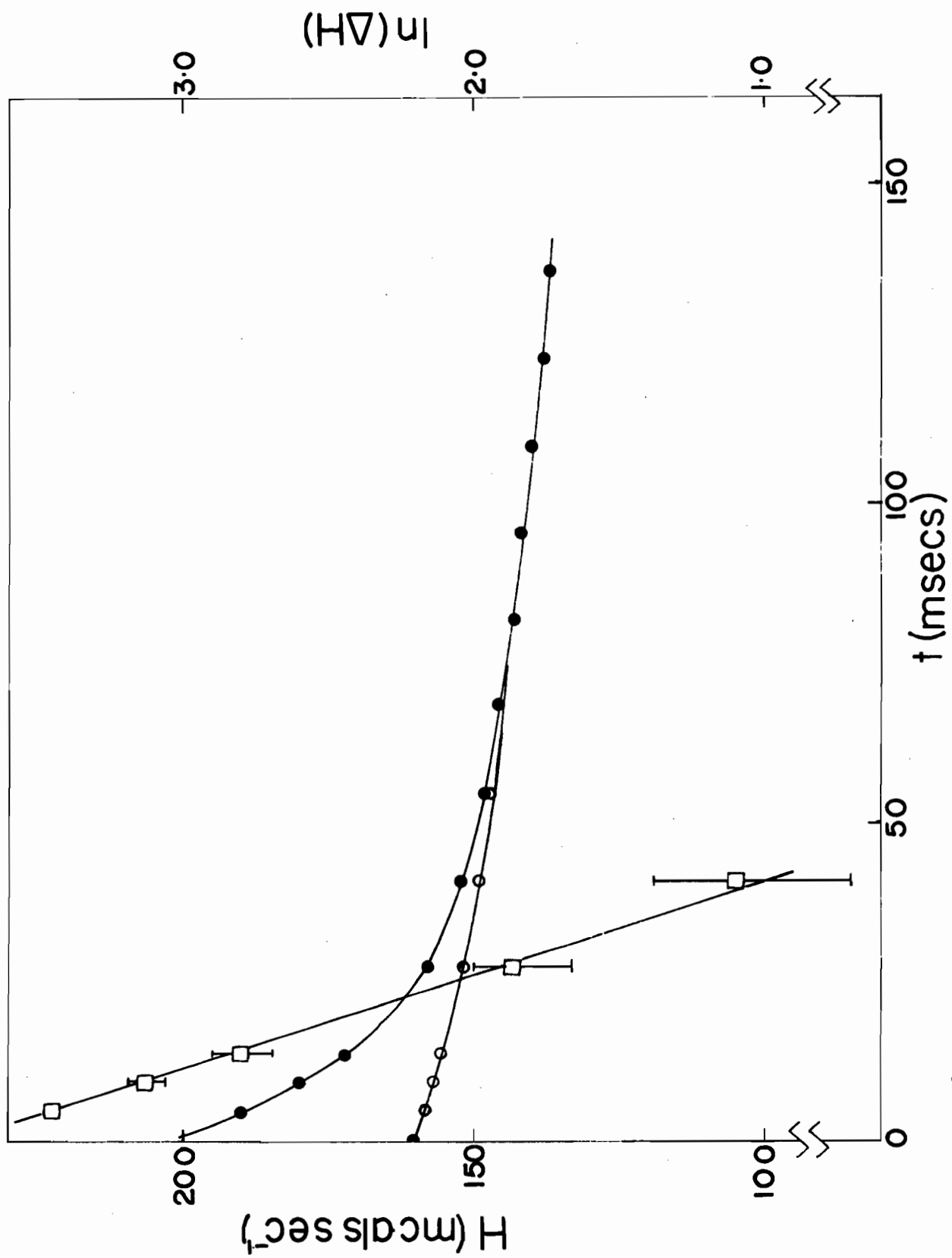
Figure 7

ACCELERATED DEACTIVATION OF N_2^* BY

SMALL AMOUNTS OF N_2O

(Data from Table VI)

- - Calculated heat release to detector (H_{calc})
- - Measured heat release to detector (H_{exp})
- - Plot of $\ln(H_{exp} - H_{calc}) = \ln(\Delta H)$



Thus a plot of k_{obs} against $[N_2O]$ should yield a straight line of slope k_{N_2O} and intercept k_w .

The results of such experiments are shown in Table VII and Fig. 8. In addition to N_2O , both CO_2 and Ar were also studied. From the slopes of these curves the following rate constants were obtained.

$$k_{N_2O} = 1.63 \times 10^{10} \text{ cm}^3 \text{ mole}^{-1} \text{ sec}^{-1}$$

$$k_{CO_2} = 4.56 \times 10^9 \text{ cm}^3 \text{ mole}^{-1} \text{ sec}^{-1}$$

$$k_{Ar} = 1.62 \times 10^8 \text{ cm}^3 \text{ mole}^{-1} \text{ sec}^{-1}$$

It is more convenient for purposes of discussion to express these rate constants in terms of a collisional deactivation efficiency, δ_M .

From kinetic theory, the number of collisions per second between M and N_2^* is given by

$$\text{No. of collisions sec}^{-1} = 1.142 \times 10^4 [N_2]^* [M] (\sigma_{N_2^*} + \sigma_M)^2 \left(\frac{T}{\mu}\right)^{\frac{1}{2}}$$

where $\sigma_{N_2^*}$ and σ_M are collision diameters and μ is the reduced molecular weight.

The rate of disappearance of N_2^* will therefore be equal to the collision frequency multiplied by the collisional deactivation efficiency.

Therefore

$$-\frac{d[N_2]^*}{dt} = k_M [M] [N_2]^* = \delta_M 1.142 \times 10^4 [M] [N_2]^* (\sigma_{N_2^*} + \sigma_M)^2 \left(\frac{T}{\mu}\right)^{\frac{1}{2}}$$

TABLE VII

M = N₂O

| P | [M] x 10 ⁹ | [N ₂] x 10 ⁷ | t ₂ - t ₁ | $\ln \frac{(\Delta H)_{t_1}}{(\Delta H)_{t_2}}$ | $k_{\text{obs}} = \frac{1}{t_2 - t_1} \ln \frac{(\Delta H)_{t_1}}{(\Delta H)_{t_2}}$ |
|-------|------------------------|-------------------------------------|---------------------------------|---|--|
| mm Hg | moles cm ⁻³ | moles cm ⁻³ | secs | | sec ⁻¹ |
| 2.74 | 3.74 | 1.44 | 0.0497 | 3.46 | 69.6 |
| 2.71 | 2.30 | 1.44 | 0.0675 | 3.20 | 47.5 |
| 2.70 | 0.81 | 1.45 | 0.112 | 3.00 | 26.8 |

M = CO₂

| | | | | | |
|------|------|------|--------|------|------|
| 2.81 | 12.1 | 1.40 | 0.0312 | 2.00 | 64.0 |
| 2.81 | 5.26 | 1.47 | 0.0610 | 2.00 | 32.8 |
| 2.81 | 3.73 | 1.49 | 0.0740 | 2.00 | 27.0 |

M = Ar

| | | | | | |
|------|------|------|--------|------|------|
| 2.84 | 17.0 | 1.37 | 0.0870 | 1.00 | 11.5 |
| 2.54 | 7.9 | 1.30 | 0.100 | 1.00 | 10.0 |

SLOPES

$$k_{\text{N}_2\text{O}} = 1.63 \times 10^{10} \text{ cm}^{-3} \text{ mole}^{-1} \text{ sec}^{-1}$$

$$k_{\text{CO}_2} = 4.56 \times 10^9 \text{ cm}^{-3} \text{ mole}^{-1} \text{ sec}^{-1}$$

$$k_{\text{Ar}} = 1.62 \times 10^8 \text{ cm}^{-3} \text{ mole}^{-1} \text{ sec}^{-1}$$

Figure 8

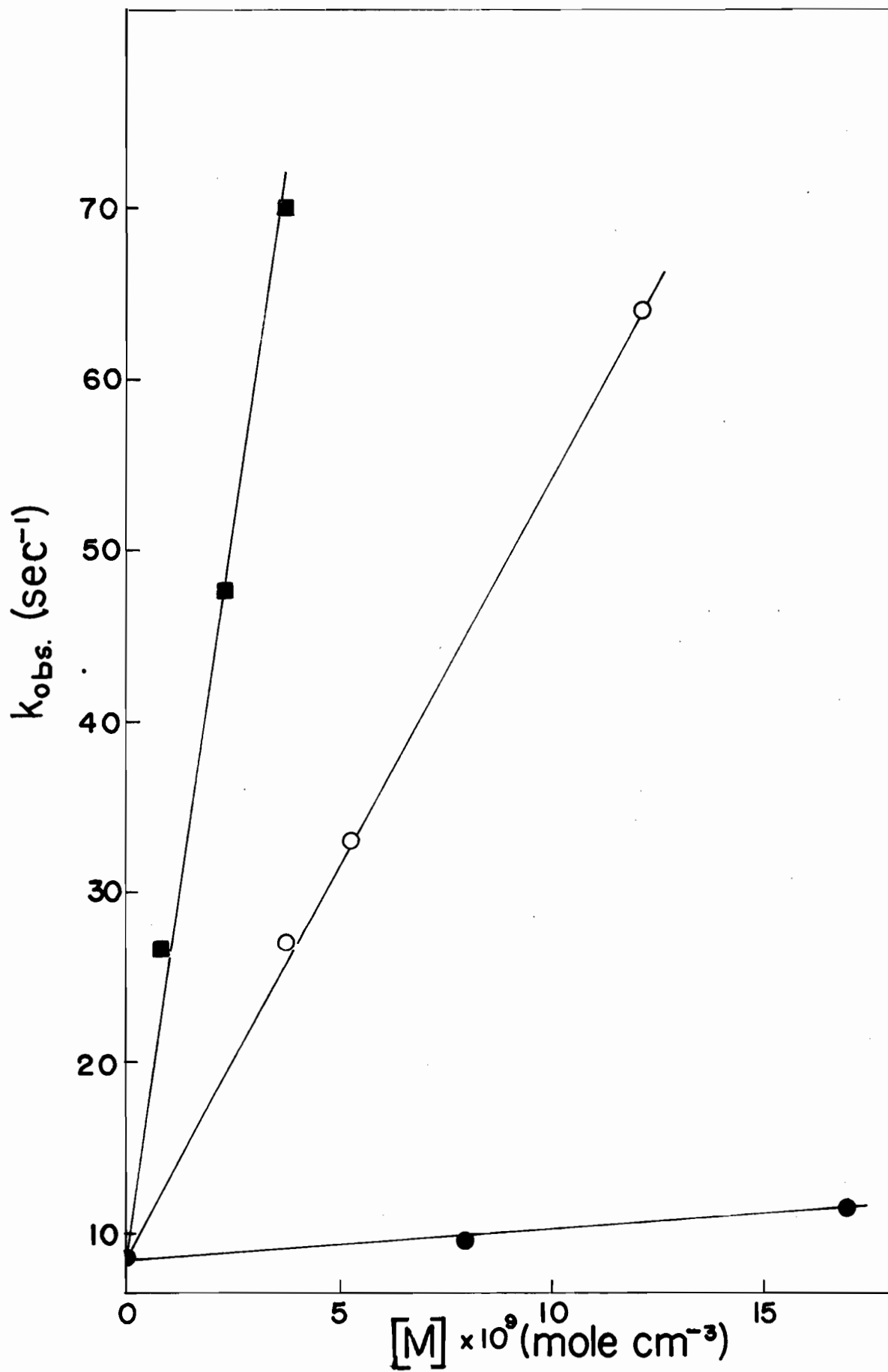
VARIATION OF k_{obs} ($= k_w + k_M[M]$) with $[M]$

(Data from Table VII)

■ - M = N₂O

○ - M = CO₂

● - M = Ar



The collisional efficiency can then be calculated from

$$\gamma_M = \frac{k_M}{1.142 \times 10^4 (\sigma_{N_2^*} + \sigma_M)^2 \left(\frac{T}{\mu}\right)^{\frac{1}{2}}}$$

(N.B. In this expression k_M must be expressed in units of $\text{cm}^3 \text{ molecules}^{-1} \text{ sec}^{-1}$.)

The values of γ_M so obtained are shown below:

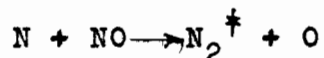
| M | σ_M (Ref. 24) | γ_M | γ_M / γ_{Ar} |
|--------|--------------------------|----------------------|--------------------------|
| N_2O | 3.2×10^{-8} cms | 1.4×10^{-4} | 90 |
| CO_2 | 3.2×10^{-8} cms | 4.0×10^{-5} | 25 |
| Ar | 2.8×10^{-8} cms | 1.6×10^{-6} | 1 |

It should be pointed out that the values of γ_M in the above table cannot be accepted unreservedly since the parameter measured in these experiments (rate of energy loss) may well be a function of both the energy distribution and the microscopic kinetics of the relaxation. They should be regarded therefore more as a convenient way of expressing the observed relaxation rate in this particular system only. The relative efficiencies, γ_M / γ_{Ar} , however, may be more widely applicable.

Examination of vibrationally excited N_2
produced by reaction of N and NO

Most of the preceding study has been devoted to the energetic species produced in the discharge. This still leaves the possibility of the production of vibrationally

excited N_2 by the reaction



As seen previously, this could conceivably result in vibrationally excited nitrogen with up to perhaps 75 kcal mole⁻¹.

There remains, however, the difficulty of separating this species from the energetic species originating in the discharge itself. Consideration of the previous results, however, shows that N_2^* produced in the discharge deactivates on pyrex with an efficiency of about 4×10^{-4} .

The corresponding figure for the recombination of nitrogen atoms on pyrex is about 2×10^{-5} (25,26,27). It should therefore be possible to remove preferentially the N_2^* arising in the discharge by increasing the surface area of the reaction vessel with only a relatively small decrease in the nitrogen-atom concentration. This was accomplished by inserting a pyrex glass wool plug in the reaction tube just downstream from the discharge. It was immediately apparent in a qualitative fashion that a large amount of energy was being released at this point. The walls of the reaction tube became extremely hot in the vicinity of the plug, although the nitrogen-atom concentration was not markedly reduced.

A quantitative study of discharged nitrogen subjected to this treatment is shown in Table VIII and Fig. 9.

Figure 9

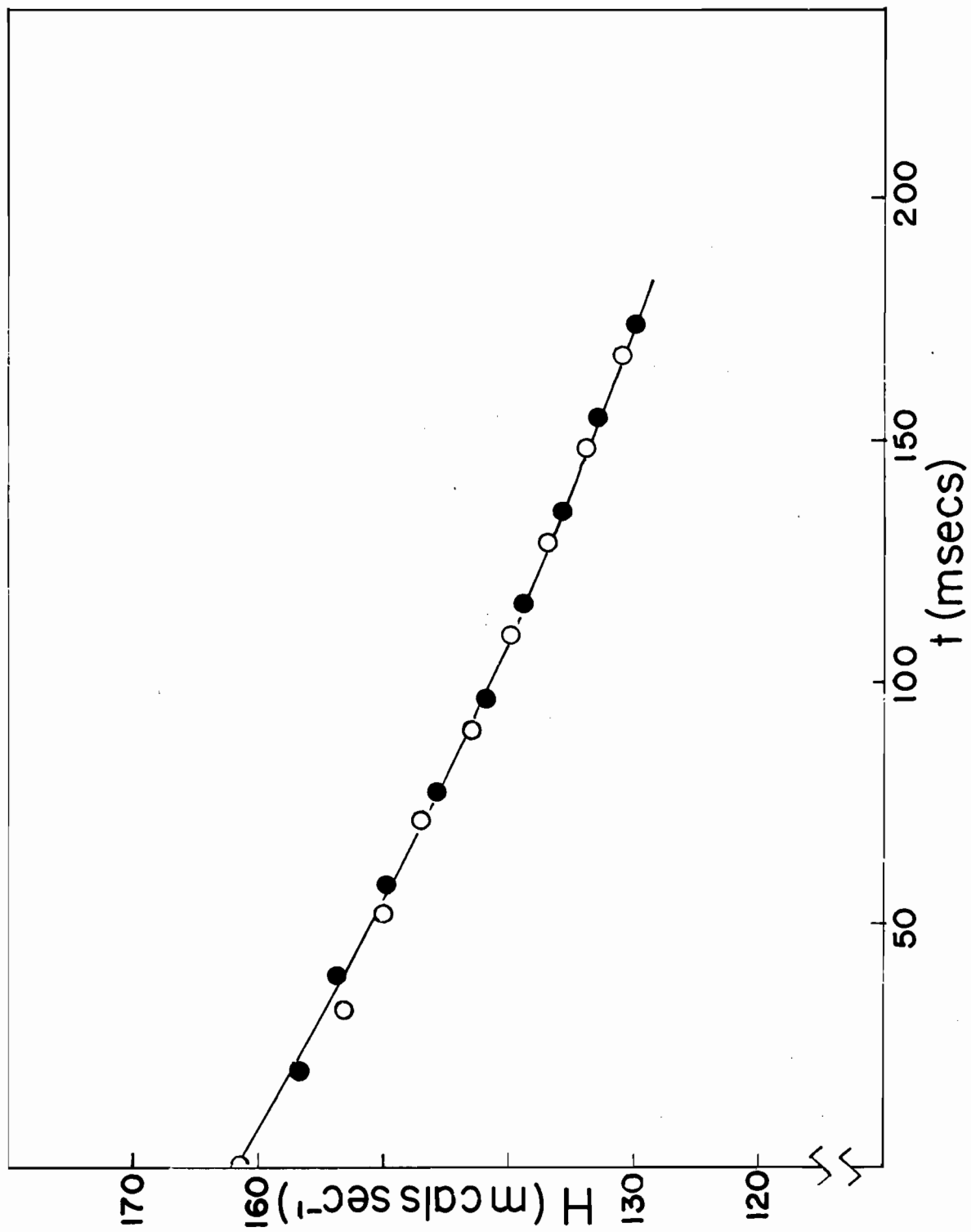
DETECTOR MEASUREMENTS IN A 'FILTERED'

N-ATOM SYSTEM

(Data from Table VIII)

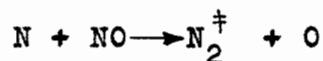
○ - Calculated heat release to detector

● - Measured heat release to detector



These results show that N_2^* from the discharge can be effectively 'filtered' out by means of glass wool to yield a system containing ground state nitrogen atoms as virtually the sole energetic species.

Obviously, if such a system is now titrated with nitric oxide, any energetic species, other than ground state oxygen atoms, can be attributed to N_2^\ddagger produced in the reaction



The results of such an experiment, using a silver peroxide coated probe, are shown in Table IX and Fig. 10. The discrepancy between H_{exp} and H_{calc} has reappeared, and this excess energy can now be assumed to be carried by N_2^\ddagger produced in the titration reaction. Since the flow rate of N_2^\ddagger must be equal to the oxygen-atom flow, such an experiment affords a quantitative estimate of the average energy carried by the N_2^\ddagger . From Fig. 10, $\ln \Delta H$ at $t = 0$ is equal to 3.1, i.e. $\Delta H_{(t=0)} = 22.2 \text{ mcals sec}^{-1}$.

The corresponding flow rate of N_2^\ddagger was $1.223 \mu\text{moles sec}^{-1}$. For this particular experiment, the energy of N_2^\ddagger , $E_{N_2^\ddagger}$, can be evaluated from

$$E_{N_2^\ddagger} = \Delta H_{(t=0)} / f_{N_2^\ddagger} = 18.2 \text{ kcals mole}^{-1}$$

Unfortunately, in these experiments, the magnitude of ΔH was quite small and was the difference between two relatively large quantities.

TABLE IX

P = 1.3 mm Hg

N₂ flow = 98.5 μmoles sec⁻¹

T = 8.5°C

NO flow = 1.223 μmoles sec⁻¹

R = 1.320 Ω

H_{calc}(t = 0) = 72 mcals sec⁻¹

Lead Resistance

= 0.185 Ω

| t msecs | I _o amps | I _f amps | H _{exp} mcals sec ⁻¹ | ΔH mcals sec ⁻¹ | ln(ΔH) |
|------------|------------------------|------------------------|--|-------------------------------|--------------|
| 108 | 0.7090 | 0.4665 | 77.5 | 9.0 ± 1.0 | 2.197 ± 0.1 |
| 96 | 0.7090 | 0.4615 | 79.0 | 10.0 ± 1.0 | 2.303 ± 0.1 |
| 84 | 0.7090 | 0.4540 | 81.0 | 11.0 ± 1.0 | 2.398 ± 0.1 |
| 72 | 0.7090 | 0.4470 | 82.4 | 12.4 ± 1.0 | 2.518 ± 0.08 |
| 60 | 0.7090 | 0.4400 | 84.5 | 14.0 ± 1.0 | 2.639 ± 0.07 |
| 48 | 0.7090 | 0.4330 | 86.0 | 15.0 ± 1.0 | 2.708 ± 0.07 |
| 36 | 0.7085 | 0.4240 | 87.8 | 16.0 ± 1.0 | 2.773 ± 0.06 |
| 24 | 0.7090 | 0.4130 | 90.3 | 18.0 ± 1.0 | 2.890 ± 0.05 |

Figure 10

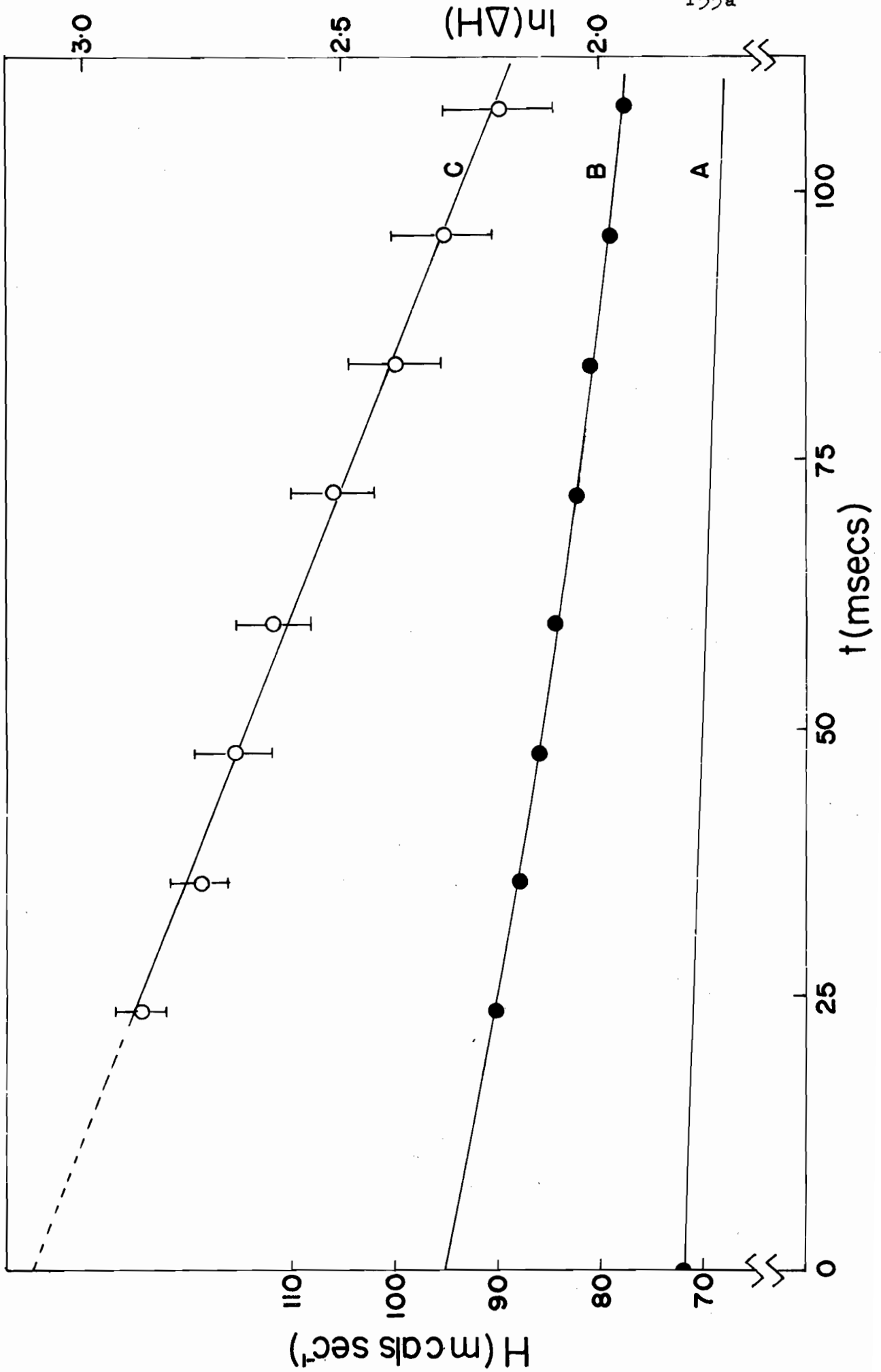
DETECTOR MEASUREMENTS IN AN OXYGEN
ATOM SYSTEM PRODUCED BY TITRATION OF
A 'FILTERED' NITROGEN ATOM STREAM WITH NO

(Data from Table IX)

A - Calculated heat release to detector (H_{calc})

B - Measured heat release to detector (H_{exp})

C - Plot of $\ln(H_{exp} - H_{calc}) = \ln(\Delta H)$



It can be seen from Fig. 10 that the resulting uncertainty in $\ln(\Delta H)$ was quite large. Despite this, the slopes of several plots of $\ln(\Delta H)$ against t yielded an average value of the rate constant for deactivation of N_2^\ddagger of $8.5 \pm 0.4 \text{ sec}^{-1}$. This can be regarded as evidence in favour of the similarity between N_2^* produced in the discharge and N_2^\ddagger produced by the N - NO reaction.

The results of these experiments are shown in Table X. The average energy of N_2^\ddagger can be estimated as $20 \pm 4 \text{ kcal mole}^{-1}$.

TABLE X

| Expt. No. | P mm Hg | NO flow (= N_2^\ddagger flow) micromoles sec^{-1} | $\Delta H(t=0)$ mcals sec^{-1} | k sec^{-1} | $\Delta H(t=0) / f_{N_2^\ddagger}$ kcal mole^{-1} |
|-----------|------------|--|--|------------------------|---|
| 86 | 1.3 | 1.223 | 22.2 | 8.2 | 18.2 |
| 86 | 2.6 | 0.985 | 23.0 | 8.06 | 23.4 |
| 87 | 3.35 | 1.02 | 21.8 | 9.10 | 21.4 |
| 88 | 2.10 | 0.970 | 17.9 | 8.77 | 18.5 |

Average energy = $20 \pm 4 \text{ kcal mole}^{-1}$

IV. DISCUSSION

The nature of the energetic species present in discharged nitrogen is open to some speculation. The evidence obtained by Dressler⁽¹⁷⁾ indicates without doubt that active nitrogen contains vibrationally excited N_2 in addition to ground state nitrogen atoms. That the species denoted in the present work by N_2^* is also probably vibrationally excited N_2 can be deduced from its relaxational behaviour.

The probability of vibrational excitation or deexcitation between two colliding molecules depends upon the duration of the collision. The more nearly adiabatic is the collision, the lower will be the probability of energy transfer between the two systems. Thus, if the duration of the collision is long compared with the period of the vibration, the probability of energy transfer will be low. This implies that the probability will be low provided⁽²⁸⁾

$$\frac{a}{v} \gg \frac{1}{\nu} \quad \text{i.e.} \quad \frac{a\nu}{v} \gg 1$$

where a is of the order of gas kinetic radii and v the relative velocity of the colliding systems when widely separated. Thus a/v , the duration of the collision, must be very much longer than $1/\nu$, the period of the vibration. For a harmonic oscillator, the amplitude, d , can be shown to be

$$d = \left(\frac{\hbar}{\pi \nu \mu} \right)^{\frac{1}{2}}$$

where μ is the reduced mass of the molecule. Furthermore, at a temperature T , the relative velocity of the colliding systems is given approximately by

$$v^2 \simeq \frac{kT}{m}$$

where m is the mass of the lighter system.

Substitution of these values shows that the probability of vibrational energy transfer will be low provided

$$\frac{a}{d} \left(\frac{h\nu m}{\pi kT \mu} \right)^{\frac{1}{2}} \gg 1$$

For the low lying levels of any diatomic molecule $a \gg d$. Thus the probability of deactivation by collision becomes dependent upon the magnitude of $h\nu/kT$. For a molecule such as N_2 , $h\nu/kT$ at $300^\circ K$ is about 11 for transitions from the first to the zeroth level. Qualitatively it would be reasonable to expect the probability of vibrational energy transfer to be low in such a system.

Vibrational relaxation times

The concept of a relaxation time, τ , for vibrational energy transfer has been defined by Landau and Teller⁽²⁹⁾ in the following expression:

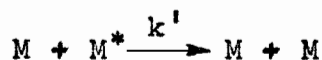
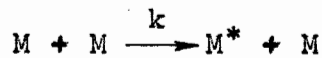
$$\frac{dE_{vib}(t)}{dt} = \frac{E_{vib}(T) - E_{vib}(t)}{\tau} \dots \dots \dots (a)$$

where $E_{vib}(t)$ = total vibrational energy at time, t ,
 $E_{vib}(T)$ = equilibrium vibrational energy at the gas kinetic temperature, T .

For a constant relaxation time, this expression implies an exponential decay of the excess vibrational energy.

For the simplest case involving transitions between the first and zeroth levels, τ can be related to a deactivational rate constant in the following manner.

Consider the reactions



where M^* represents a molecule in the first vibrational level.

Thus

$$\frac{d[M^*]}{dt} = k[M]^2 - k'[M][M^*]$$

Now

$$\frac{k}{k'} = \frac{[M^*]_{eq}}{[M]_{eq}}$$

$$\text{Therefore } \frac{d[M^*]}{dt} = \frac{k'[M^*]_{eq}}{[M]_{eq}} [M]^2 - k'[M][M^*]$$

Provided both $[M^*]$ and $[M^*]_{eq} \ll [M]$, $[M]$ will not change appreciably during the relaxation

$$\text{Therefore } \frac{d[M^*]}{dt} \approx k'[M^*]_{eq} [M] - k'[M][M^*]$$

$$\text{Substituting } [M^*] = \frac{E_{vib}(t)}{h\nu} \quad \text{and} \quad [M^*]_{eq} = \frac{E_{vib}(T)}{h\nu}$$

leads to

$$\frac{dE_{vib}(t)}{dt} = k'[M] \left(E_{vib}(T) - E_{vib}(t) \right)$$

Comparison with equation (a) shows that

$$\tau = \frac{1}{k'[M]}$$

The relaxation time defined by Landeau and Teller, however, does not stipulate that the excitation be restricted to a single level. Thus for a system in which appreciable populations of the levels other than the zeroth and first exist, τ , as defined by equation (a), can no longer be identified with the rate constant for deexcitation of a particular level. In fact, in such a system, τ may no longer be strictly constant. The mathematical treatment of relaxation of multistate systems has received a large amount of theoretical study. Shuler et al. (30,31,32,33,34) have published a series of papers dealing with the relaxation of such systems. In particular, they have examined the effect of relaxation from both Boltzman distributions in which the relaxation occurs through a series of consecutive Boltzman distributions of decreasing vibrational temperature and also of extreme non-Boltzman distributions such as a delta function distribution centred on a particular level. In the latter case the initial delta function broadens as it progresses to lower vibrational levels. These analyses have been performed both for a system of harmonic oscillators and also for anharmonic oscillators. The effect of anharmonicity, however, is small.

In all these cases, the vibrational energy decreases exponentially with a single over-all relaxation time although, as pointed out previously, this macroscopic relaxation time cannot be identified with the microscopic kinetics of individual levels.

Temperature dependence of
relaxation times

The temperature dependence of the relaxation time has been examined theoretically by Landau and Teller⁽²⁹⁾. These workers expressed τ as a function of temperature by an expression of the form

$$\log \tau = A + BT^{-1/3}$$

More recently, Parker⁽³⁵⁾, in an analysis of vibrational and rotational relaxation, has set up a model from which τ can be calculated from molecular parameters. This led to a temperature dependence in which $\log \tau$ varies approximately as $T^{-1/2}$. However, the experimental data (vide infra) over a wide temperature range are fitted much more closely by the $T^{-1/3}$ dependence.

Vibrational relaxation of nitrogen

For the purposes of the present discussion, it is more convenient to replace the relaxation time, τ , by the collision efficiency, γ , or by the number of collisions, N_c , necessary to deactivate a single molecule. These three quantities are related by

$$N_c = \frac{1}{\gamma} = \tau Z$$

where Z = number of collisions made by an excited molecule per second.

It was seen earlier that the excited species, N_2^* , produced in the discharge, appeared to decay exponentially,

i.e. with a single relaxation time. However, the rate constant of this decay was pressure independent and must therefore be attributed to a heterogeneous relaxation process with an efficiency of $\gamma_{\text{pyrex}} = 4.8 \times 10^{-4}$. Thus about 2000 collisions with the wall are required for heterogeneous deactivation.

The inability to detect any homogeneous deactivation in pure nitrogen is consistent with the work of previous investigators of the vibrational relaxation of nitrogen^(36,37,38,39,40). The results of these investigations are shown in Fig. 11 in which $\log N_c$ is plotted as a function of $T^{-1/3}$. It is apparent that the data from 5500 - 1000°K, covering a range of N_c from 5×10^3 to 5×10^6 , are accurately expressed by the Landau-Teller temperature dependence. The results of Huber and Kantrowitz⁽³⁶⁾ are rather low, but correction⁽³⁷⁾ for the presence of water vapour also brings these results into line. The calculated value of Schwartz, Slawsky and Herzfeld⁽⁴¹⁾ is also in good agreement with the extrapolated experimental data. Extrapolation of these data to 300°K would predict a value for N_c of about 10^{10} collisions. Thus the failure in the present work to detect any significant homogeneous deactivation of N_2^* is consistent with the identification of this species as vibrationally excited nitrogen.

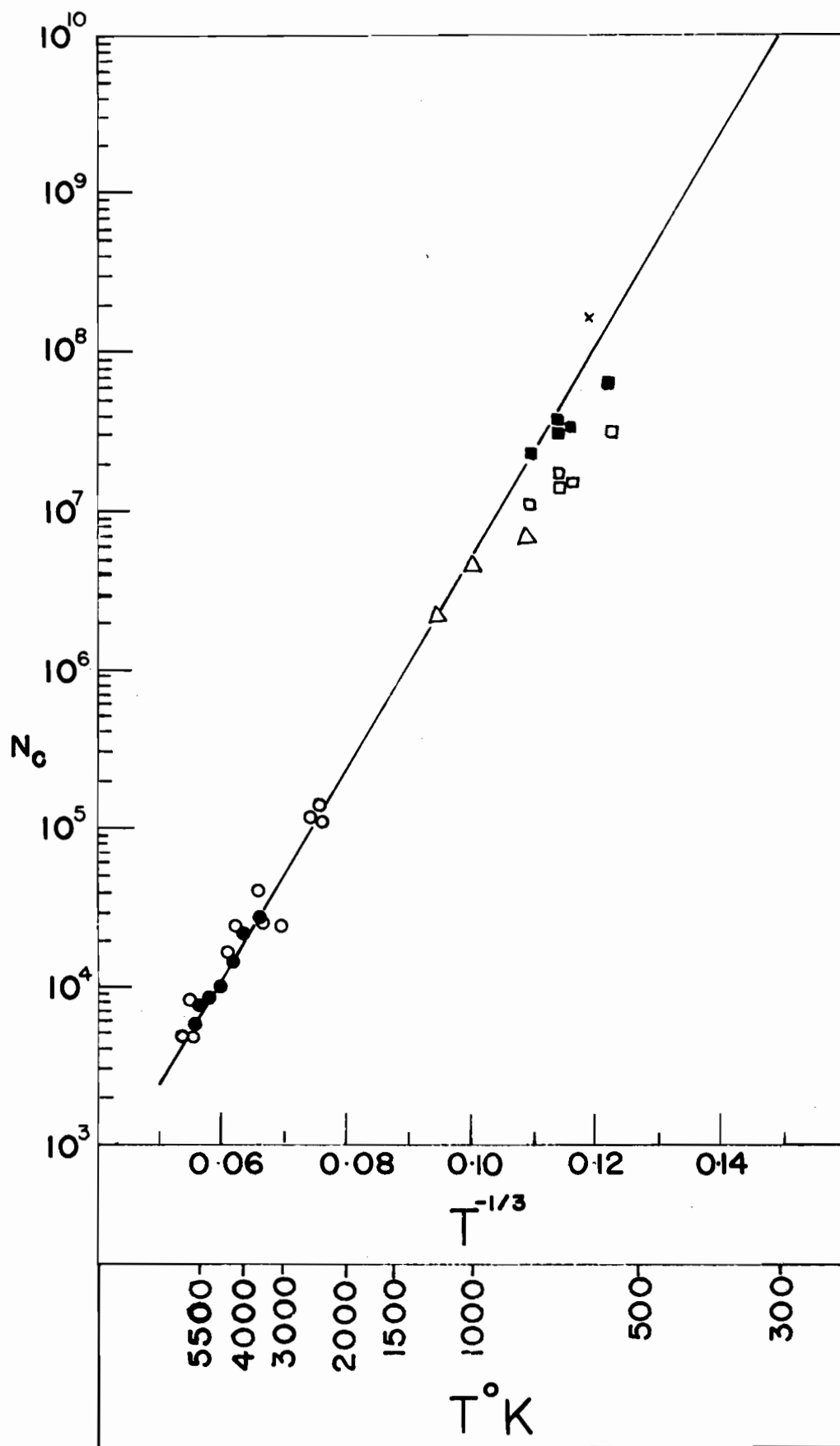
Effect of impurity on relaxation rate

The marked increase in relaxation rate brought about by the presence of foreign molecules has been examined

Figure 11

PLOT OF NUMBER OF COLLISIONS, N_c ,
AS A FUNCTION OF TEMPERATURE REQUIRED
TO DEACTIVATE VIBRATIONALLY EXCITED NITROGEN

- - Strenlow and Cohen (shock tube) Ref. (39)
- - Blackman (shock tube) Ref. (40)
- △ - Lukasik and Young (acoustical) Ref. (37)
- - Huber and Kantrowitz (impact tube) Ref. (36)
- - Huber and Kantrowitz⁽³⁶⁾ as corrected in
Ref. (37)
- × - Schwartz, Slawsky and Herzfeld (calculated)
Ref. (41)



by Schwartz et al.⁽⁴¹⁾. They have shown that the relaxation rate is influenced both by the mass of the colliding system and also by resonance effects if the colliding system has several degrees of freedom among which the energy can be partitioned.

These effects are illustrated in the following table.

| Gases | | Temp. °K | $N_c^{(1 \rightarrow 0)}$ | $N_c^{(1 \rightarrow 0)}$ |
|----------------|----------------|-------------|---------------------------|---------------------------|
| A | B | | (A, A) | (A, B) |
| N ₂ | A | 600 | 1.4×10^8 | 3.3×10^7 |
| N ₂ | H ₂ | 600 | 1.4×10^8 | 1.1×10^3 |
| O ₂ | N ₂ | 288 | 1.2×10^7 | 3.3×10^6 |
| CO | N ₂ | 600 | 1.7×10^7 | 6.7×10^2 |
| O ₂ | CO | 288 | 1.2×10^7 | 5×10^5 |

In this table $N_c^{(1 \rightarrow 0)}$ _(A,A) is the number of collisions required between like molecules, A, to effect deactivation from the first level. $N_c^{(1 \rightarrow 0)}$ _(A,B) is the number of collisions required between molecules, A and B, to effect deactivation of A.

As might be expected, argon, with its fairly large mass and its lack of any vibrational degrees of freedom, is very inefficient in deactivating vibrationally excited

nitrogen. This is of course consistent with the results of the present investigation.

On the other hand, hydrogen, with its low mass coupled with fairly close matching of energy levels, is very efficient.

The importance of energy level matching is dramatically illustrated by the last three entries in the foregoing table. Both N_2 and CO, with their widely spaced energy levels, relax extremely slowly when pure. However, the relaxation rate of CO when N_2 is added as an impurity is very markedly increased, but it will be noticed that neither N_2 nor CO is very efficient in deactivating O_2 where the energy level matching is much less close.

In the present work a similar effect can be noted with N_2O and CO_2 .

It has been suggested by Callear⁽⁴²⁾ that the deactivation of vibrationally excited nitrogen by N_2O proceeds in the following manner:



Such a process should be very rapid since N_2O has a fundamental frequency at about 2223 cm^{-1} which is only 108 cm^{-1} below that of N_2 . Callear has estimated that such an exchange should take place in about 10^3 collisions. The rate determining step for degradation of the vibrational energy to translational energy is therefore determined by the rate of deactivation of the N_2O which is governed by its

lowest vibrational frequency at 588 cm^{-1} . Callear has calculated that about 10^4 collisions are necessary to achieve deactivation of N_2O .

For CO_2 the matching is even closer since CO_2 has a fundamental frequency at 2349 cm^{-1} compared with 2331 cm^{-1} for N_2 . The observed fact that CO_2 is actually less efficient than N_2O is undoubtedly due to the rather larger minimum vibrational frequency of CO_2 (667 cm^{-1}). In fact, Lambert and Salter⁽⁴³⁾ have concluded from a study of many experimental results that $\log N_c$ is proportional to the minimum vibrational frequency. Thus, for CO_2 and N_2O , one would expect their efficiencies to be in the ratio 1 : 3.3 compared with that found here of 1 : 3.6.

The agreement between the predicted value and that observed experimentally is very good.

Energy distribution between the vibrational levels of nitrogen

The total vibrational energy carried by the discharged nitrogen was shown earlier to be about 6 kcal/mole⁻¹. It is perhaps coincidental that this value is quite close to the first vibrational level of N_2 . However, it is not inconceivable that initially all the nitrogen was excited to levels above the zeroth and which then decayed rapidly down to the first level.

Since the experimental measurements were made after a considerable time lapse, the extrapolation of these

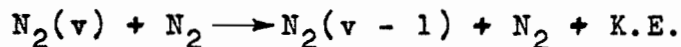
measurements to zero time would not include very rapid relaxation processes which would be essentially complete before the gas reached the measurement zone.

Since the anharmonicity of the levels in N_2 is small, cascade processes such as



could conceivably be quite rapid.

It is obvious that the method employed in the present investigation is entirely incapable of detecting such a process. It can, in fact, only measure vibrational energy loss by a process such as



It is therefore possible that this present technique is only sensitive to changes from the first to the zeroth level and is obviously incapable of yielding information concerning the vibrational energy distribution.

Excitation produced by the N/NO reaction

The energetic species produced as a product of the reaction between nitrogen atoms and nitric oxide can be fairly confidently identified as vibrationally excited nitrogen.

The average energy of the nitrogen produced in this way was seen to be about 20 kcal mole⁻¹ which corresponds to excitation to at least the third vibrational level. However, within the limit of the (rather large) experimental error, the relaxation rate appeared to be the same as for the excited

nitrogen produced in the discharge. Again, there is no way of deciding from these experiments whether the relaxation process involves a slow relaxation from high levels directly to kinetic energy or whether there is a rapid vibration-vibration interchange followed by a slow relaxation from the first to the zeroth level. Fortunately this species has been studied in this laboratory by a different technique. It has been shown by Phillips and Schiff⁽⁴⁴⁾ that this vibrationally excited nitrogen is capable of partially decomposing ozone. This requires the nitrogen molecule to have at least 24 kcal/mole of excess energy. Phillips found that about 75% of the vibrationally excited nitrogen initially produced in the N/NO reaction was capable of decomposing ozone. To reconcile this with the fact that the average energy is only 20 ± 4 kcal/mole strongly indicates an extreme non-Boltzmann distribution with a maximum in the region of the fourth level. Furthermore, the relaxation rate of this vibrationally excited N₂, as measured by its ability to decompose ozone, was considerably faster than its rate of loss of vibrational energy as determined in this present work. This, of course, is completely explicable when one realizes that the chemical method measures the rate at which the molecules decay to levels below the fourth. As suggested earlier, this process can probably occur with greater rapidity than processes involving vibrational-translational transfer. This problem has been discussed at greater length elsewhere⁽⁴⁵⁾.

BIBLIOGRAPHY

1. S. Glasstone, 'Textbook of Physical Chemistry', p. 332 et seq., Macmillan & Co., London (1956).
2. G. Herzberg, 'Molecular Spectra and Molecular Structure', Vol. I, Prentice-Hall, New York (1939).
3. D. Garvin, J. Am. Chem. Soc., 81, 3173 (1959).
4. J.D. McKinley, D. Garvin and M. Boudart, J. Chem. Phys., 23, 784 (1955).
5. D. Garvin, H.P. Broida and J. Kostkowski, J. Chem. Phys., 32, 880 (1960).
6. F.J. Lipscombe, R.G.W. Norrish and B.A. Thrush, Proc. Roy. Soc., A233, 455 (1956).
7. J.K. Cashion and J.C. Polanyi, J. Chem. Phys., 30, 1097 (1959).
8. W.D. McGrath and R.G.W. Norrish, Z. Physik Chem., 15, 245 (1958).
9. N. Basco and R.G.W. Norrish, Proc. Roy. Soc., A260, 293 (1961).
10. N. Basco and R.G.W. Norrish, Can. J. Chem., 38, 1769 (1960).
11. J.K. Cashion and J.C. Polanyi, J. Chem. Phys., 29, 455 (1958).
12. J.K. Cashion and J.C. Polanyi, J. Chem. Phys., 30, 316 (1959).
13. J.P. Simons, Nature, 186, 551 (1960).
14. J.C. Polanyi, J. Chem. Phys., 31, 1338 (1959).
15. F.T. Smith, J. Chem. Phys., 31, 1352 (1959).
16. F. Kaufman and J.R. Kelso, J. Chem. Phys., 28, 510 (1958).
17. K. Dressler, J. Chem. Phys., 30, 1621 (1959).
18. P. Harteck and V. Kopsch, Z. Physik Chem., B12, 327 (1931).
19. J.W. Linnett and D.G.H. Marsden, Proc. Roy. Soc., A234, 489, 504 (1956).
20. E.L. Tollefson and D.J. Le Roy, J. Chem. Phys., 16, 1057 (1948).

21. L. Elias, E.A. Ogryzlo and H.I. Schiff, *Can. J. Chem.*, 37, 1680 (1959).
22. J. Berkowitz, W. Chupka and G.B. Kistiakowsky, *J. Chem. Phys.*, 25, 457 (1956).
23. G.E. Beale and H.P. Broida, *J. Chem. Phys.*, 31, 1030 (1959).
24. A. Farkas and H.W. Melville, 'Experimental Methods in Gas Reactions', pp. 2 and 3, Macmillan Co., London (1939).
25. J.T. Herron, J.L. Franklin, P. Brandt and J.H. Dibeler, *J. Chem. Phys.*, 30, 879 (1959).
26. T. Wentinck, Jr., J.O. Sullivan and K.L. Wray, *J. Chem. Phys.*, 29, 231 (1958).
27. R.A. Young, *J. Chem. Phys.*, 34, 1292 (1961).
28. H.S.W. Massey and E.H.S. Burhop, 'Electronic and Ionic Impact Phenomena', p. 454, Oxford University Press, London and New York (1952).
29. L. Landau and E. Teller, *Phys. Z. Sowjetunion*, 10, 34 (1936).
30. R.J. Rubin and K.E. Shuler, *J. Chem. Phys.*, 25, 59 (1956).
31. K.E. Shuler, *J. Phys. Chem.*, 61, 849 (1957).
32. E.W. Montroll and K.E. Shuler, *J. Chem. Phys.*, 26, 454 (1957).
33. N.W. Bazeley, E.W. Montroll, R.J. Rubin and K.E. Shuler, *J. Chem. Phys.*, 28, 700 (1958).
34. K.E. Shuler, *Phys. Fluids*, 2, 442 (1959).
35. J.G. Parker, *Phys. Fluids*, 2, 449 (1959).
36. P.W. Huber and A. Kantrowitz, *J. Chem. Phys.*, 15, 275 (1947).
37. S.J. Lukasik and J.E. Young, *J. Chem. Phys.*, 27, 1149 (1957).
38. W. Bleakney, *Proc. Conference of Chem. Aeronomy*, Cambridge, Mass., p. 275, (1956).
39. R.A. Strenlow and A. Cohen, *J. Chem. Phys.*, 30, 257 (1959).
40. V.H. Blackman, *J. Fluid Mech.*, 1, 61 (1956).
41. R.N. Schwartz, Z.I. Slawsky and K.F. Herzfeld, *J. Chem. Phys.*, 20, 1591 (1952).

42. A.B. Callear, Private communication.
43. J.D. Lambert and R. Salter, Proc. Roy. Soc., 253A, 277 (1959).
44. L.F. Phillips and H.I. Schiff, J. Chem. Phys.,
36, 3283 (1962).
45. J.E. Morgan, L.F. Phillips and H.I. Schiff,
Disc. Faraday Soc., 33, 118 (1962).

APPENDIX A

PARAMETERS FOR USE IN THE EQUATION FOR
THE EQUILIBRIUM CONSTANT (Part I, p. 20)

| <u>i</u> | <u>d_i</u> | <u>e_i</u> | <u>θ_i</u> |
|----------|--------------------------|----------------------|---------------------------|
| 1 | 1.595 x 10 ⁴ | - 2.423 | - 1.217 x 10 ⁴ |
| 2 | 1.698 x 10 ⁻² | 1.043 | - 4.715 x 10 ⁴ |
| 3 | 1.064 x 10 ⁻⁶ | 3.466 | - 3.498 x 10 ⁴ |
| 4 | 2.710 x 10 ² | - 1.380 | - 5.932 x 10 ⁴ |

| <u>i</u> | <u>b_{i1}</u> | <u>b_{i2}</u> | <u>b_{i3}</u> |
|----------|----------------------------|----------------------------|-----------------------------|
| 1 | 4.499 x 10 ⁻³ | - 1.370 x 10 ⁻⁶ | 2.091 x 10 ⁻¹⁰ |
| 2 | - 3.277 x 10 ⁻³ | 1.222 x 10 ⁻⁶ | - 2.091 x 10 ⁻¹⁰ |
| 3 | - 7.776 x 10 ⁻³ | 2.592 x 10 ⁻⁶ | - 4.182 x 10 ⁻¹⁰ |
| 4 | 1.222 x 10 ⁻³ | - 1.48 x 10 ⁻⁷ | - |

APPENDIX B

DIFFUSION IN FLOW SYSTEMS

1. Effect of axial diffusion on the measured rate constant of a first order reaction

A reacting gas flowing through a tube will set up a concentration gradient along the length of the tube which will cause a diffusive flow tending to remove the gradient. Provided there is no mechanical mixing, the concentration at any particular point in the tube, however, will quickly reach an equilibrium value which will remain unchanged with time. If the concentration of the reactive species is sufficiently low that removal does not affect the linear gas velocity, the condition that the concentration C , at any point, x , in the tube remains constant leads to the following differential equation

$$D \frac{d^2C}{dx^2} - v \frac{dC}{dx} - kC^n = 0$$

where D = diffusion coefficient.

k = rate constant of the removal reaction.

n = order of the removal reaction.

v = linear gas velocity.

For a first order reaction, i.e. $n = 1$, this equation can be solved under the boundary conditions:

$$C = C_0 \text{ at } x = 0$$

$$C = 0 \text{ at } x = \infty$$

to yield

$$C = C_0 \exp \left(\frac{v - \sqrt{v^2 + 4kD'}}{2D} \right) x \dots\dots\dots (1)$$

The observed rate constant, k' , obtained from such a system is defined by:

$$C = C_0 \exp \left(- \frac{k' x}{v} \right)$$

Thus the true rate constant can be obtained from the relation

$$k = k' \left(1 + \frac{k' D}{v^2} \right) \dots\dots\dots (2)$$

Obviously the condition required for diffusion to be negligible is therefore

$$\frac{Dk'}{v^2} \ll 1$$

The solutions of the original differential equation for $n \neq 1$ do not lead to simple solutions. However, the condition for diffusion to be negligible can be obtained quite simply.

The essential criterion is that the diffusive term, $D \frac{d^2C}{dx^2}$, be negligible compared with the convective flow term,

$$- v \frac{dC}{dx}.$$

$$\text{Now } \frac{dC}{dx} = \frac{dC}{dt} \cdot \frac{dt}{dx} = \frac{k}{v} C^n$$

$$\frac{d^2C}{dx^2} = \frac{d}{dx} \left(\frac{dC}{dx} \right) = \frac{k^2}{v^2} n C^{2n-1}$$

$$\text{Therefore for } D \frac{d^2C}{dx^2} \ll - v \frac{dC}{dx},$$

$$\text{leads to } \frac{nDkC^{n-1}}{v^2} \ll 1$$

2. Perturbation produced by a catalytic probe

The use of a catalytic probe to measure atom concentrations in a flow system has been criticized by Wise and Ablow*. This criticism, if valid, will also apply to present use of a probe to follow the decay of vibrationally excited nitrogen. That negligible error is introduced by such probe when used to follow a first order reaction is shown by the following analysis.

The differential equation expressing C as a function of x remains unchanged. However, the presence of a probe, capable of completely removing the reactant, situated at x = L leads to the following boundary conditions.

$$C' = C_0 \text{ at } x = 0$$

$$C' = 0 \text{ at } x = L$$

where C' is now the perturbed concentration.

The solution is now

$$C' = \frac{C_0 e^{(\frac{v}{2D} - R)x}}{1 - e^{-2RL}} \left(1 - e^{-2R(L - x)} \right) \dots\dots\dots (3)$$

$$\text{where } R = \frac{\sqrt{v^2 + 4kD}}{2D}$$

*H. Wise and C.M. Ablow, J. Chem. Phys., 35, 10 (1961)

Comparison with equation (1) shows that the fractional change in concentration, due to the presence of the probe, is given by:

$$\frac{C'}{C} = \frac{1 - e^{-2R(L - x)}}{1 - e^{-2RL}} \dots\dots\dots (4)$$

The parameters in R for typical operating conditions have the following approximate values:

$$v \simeq 100 \text{ cm sec}^{-1}$$

$$k \simeq 8 \text{ sec}^{-1}$$

$$D \simeq 30 \text{ cm}^2 \text{ sec}^{-1} \text{ (calculated from simple kinetic theory)}$$

$$\text{Thus } R \simeq 1.7$$

Since L in practice is never less than 10 cms, the denominator in equation (4) is almost identically equal to unity.

The relative concentration 1 cm upstream from the probe, i.e. $L - x = 1$, is therefore equal to

$$\frac{C'}{C} = 1 - e^{-3.4} = 0.967$$

Thus the perturbed concentration, C' , due to the presence of the probe, is 96.7% of the unperturbed value.

For $L - x = 2$, C' becomes 99.9% of the unperturbed value. It is therefore apparent that the perturbation introduced by the probe extends only a very short distance upstream.

However, it is important to realize that such a

probe does not in fact measure concentrations directly (one of the boundary conditions was that $C' = 0$ at $x = L$). Rather it measures a particle flux from which a concentration, C_{exp} , for use in the kinetic equations, is calculated from the relation

$$C_{exp} = \frac{N}{av}$$

where N = particle flux,

a = cross-sectional area of reaction tube.

Thus one must compare C_{exp} rather than C' with the unperturbed concentration, C .

The number of particles, N_x , crossing a plane per second, will be the sum of the particles crossing by convective flow plus those crossing by diffusive flow. This can be calculated as follows:

$$\text{Diffusive flow} = - \frac{aDdC'}{dx}$$

$$\text{Convective flow} = avC'$$

$$\text{i.e. } N_x = \frac{aDdC'}{dx} + avC' \dots\dots\dots (5)$$

Differentiation and substitution of equation (3) in equation (5) then yields

$$N_x = aDA_xR \left(1 + e^{-2R(L-x)} \right) + \frac{A_x v}{2} \left(1 - e^{-2R(L-x)} \right)$$

$$\text{where } A_x = \frac{C_0 e^{\left(\frac{v}{2D} - R\right)x}}{1 - e^{-2RL}}$$

At $x = L$

$$N_L = 2aDA_L R$$

$$= \frac{2aDR C_o e^{\left(\frac{v}{2D} - R\right)L}}{1 - e^{-2RL}}$$

Thus

$$C_{\text{exp}} = \frac{N_L}{av} = \frac{2DR}{v} \frac{C_o e^{\left(\frac{v}{2D} - R\right)L}}{1 - e^{-2RL}}$$

Now

$$\frac{2DR}{v} = \left(1 + \frac{4kD}{v^2}\right)^{\frac{1}{2}}$$

Therefore

$$C_{\text{exp}} = \left(1 + \frac{4kD}{v^2}\right)^{\frac{1}{2}} \frac{C_o}{1 - e^{-2RL}} e^{\left(\frac{v}{2D} - R\right)L} \dots (6)$$

This can be compared with the unperturbed concentration, C , given by equation (1) to yield

$$\frac{C_{\text{exp}}}{C} = \left(1 + \frac{4kD}{v^2}\right)^{\frac{1}{2}} \frac{1}{1 - e^{-2RL}}$$

As noted previously, the term $1 - e^{-2RL}$ can be set equal to unity without appreciable error.

Using the previously tabulated values of k , D , and v , the term

$$\left(1 + \frac{4kD}{v^2}\right)^{\frac{1}{2}} \simeq 1.05$$

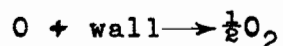
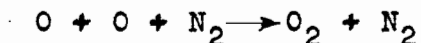
Thus an error of about 5% is introduced into the concentration determination.

However, since the system obeys first order kinetics, it is not necessary, for rate determinations, to estimate concentrations absolutely. The presence of the constant term $(1 + \frac{4kD}{v^2})^{\frac{1}{2}}$ introduces no error, and the use of a probe in such a system can be completely justified. Of course the rate constants so determined must be corrected, if necessary, for the normal diffusion effects as shown by equation (2). In the present system this correction is also negligible.

SUMMARY AND CONTRIBUTIONS TO KNOWLEDGE

1. The reaction $N + NO \rightarrow N_2 + O$ has been successfully employed to produce a system essentially free from molecular oxygen and containing a known concentration of oxygen atoms.
2. This system has been used to confirm the validity of the NO_2/O reaction as a quantitative method for determining oxygen-atom concentrations.
3. A rapid method for following the concentration of atomic oxygen as a function of time in a fast flow system has been devised and used to study the kinetics of the atom recombination.

The results are consistent with the mechanism



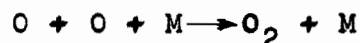
The rate constant for the homogeneous recombination was found to be sensitive to small amounts of condensable impurity (mainly water vapour) present in undried tank nitrogen.

For undried nitrogen, the homogeneous recombination rate constant was found to be $1.5 \times 10^{15} \text{ cm}^6 \text{ mole}^{-2} \text{ sec}^{-1}$.

Removal of the condensable material from the nitrogen by passage through two liquid air traps reduced this rate constant to $1.0 \times 10^{15} \text{ cm}^6 \text{ mole}^{-2} \text{ sec}^{-1}$.

Efficiencies of third bodies other than N_2 in the homogeneous recombination reaction were also examined.

Rate constants for the reaction



were evaluated as $3.3 \times 10^{15} \text{ cm}^6 \text{ mole}^{-2} \text{ sec}^{-1}$ ($M = \text{SF}_6$),
 $3.3 \times 10^{15} \text{ cm}^6 \text{ mole}^{-2} \text{ sec}^{-1}$ ($M = \text{CO}_2$), $1.37 \times 10^{15} \text{ cm}^6$
 $\text{mole}^{-2} \text{ sec}^{-1}$ ($M = \text{N}_2\text{O}$), $3 \times 10^{14} \text{ cm}^6 \text{ mole}^{-2} \text{ sec}^{-1}$ ($M = \text{He}$),
 $\leq 3 \times 10^{14} \text{ cm}^6 \text{ mole}^{-2} \text{ sec}^{-1}$ ($M = \text{Ar}$).

Removal of vibrationally excited nitrogen, normally present in active nitrogen, did not affect the recombination rate.

4. The rate constant for the heterogeneous recombination was found to be 0.4 sec^{-1} yielding a recombination coefficient for oxygen atoms on pyrex of 1.65×10^{-5} .

5. The presence of vibrationally excited nitrogen in active nitrogen has been demonstrated by the discrepancy between the heat content measured experimentally by an isothermal calorimetric probe and that calculated from the known nitrogen-atom concentration.

6. The vibrational energy content of active nitrogen leaving a microwave discharge was estimated as $6.03 \text{ kcal mole}^{-1}$. The relaxation of this species was found to be due almost entirely to heterogeneous deactivation on the walls of the reaction vessel with an efficiency of 4.8×10^{-4} .

A marked increase in the homogeneous relaxation rate was produced by the addition of other inert gases

(Ar, CO₂, N₂O). The collisional efficiencies of these gases were estimated as: 1.6×10^{-6} (Ar), 4.0×10^{-5} (CO₂), and 1.4×10^{-4} (N₂O).

7. The preferential elimination of vibrationally excited nitrogen by passage of active nitrogen through a glass-wool plug was employed to produce a system containing atomic nitrogen as virtually the sole energetic species. This system was used to confirm the stoichiometry of the reaction $N + NO \rightarrow N_2 + O$.

Probe measurements in such a system showed that virtually all of the atomic nitrogen was in the ground (⁴S) state.

8. The reaction between atomic nitrogen and nitric oxide was found to produce vibrationally excited nitrogen with an average energy of 20 ± 4 kcal mole⁻¹.

9. The perturbation produced by a catalytic probe placed in a reacting flow system has been calculated, using a simple mathematical model.

It has been shown that the concentration calculated from probe measurements in a system in which the reactant disappears by a first order reaction can be made to approximate closely the unperturbed value by a suitable choice of experimental conditions.